58 DSP ($Ca_2Sr(CH_3CH_2COO)_6$) family

58A Pure compounds

No. 58A-1 $Ca_2Sr(CH_3CH_2COO)_6$, Dicalcium strontium propionate (DSP)

(M = 606.21; [D: 636.39])

1a Ferroelectricity in DSP was discovered by Matthias and Remeika in 1957. 57Mat

b

phase	III [a])	II [b])	I [b])
state		F [b])	P [b])
crystal system	monoclinic [c])	tetragonal [d])	tetragonal [e])
space group		$P4_1 - C_4^2$ or $P4_3 - C_4^4$ [d])	$P4_12_12 - D_4^4$ or $P4_32_12 - D_4^8$ [e])
Θ [K]	104.2 [a])	282.6 [a]) [D: 279.5] [f])	

[a]) 65Nak
[b]) 57Mat
[c]) 78Hos
[d]) 67Miz
[e]) 67Mar
[f]) 86Yag, 87Yag1

Θ vs. p: see Fig. 58A-1-023, Fig. 58A-1-024, Fig. 58A-1-025 in subsection 5a.
P_s || [001]. 57Mat
Transparent, colorless.

2a Crystal growth: evaporation or heating method from aqueous solution. 65Kob
Solubility: Fig. 58A-1-001.

b Crystal form: Fig. 58A-1-002.

3a Unit cell parameters:
Phase I: a = 12.515(2) Å, c = 17.257(2) Å at T = 25 °C. 81Ito
Phase II: a = 12.475(2) Å, c = 17.141(4) Å at T = –40 °C. 82Mis
Unit cell parameters of $Ca_2Sr(C_2D_5CO_2)_6$: Table 58A-1-001.

b Z = 4.
Crystal structure: Fig. 58A-1-003, Fig. 58A-1-004, Fig. 58A-1-005, Fig. 58A-1-006, Fig. 58A-1-007, Fig. 58A-1-008.
Fractional coordinates and temperature parameters
for nondeuterated crystal: Table 58A-1-002, Table 58A-1-003, Table 58A-1-004, Table 58A-1-005; Fig. 58A-1-009, Fig. 58A-1-010;
for deuterated crystal: Table 58A-1-006, Table 58A-1-007.
Interatomic distances and bond angles
for nondeuterated crystal: Table 58A-1-008, Table 58A-1-009, Table 58A-1-010, Table 58A-1-011;
for deuterated crystal: Table 58A-1-012, Table 58A-1-013.
Shapes of propionate groups: Fig. 58A-1-011, Fig. 58A-1-012.
Occupancy of C atoms: Table 58A-1-014, Table 58A-1-015.

4 Lattice distortion: Fig. 58A-1-013.

5a Dielectric constant: Fig. 58A-1-014, Fig. 58A-1-015, Fig. 58A-1-016, Fig. 58A-1-017.
κ_a decreases from 6.6 at –178 °C to 4.3 at 32 °C with increasing temperature (f = 326 kHz). 61Kob
Effect of hydrostatic pressure: Fig. 58A-1-018, Fig. 58A-1-019, Fig. 58A-1-020, Fig. 58A-1-021, Fig. 58A-1-022.
Phase diagram in regard to p: Fig. 58A-1-023, Fig. 58A-1-024, Fig. 58A-1-025, Fig. 58A-1-026.

	Dielectric dispersion: Fig. 58A-1-027, Fig. 58A-1-028, Fig. 58A-1-029, Fig. 58A-1-030, Fig. 58A-1-031, Fig. 58A-1-032; see also Fig. 58A-3-014 in No. 58A-3 and	67Nak
	Effect of heat-treatment on the dielectric dispersion: see	83Shi
	Effect of CH_3CO_2 addition: see No. 58B-4 and	69Nak
b	Effect of bias field on κ: Fig. 58A-1-033.	
c	Spontaneous polarization: Fig. 58A-1-034, Fig. 58A-1-035, Fig. 58A-1-036; see also Fig. 58A-1-016 in subsection 5a.	
d	Pyroelectric coefficient: $p_3 = -0.90 \cdot 10^{-4}$ C K^{-1}m^{-2} at 0 °C (primary effect: $-0.40 \cdot 10^{-4}$ C K^{-1} m^{-2}; secondary effect: $-0.50 \cdot 10^{-4}$ C K^{-1} m^{-2}); see also Fig. 58A-1-034 in subsection 5c.	81Bha
6a	Heat capacity: Fig. 58A-1-037.	
	Transition heat, transition entropy:	65Nak

transition	III–II	II–I
ΔQ_m [J mol^{-1}]	818	940
ΔS_m [J K^{-1} mol^{-1}]	2.55	13.4

7a	Piezoelectricity: Fig. 58A-1-038.	
b	Electrostriction: Fig. 58A-1-039, Fig. 58A-1-040.	
8a	Elastic stiffness: Fig. 58A-1-041, Fig. 58A-1-042; see also	66Ham
	Ultrasonic wave velocity: Fig. 58A-1-043, Fig. 58A-1-044, Fig. 58A-1-045, Fig. 58A-1-046.	
	Ultrasonic attenuation: Fig. 58A-1-047, Fig. 58A-1-048.	
	Relaxation time obtained from ultrasonic attenuation: see	94Val
b	The tetragonal c axis is rotated by 90° under appropriate external stress in phase I.	77Saw
9a	Refractive indices: Table 58A-1-016, Table 58A-1-017.	
	Birefringence: Fig. 58A-1-049.	
b	Electrooptic constant: Fig. 58A-1-050.	
d	Optical activity: Fig. 58A-1-051, Fig. 58A-1-052, Fig. 58A-1-053, Fig. 58A-1-054.	
	The crystal of space group $P4_32_12$ is dextrorotatory.	81Gla
e	Nonlinear optical properties: Fig. 58A-1-055.	
	Nonlinear optical susceptibilities: $\lvert d_{31}\rvert = 0.19(2)\, d_{11}^{quartz}$, $\lvert d_{33}\rvert = 0.37(4)\, d_{11}^{quartz}$, $d_{31} \cdot d_{33} < 0$ at –20 °C for $\lambda = 1.06$ µm.	74Ish
10a	Raman scattering: Table 58A-1-018, Table 58A-1-019; Fig. 58A-1-056, Fig. 58A-1-057.	
b	Brillouin scattering: Fig. 58A-1-058, Fig. 58A-1-059; see also	73Shi
13a	NMR: Fig. 58A-1-060, Fig. 58A-1-061; see also	68Nak, 71Shi
b	ESR of X-irradiated crystal: Fig. 58A-1-062.	
	ESR of Mn^{2+} doped crystal: Table 58A-1-020; Fig. 58A-1-063, Fig. 58A-1-064; see also	73Ram, 89Mis1, 89Mis2
14a	Neutron scattering from disordered structure: Fig. 58A-1-065, Fig. 58A-1-066.	
b	Neutron diffuse scattering: Fig. 58A-1-067, Fig. 58A-1-068.	

15a	Ferroelectric domains are observed by powder pattern method and by electron mirror microscope.	67Moc 71Som
b	Domain switching: Fig. 58A-1-069. Switching time depends linearly on the applied electric field.	82Rav
16	Etchant: methanol.	88Cha

Table 58A-1-001. $Ca_2Sr(CD_3CD_2COO)_6$ (DDSP). Unit cell parameters *a*, *c* vs. *T* [88Mac].

T [K]	*a* [Å]	*c* [Å]
337	12.507(4)	17.281(4)
294	12.483(4)	17.222(5)
284	12.469(3)	17.210(5)
258	12.469(3)	17.144(3)
184	12.428(5)	17.037(5)
120	12.388(6)	17.992(7)

Table 58A-1-002. $Ca_2Sr(CH_3CH_2COO)_6$ (DSP). Fractional coordinates of atoms in the unit cell and isotropic temperature parameters in the phase I (20 °C) [67Miz]. X(ij): The j th atom X in the i th propionate radical. *B* is defined by Eq. (e) in Introduction. See Fig. 58A-1-004.

Atom	*x*	*y*	*z*	*B* [Å^2]
Sr	0.2771	0.2771	0.0000	3.4
Ca	0.2596	0.0660	0.1582	4.6
O(1)	0.184	0.086	0.037	6.9
O(2)	0.383	0.463	0.040	8.4
O(31)	0.395	0.156	0.091	5.6
O(32)	0.546	0.171	0.032	8.4
O(41)	0.196	0.236	0.168	8.7
O(42)	0.184	0.387	0.114	5.5
C(11)	0.10	0.10	0.00	7.0
C(12)	0.01	0.01	0.00	
C(21)	0.46	0.46	0.00	7.5
C(22)	0.56	0.56	0.00	
C(31)	0.493	0.152	0.086	4.5
C(32)	0.56	0.14	0.18	
C(41)	0.173	0.332	0.172	5.1
C(42)	0.13	0.38	0.24	

Table 58A-1-003. $Ca_2Sr(CH_3CH_2COO)_6$ (DSP). Fractional coordinates of atoms in the unit cell and isotropic temperature parameters in the phase II (–50 °C) [67Mar]. X(ij): The j th atom X in the i th propionate radical. *B* is defined by Eq. (e) in Introduction. See Fig. 58A-1-005.

Atom	*x*	*y*	*z*	*B* [Å^2]
Sr	0.2780	0.2776	0.0000	3.0
Ca(1)	0.2587	0.0670	0.1578	3.8
Ca(2)	0.0684	0.2610	–0.1597	3.6
O(11)	0.189	0.087	0.044	6.3
O(12)	0.079	0.189	–0.033	5.9
O(21)	0.384	0.470	0.041	8.3
O(22)	0.474	0.373	–0.044	6.9
O(31)	0.392	0.157	0.089	3.8
O(32)	0.562	0.171	0.031	7.3
O(41)	0.162	0.389	–0.085	3.2
O(42)	0.175	0.546	–0.032	8.4
O(51)	0.199	0.234	0.166	6.1
O(52)	0.182	0.394	0.112	5.1
O(61)	0.228	0.197	–0.161	7.5
O(62)	0.398	0.179	–0.109	4.9
C(11)	0.10	0.10	0.00	5.3
C(12)	0.02	–0.01	–0.02	6.9
C(13)	0.04	–0.10	–0.01	13.0
C(21)	0.46	0.48	0.01	4.7
C(22)	0.53	0.55	0.06	9.8
C(23)	0.52	0.63	0.08	17.0
C(31)	0.49	0.16	0.09	4.1
C(32)	0.53	0.10	0.16	6.2
C(33)	0.57	0.21	0.18	13.3
C(41)	0.15	0.50	–0.09	4.3
C(42)	0.10	0.54	–0.16	5.4
C(43)	0.15	0.55	–0.23	14.3
C(51)	0.17	0.34	0.18	4.5
C(52)	0.11	0.39	0.24	4.6
C(53)	0.18	0.36	0.30	15.3
C(61)	0.34	0.17	–0.17	6.4
C(62)	0.37	0.15	–0.25	9.5
C(63)	0.34	0.19	–0.33	17.5

Table 58A-1-004. $Ca_2Sr(CH_3CH_2COO)_6$ (DSP). Fractional coordinates and anisotropic temperature parameters at 25(1) °C [81Ito]. U_{ij} is defined by Eq. (d) in Introduction. The values of U_{ij} are given in 10^{-2} Å^2. Primed and double primed atoms indicate disordered atoms as shown in Fig. 58A-1-011.

Atom	*x*	*y*	*z*	U_{11}	U_{22}	U_{33}	U_{12}	U_{13}	U_{23}
Sr	0.27666(2)	0.27666(2)	0.0	2.40(1)	2.40(1)	2.46(2)	–0.16(2)	0.09(1)	–0.09(1)
Ca(1)	0.26045(7)	0.06587(6)	0.15841(5)	5.02(5)	2.77(4)	4.35(4)	–0.08(4)	0.97(4)	1.46(3)
O(11)	0.0856(4)	0.1833(3)	–0.0375(2)	8.7(3)	7.3(3)	7.0(2)	–2.9(2)	–2.7(2)	2.5(2)
O(21)	0.3773(4)	0.4687(4)	0.0384(3)	7.0(3)	7.4(3)	13.1(4)	0.8(2)	4.1(3)	–3.9(3)
O(31)	0.3957(2)	0.1566(3)	0.0886(2)	3.9(2)	5.1(2)	5.6(2)	–0.3(1)	0.4(2)	1.7(2)
O(32)	0.5495(3)	0.1695(4)	0.0301(2)	7.0(3)	13.3(4)	6.1(2)	–1.2(3)	2.3(2)	1.7(2)
O(41)	0.1988(4)	0.2359(3)	0.1664(3)	9.8(3)	4.0(2)	14.6(4)	2.7(2)	1.7(3)	1.0(2)
O(42)	0.1860(3)	0.3898(3)	0.1137(2)	9.2(3)	3.9(2)	5.5(2)	1.1(2)	2.4(2)	–0.2(2)
C(11)	0.1000(4)	0.1000(4)	0.0	8.0(4)	8.0(4)	5.6(4)	–5.0(4)	–2.0(4)	2.0(4)
C(12)	0.0153(5)	0.0153(5)	0.0	15.8(10)	15.8(10)	23.0(16)	–12.9(11)	–9.0(12)	9.0(12)
C(13)'	0.0355(25)	–0.0912(19)	0.0215(27)	19.5(23)	9.8(13)	41.2(53)	–8.6(14)	–12.5(31)	11.4(2)
C(21)	0.4592(4)	0.4592(4)	0.0	4.5(2)	4.5(2)	9.7(6)	–0.9(3)	2.8(3)	–2.8(3)
C(22)'	0.5225(18)	0.5610(18)	–0.0052(36)	9.1(19)	8.4(18)	39.1(37)	–4.5(16)	–3.1(25)	–8.1(27)
C(23)'	0.6157(19)	0.5592(25)	–0.0409(19)	11.2(16)	25.4(36)	25.7(34)	–10.3(22)	5.4(19)	–1.2(25)
C(31)	0.4951(4)	0.1533(4)	0.0871(3)	4.0(2)	5.8(3)	4.2(2)	–0.1(2)	0.1(2)	1.6(2)
C(32)	0.5500(6)	0.1212(9)	0.1586(5)	7.6(5)	18.2(9)	11.7(6)	0.6(5)	–3.0(5)	7.8(7)
C(33)'	0.5671(43)	0.2109(33)	0.2113(14)	47.5(67)	25.3(34)	11.7(16)	–1.3(41)	–15.7(28)	–4.3(21)
C(33)"	0.6588(16)	0.1502(23)	0.1661(16)	8.4(12)	20.9(24)	22.7(24)	–3.0(14)	–7.2(15)	7.9(20)
C(41)	0.1748(4)	0.3302(4)	0.1703(3)	7.0(3)	3.5(2)	6.0(3)	0.7(2)	2.4(3)	0.3(2)
C(42)	0.1239(8)	0.3775(6)	0.2412(4)	17.8(8)	10.4(5)	5.4(3)	2.4(5)	5.5(5)	1.4(4)
C(43)	0.1651(13)	0.3253(17)	0.3177(5)	21.6(14)	34.4(22)	6.9(5)	2.7(14)	–0.4(7)	3.6(9)

Table 58A-1-005. $Ca_2Sr(CH_3CH_2COO)_6$ (DSP). Fractional coordinates and anisotropic temperature parameters at T = –40 °C [82Mis]. U_{ij} and U are defined by Eq. (d) in Introduction and the temperature factor exp $[-8\pi^2 U(\sin\theta/\lambda)^2]$, respectively. U_{ij}, U in [10^{-2} Å^2]. Last column: equivalent atom above Θ_f. See Table 58A-1-004 about the equivalent atoms above Θ_f. See Table 58A-1-008 for symmetry code v. For atoms labelled 3a, 3b, 4a, 4b, see Fig. 58A-1-007 and Fig. 58A-1-012.

Atom	x	y	z	U_{11}, U	U_{22}	U_{33}	U_{12}	U_{13}	U_{23}	Atom above Θ_f
Sr	0.27583(5)	0.27879(5)	0.0	1.58(3)	1.40(3)	2.43(3)	–0.06(2)	0.04(3)	–0.08(3)	Sr
Ca(1)	0.25634(13)	0.07032(12)	0.16176(11)	3.60(8)	1.76(7)	4.08(9)	–0.28(6)	0.48(7)	1.11(7)	Ca(1)
Ca(2)	0.06624(12)	0.26805(14)	–0.15729(11)	2.03(7)	4.00(9)	3.98(9)	0.01(7)	–1.16(7)	–0.76(8)	Ca(1^v)
O(11)	0.0755(6)	0.1918(6)	–0.0337(4)	6.6(5)	5.1(4)	5.3(4)	–2.1(4)	–1.3(4)	1.4(3)	O(11)
O(12)	0.1788(6)	0.0942(6)	0.0398(5)	5.2(4)	5.5(4)	6.4(5)	–2.3(3)	–1.8(4)	2.1(4)	O(11^v)
O(21)	0.3689(6)	0.4715(6)	0.0361(5)	5.5(4)	3.9(4)	10.5(7)	–0.5(3)	3.6(4)	–3.0(4)	O(21)
O(22)	0.4668(7)	0.3838(6)	–0.0427(6)	6.4(5)	5.5(5)	11.8(7)	1.7(4)	4.2(5)	–2.1(5)	O(21^v)
O(3a1)	0.3929(4)	0.1611(5)	0.0924(4)	2.5(3)	3.6(3)	5.3(4)	0.0(2)	0.3(3)	1.6(3)	O(31)
O(3a2)	0.5497(6)	0.1798(8)	0.0345(5)	4.8(4)	11.9(7)	4.5(4)	–0.9(5)	1.4(3)	2.1(5)	O(32)
O(3b1)	0.1575(4)	0.4025(4)	–0.0876(4)	2.9(3)	2.9(3)	4.3(3)	–0.3(2)	–1.0(3)	0.3(3)	O(31^v)
O(3b2)	0.1595(7)	0.5604(6)	–0.0299(5)	8.7(6)	4.7(4)	5.7(5)	–1.1(4)	–1.1(4)	–1.1(4)	O(32^v)
O(4a1)	0.1887(8)	0.2366(6)	0.1765(7)	9.3(6)	2.9(4)	13.9(9)	2.8(4)	3.0(6)	0.6(5)	O(41)
O(4a2)	0.1795(5)	0.3889(5)	0.1123(4)	5.5(4)	3.0(3)	4.2(3)	–1.1(3)	1.3(3)	–0.5(3)	O(42)
O(4b1)	0.2383(5)	0.2039(6)	–0.1573(5)	3.1(3)	5.3(4)	8.4(5)	1.8(3)	–1.0(4)	–1.0(4)	O(41^v)
O(4b2)	0.3966(5)	0.1858(6)	–0.1110(4)	2.6(3)	8.1(5)	5.1(4)	–0.1(3)	–0.6(3)	–2.4(4)	O(42^v)
C(11)	0.0949(8)	0.1066(8)	0.0053(7)	5.4(6)	6.0(6)	4.5(5)	–3.5(5)	–1.3(5)	1.4(5)	C(11)
C(12)	0.0097(13)	0.0219(14)	0.0086(16)	8.1(9)	11.0(12)	18.5(17)	–8.1(9)	–5.8(11)	8.4(14)	C(12)
C(13)'	–0.1012(12)	0.0495(14)	–0.0160(16)	4.6(8)	8.7(11)	16.9(22)	–3.6(8)	–3.1(11)	4.2(14)	C(13)'
C(13)''	0.0352(66)	–0.0694(66)	0.0240(48)	9.1(22)						C(13^v)'
C(21)	0.4532(7)	0.4654(7)	–0.0011(8)	3.0(4)	3.5(4)	6.5(6)	0.0(3)	2.0(5)	–1.7(5)	C(21)
C(22)	0.5348(19)	0.5472(21)	0.0004(24)	13.6(19)	16.8(19)	23.9(26)	–12.6(16)	–3.8(19)	2.2(21)	C(22)'
C(23)'	0.5630(32)	0.5998(39)	0.0592(36)	10.0(25)	15.2(33)	21.7(46)	–2.7(24)	2.0(29)	–8.9(35)	C(23)'
C(23)''	0.6244(60)	0.5352(60)	0.0453(50)	18.1(24)						C(23^v)'
C(3a1)	0.4928(7)	0.1548(7)	0.0913(6)	3.4(4)	4.2(5)	4.3(5)	0.3(4)	0.3(4)	1.2(4)	C(31)
C(3a2)	0.5449(10)	0.1115(14)	0.1631(10)	4.4(6)	12.5(12)	10.7(11)	–0.6(7)	–2.6(7)	6.0(10)	C(32)
C(3a3)'	0.5593(87)	0.2041(87)	0.2255(64)	12.0(30)						C(33)'
C(3a3)''	0.6632(12)	0.1411(22)	0.1704(15)	4.0(8)	16.8(21)	14.3(20)	–2.5(11)	–3.9(11)	5.7(17)	C(33)''
C(3b1)	0.1566(7)	0.5042(7)	–0.0873(5)	4.2(5)	3.2(4)	3.5(4)	0.0(4)	–0.9(4)	0.3(4)	C(31^v)
C(3b2)	0.1397(12)	0.5577(11)	–0.1650(9)	9.3(9)	6.7(8)	7.8(9)	0.7(7)	–2.6(8)	2.2(7)	C(32^v)
C(3b3)'	0.2422(24)	0.5475(32)	–0.2104(18)	9.8(19)	18.8(31)	9.4(19)	–1.4(21)	2.5(16)	5.2(21)	C(33^v)'
C(3b3)''	0.1494(41)	0.6600(41)	–0.1713(31)	10.0(14)						C(33^v)''
C(4a1)	0.1643(7)	0.3342(7)	0.1714(6)	4.4(5)	2.5(4)	5.1(5)	0.4(4)	1.2(4)	0.2(4)	C(41)
C(4a2)	0.1111(11)	0.3835(9)	0.2393(6)	10.3(9)	5.9(6)	2.6(5)	1.2(6)	2.2(6)	0.4(5)	C(42)
C(4a3)	0.1471(19)	0.3490(10)	0.3186(10)	15.2(17)	17.6(20)	4.9(8)	2.0(16)	1.3(10)	1.7(10)	C(43)
C(4b1)	0.3320(7)	0.1812(8)	–0.1664(7)	3.1(5)	4.5(5)	6.9(7)	0.6(4)	0.5(5)	–2.6(5)	C(41^v)
C(4b2)	0.3759(14)	0.1395(20)	–0.2443(10)	9.6(11)	21.3(21)	7.2(9)	2.9(12)	–1.5(9)	–9.6(13)	C(42^v)
C(4b3)	0.3109(24)	0.1783(23)	–0.3127(11)	19.3(23)	19.3(23)	6.0(10)	4.6(19)	–2.4(13)	–0.6(13)	C(43^v)

Table 58A-1-006. $Ca_2Sr(CD_3CD_2COO)_6$ (DDSP). Fractional coordinates and anisotropic temperature parameters at 294 K [88Mac]. U_{ij} is defined by Eq. (d) in Introduction. The values of U_{ij} are given in 10^{-2} Å^2. Primed and double primed atoms indicate disordered atoms, as shown in Fig. 58A-1-011.

Atom	*x*	*y*	*z*	U_{11}	U_{22}	U_{33}	U_{12}	U_{13}	U_{23}
Sr	0.27670(2)	0.27670(2)	0.0	3.758(9)	3.758(9)	3.53(2)	–0.11(2)	0.06(1)	–0.06(1)
Ca	0.26069(7)	0.06615(5)	0.15857(4)	6.26(4)	3.87(3)	5.08(3)	–0.14(3)	0.90(4)	1.42(3)
O(11)	0.0855(3)	0.1828(3)	–0.0372(2)	9.7(2)	9.2(2)	7.5(2)	–3.0(2)	–2.9(2)	2.9(2)
C(11)	0.1000(7)	0.1000(7)	0.0	8.7(5)	8.7(5)	7.0(4)	–4.1(3)	–1.3(7)	1.3(7)
C(12)	0.0148(8)	0.0148(8)	0.0	14.9(7)	14.9(7)	22(1)	–11.3(4)	–7(1)	7(1)
C(13)	0.032(1)	–0.085(1)	0.018(1)	20(1)	10.8(8)	19(1)	–8.9(7)	–8(1)	5.6(9)
O(21)	0.3769(3)	0.4682(3)	0.0384(2)	8.0(2)	8.6(2)	13.1(3)	0.9(2)	4.2(2)	–4.1(2)
C(21)	0.4589(7)	0.4589(7)	0.0	5.7(4)	5.7(4)	10.5(4)	–0.9(3)	2.0(5)	–2.0(5)
C(22)	0.5215(9)	0.5633(9)	–0.003(2)	8.6(7)	9.2(7)	33(2)	–4.3(5)	0(2)	–6(1)
C(23)	0.606(1)	0.570(1)	–0.038(1)	16(1)	20(2)	30(2)	–8.5(9)	14(1)	–4(1)
O(31)	0.3959(2)	0.1570(2)	0.0895(2)	4.9(1)	6.1(2)	6.6(2)	0.0(2)	0.1(2)	1.2(2)
O(32)	0.5497(3)	0.1695(4)	0.0294(2)	8.5(2)	15.7(3)	6.4(2)	–1.6(2)	2.2(2)	2.4(2)
C(31)	0.4949(3)	0.1533(3)	0.0870(2)	5.5(2)	6.5(2)	5.5(2)	0.0(2)	0.1(2)	1.2(2)
C(32)	0.5513(5)	0.1225(7)	0.1619(4)	8.5(4)	21.4(7)	9.8(3)	0.3(4)	–2.6(3)	6.7(4)
C(33)'	0.560(2)	0.209(2)	0.2117(8)	24(2)	33(3)	7.5(7)	2(2)	–6.0(9)	–2(1)
C(33)"	0.650(1)	0.158(1)	0.1756(8)	8.7(8)	25(2)	14(1)	–2(1)	–5.6(7)	7(1)
O(41)	0.1970(3)	0.2361(3)	0.1664(2)	10.6(3)	4.9(2)	16.6(3)	2.0(2)	1.8(2)	1.4(2)
O(42)	0.1863(3)	0.3903(2)	0.1139(2)	10.7(2)	5.1(2)	5.8(2)	–1.1(2)	2.4(2)	–0.1(1)
C(41)	0.1746(4)	0.3310(3)	0.1703(3)	7.6(3)	5.0(2)	7.2(3)	0.9(2)	2.2(2)	0.1(2)
C(42)	0.1236(6)	0.3797(5)	0.2421(3)	19.3(6)	11.3(4)	5.6(2)	3.0(4)	5.5(3)	0.9(3)
C(43)	0.1668(9)	0.3353(9)	0.3143(4)	24(1)	28(1)	7.3(4)	6.0(9)	0.9(6)	1.7(6)

Table 58A-1-007. $Ca_2Sr(CD_3CD_2COO)_6$ (DDSP). Fractional coordinates and anisotropic temperature parameters at 258 K [88Mac]. U_{ij} is defined by Eq. (d) in Introduction. The values of U_{ij} are given in 10^{-2} Å^2.

Atom	*x*	*y*	*z*	U_{11}	U_{22}	U_{33}	U_{12}	U_{13}	U_{23}
Sr	0.27599(4)	0.27790(4)	0.0	3.15(2)	2.93(2)	3.21(2)	–0.09(2)	0.04(2)	–0.08(2)
Ca(1)	0.2582(1)	0.06876(9)	0.16029(8)	5.18(6)	3.07(5)	4.62(6)	–0.21(5)	0.65(6)	1.18(5)
Ca(2)	0.06633(9)	0.2656(1)	–0.15805(8)	3.17(5)	5.37(6)	4.44(6)	–0.20(5)	–1.22(5)	–0.77(6)
O(11)	0.0792(4)	0.1879(4)	–0.0360(3)	7.3(3)	7.3(3)	6.4(3)	–2.0(3)	–1.9(3)	2.1(3)
O(12)	0.1811(4)	0.0913(5)	0.0380(3)	7.1(3)	8.2(3)	6.9(3)	–2.8(3)	–2.5(3)	2.6(3)
C(11)	0.0957(6)	0.1050(6)	0.0015(6)	6.9(4)	6.3(3)	6.3(4)	–3.4(3)	–1.3(4)	1.0(4)
C(12)	0.0117(7)	0.0185(7)	0.005(1)	11.7(5)	12.5(5)	20(1)	–10.0(4)	–7.0(8)	7.4(8)
C(13)"	0.037(8)	–0.087(8)	0.017(7)	15(3)	–	–	–	–	–
C(13)'	–0.0958(9)	0.044(1)	–0.018(1)	8.0(6)	13.6(9)	20(2)	–5.8(6)	–4.6(9)	4(1)
O(21)	0.3712(4)	0.4695(4)	0.0363(4)	6.9(3)	5.8(3)	11.1(4)	0.4(2)	4.0(3)	–2.7(3)
O(22)	0.4683(5)	0.3815(5)	–0.0411(4)	8.8(3)	7.1(3)	11.9(4)	1.4(3)	5.1(3)	–2.2(3)
C(21)	0.4547(5)	0.4625(5)	–0.0013(6)	5.0(3)	4.4(3)	8.5(4)	–0.7(3)	1.9(4)	–1.7(4)
C(22)	0.535(1)	0.5540(9)	–0.002(2)	12.7(7)	12.0(7)	30(2)	–8.1(5)	–2(1)	0(1)
C(23)"	0.620(2)	0.562(3)	–0.031(3)	7(1)	18(3)	39(5)	–3(2)	11(2)	–10(3)
C(23)'	0.580(2)	0.589(2)	0.048(2)	18(2)	21(2)	33(3)	–11(1)	–4(2)	–15(1)
O(3a1)	0.3945(3)	0.1594(4)	0.0910(3)	4.4(2)	4.8(2)	5.9(3)	–0.3(2)	–0.3(2)	1.6(2)
O(3a2)	0.5485(4)	0.1758(6)	0.0317(3)	6.6(3)	12.8(5)	5.2(3)	–1.4(3)	1.8(3)	1.6(3)
C(3a1)	0.4947(5)	0.1532(5)	0.0893(4)	4.3(3)	5.1(3)	4.7(3)	0.0(3)	0.0(3)	0.9(3)
C(3a2)	0.5450(7)	0.118(1)	0.1645(6)	5.9(5)	19.1(9)	10.5(6)	0.5(6)	–2.4(5)	8.5(5)
C(3a3)"	0.656(1)	0.149(1)	0.174(1)	9.2(7)	29(2)	19(1)	–5(1)	–5.8(8)	10(1)
O(3b1)	0.1579(3)	0.4000(3)	–0.0882(3)	4.6(2)	4.0(2)	5.1(2)	–0.4(2)	–1.3(2)	0.0(2)
O(3b2)	0.1632(6)	0.5579(4)	–0.0299(3)	13.1(5)	6.1(3)	5.6(3)	–1.0(3)	–1.9(3)	–1.1(3)
C(3b1)	0.1556(5)	0.5001(5)	–0.0885(4)	5.4(3)	4.7(3)	4.3(3)	0.0(3)	–1.2(3)	0.0(3)
C(3b2)	0.136(1)	0.5554(7)	–0.1660(6)	16.4(9)	6.3(5)	6.8(5)	1.1(6)	–4.0(6)	1.8(4)
C(3b3)'	0.230(2)	0.557(2)	–0.2122(9)	24(2)	26(2)	6.9(7)	–2(2)	2(1)	7(1)
C(3b3)"	0.163(5)	0.648(5)	–0.179(4)	13(4)	–	–	–	–	–
O(4a1)	0.1923(5)	0.2375(4)	0.1731(5)	9.3(4)	3.9(2)	17.1(7)	2.8(3)	1.8(5)	0.6(4)
O(4a2)	0.1820(4)	0.3898(4)	0.1121(3)	8.3(3)	4.2(2)	4.4(2)	–1.1(2)	1.5(2)	–0.3(2)
C(4a1)	0.1671(6)	0.3326(5)	0.1706(5)	6.1(4)	4.6(3)	5.8(4)	0.4(3)	1.5(3)	0.0(3)
C(4a2)	0.1147(9)	0.3840(7)	0.2400(5)	14.5(7)	8.4(5)	3.9(4)	2.4(5)	3.4(4)	0.5(4)
C(4a3)	0.151(1)	0.339(2)	0.3137(7)	20(2)	25(2)	5.6(7)	1(1)	0.8(9)	1(1)
O(4b1)	0.2353(4)	0.1997(5)	–0.1595(4)	4.3(2)	7.2(3)	11.2(4)	1.2(2)	–1.6(3)	–1.0(3)
O(4b2)	0.3943(4)	0.1851(5)	–0.1122(3)	4.7(2)	9.3(3)	5.2(3)	–0.5(3)	–0.1(2)	–2.0(3)
C(4b1)	0.3316(5)	0.1766(6)	–0.1677(5)	3.7(3)	6.8(4)	6.5(4)	0.7(3)	–0.4(3)	–2.2(4)
C(4b2)	0.3767(9)	0.130(1)	–0.2434(6)	11.0(7)	21(1)	6.6(4)	3.7(7)	–1.4(6)	–7.8(5)
C(4b3)	0.329(1)	0.178(1)	–0.3149(7)	22(2)	22(2)	6.4(7)	3(1)	–2.1(9)	1.4(9)

Table 58A-1-008. $Ca_2Sr(CH_3CH_2COO)_6$ (DSP). Interatomic distances [Å] and angles [°] around Sr and Ca [81Ito]. $T = 25$ °C.

Sr–O(11)	2.739(4)	Sr–O(21)	2.793(5)
Sr–O(31)	2.611(3)	Sr–O(32)	3.705(3)
Sr–O(41)	3.075(4)	Sr–O(42)	2.672(4)
Sr–Ca	3.8044(9)	Sr–Ca^{iv-c}	3.9767(9)
Ca–Sr–Ca^{iv-c}	104.66(2)	Ca–Sr–Ca^{v}	116.26(2)
Ca^{iv-c}–Sr–Ca^{v}	109.83(2)	Ca^{iv-c}–Sr–Ca^{vii}	111.75(2)
Ca–$O(11^{v})$	2.313(5)	Ca–$O(21^{vii-b})$	2.301(5)
Ca–O(31)	2.368(3)	Ca–$O(32^{iii-b})$	2.284(4)
Ca–O(41)	2.268(5)	Ca–$O(42^{vii-b})$	2.335(4)

Symmetry code:

(i) x, y, z	(v) $y, x, \bar{z}$
(ii) $\bar{x}, \bar{y}, 1/2 + z$	(vi) $\bar{y}, \bar{x}, 1/2 - z$
(iii) $1/2 - y, 1/2 + x, 1/4 + z$	(vii) $1/2 - x, 1/2 + y, 1/4 - z$
(iv) $1/2 + y, 1/2 - x, 3/4 + z$	(viii) $1/2 + x, 1/2 - y, 3/4 - z$

The translation operation by a cell constant is denoted by $\pm a, \pm b, \pm c$.
For simplicity the code (i) is omitted throughout.

Table 58A-1-009. $Ca_2Sr(CH_3CH_2COO)_6$ (DSP). Distances between C atoms of the methyl groups at $T = 25(1)$ °C [81Ito]. Corrected values for hindered rotation about C^{α}–C^{β} are given in the third column. Symmetry code: see Table 58A-1-008.

$CH_3(1^{iv})'$–$CH_3(2^{+c})'$	4.31(5) Å	(4.36) Å
–$CH_3(2^{v+a+b})'$	4.12(6)	(4.10)
–$CH_3(3^{ii+a+b})'$	4.20(5)	(4.24)
–$CH_3(3^{v+c})'$	2.81(5)	(2.69)
–$CH_3(3^{v+c})''$	4.19(5)	(4.20)
–$CH_3(4^{v+c})$	4.18(4)	(4.09)
$CH_3(2)'$–$CH_3(3^{iv+b-c})''$	3.63(4)	(3.60)
–$CH_3(3^{vii+a})''$	3.73(4)	(3.67)
–$CH_3(4^{ii+a+b-c})$	3.95(3)	(3.80)
–$CH_3(4^{iv-c})$	4.28(3)	(4.15)
$CH_3(3)'$–$CH_3(3^{vi+a+b})'$	4.15(7)	(4.03)
–$CH_3(3^{vi+a+b})''$	4.43(5)	(4.32)
–$CH_3(4^{iv-c})$	4.36(5)	(4.35)
–$CH_3(4^{viii})$	4.03(3)	(4.02)
$CH_3(3)''$–$CH_3(3^{vi+a+b})''$	4.45(4)	(4.32)
–$CH_3(4^{iv-c})$	3.55(3)	(3.41)
–$CH_3(4^{vi+a})$	3.96(3)	(4.02)

Table 58A-1-010. $Ca_2Sr(CH_3CH_2COO)_6$ (DSP). Interatomic distances [Å] and angles [°] around Sr and Ca [82Mis]. $T = -40$ °C. For labelling of atoms, see caption of Table 58A-1-005.

Interatomic distances [Å]				Bond angles [°]	
Sr–O(11)	2.785(8)	Sr–Ca(2)	3.758(2)	Ca(1)–Sr–Ca(2)	116.97(6)
Sr–O(21)	2.741(7)	Sr–Ca(2^{iii})	3.960(2)	Ca(1^{iv-c})–Sr–Ca(2^{iii})	122.22(5)
Sr–O(12)	2.689(7)	Ca(1)–O(12)	2.323(8)	Ca(1)–Sr–Ca(1^{iv-c})	105.03(6)
Sr–O(22)	2.815(8)	Ca(1)–O(22^{iii-b})	2.309(9)	Ca(1)–Sr–Ca(2^{iii})	108.50(6)
Sr–O(3a1)	2.608(6)	Ca(2)–O(11)	2.325(8)	Ca(2)–Sr–Ca(2^{iii})	102.94(6)
Sr–O(3a2)	2.681(8)	Ca(2)–O(21^{iv-a-c})	2.293(8)	Ca(2)–Sr–Ca(1^{iv-c})	111.35(6)
Sr–O(3b1)	2.611(6)	Ca(1)–O(3a1)	2.366(6)		
Sr–O(3b2)	3.835(8)	Ca(1)–O($3a2^{iii-b}$)	2.264(8)		
Sr–O(4a1)	3.258(11)	Ca(2)–O(3b1)	2.352(6)		
Sr–O(4a2)	2.652(6)	Ca(2)–O($3b2^{iv-a-c}$)	2.289(8)		
Sr–O(4b1)	2.891(8)	Ca(1)–O(4a1)	2.254(8)		
Sr–O(4b2)	2.690(7)	Ca(1)–O($4b2^{iii-b}$)	2.318(6)		
Sr–Ca(1)	3.809(2)	Ca(2)–O(4b1)	2.291(6)		
Sr–Ca(1^{iv-c})	3.997(2)	Ca(2)–O($4a2^{iv-a-c}$)	2.331(6)		

Symmetry code: (i) x, y, z
(ii) $\bar{x}, \bar{y}, 1/2 + z$
(iii) $1/2 - y, 1/2 + x, 1/4 + z$
(iv) $1/2 + y, 1/2 - x, 3/4 + z$

The translation oparation by a cell constant is denoted by $\pm a$, $\pm b$, $\pm c$.
For simplicity the code (i) is omitted throughout.

Table 58A-1-011. $Ca_2Sr(CH_3CH_2COO)_6$ (DSP). Distances between C atoms of the methyl groups at $T = -40$ °C [82Mis]. Symmetry code: see Table 58A-1-010. See also caption of Table 58A-1-005.

$CH_3(1^{iv})'$–$CH_3(2^{ii+a+b})'$	4.15(8) Å
–$CH_3(2^{ii+a+b})''$	4.25(12)
–$CH_3(3a^{ii+a+b})'$	2.79(14)
–$CH_3(3a^{ii+a+b})''$	4.31(11)
–$CH_3(3b^{+c})'$	4.01(18)
–$CH_3(4a^{ii+a+b})$	4.10(17)
$CH_3(1^{iv})''$–$CH_3(2^{ii+a+b})'$	3.77(10)
–$CH_3(2^{ii+a+b})''$	3.98(12)
–$CH_3(3a^{ii+a+b})'$	4.21(14)
–$CH_3(3b^{+c})'$	2.58(9)
–$CH_3(3b^{+c})''$	4.37(10)
–$CH_3(4b^{+c})$	4.15(9)
$CH_3(2)'$–$CH_3(3a^{iv+b-c})''$	3.92(6)
–$CH_3(3b^{iii+a})''$	3.53(7)
–$CH_3(4b^{ii+a+b})$	3.87(6)
$CH_3(2)''$–$CH_3(3a^{iv+b-c})''$	4.33(8)
–$CH_3(3b^{iii+a})''$	3.10(9)
–$CH_3(4a^{iv-c})$	3.63(8)
–$CH_3(4b^{ii+a+b})$	4.40(8)
$CH_3(3a)'$–$CH_3(3b^{ii+a+b})'$	4.12(11)
–$CH_3(3b^{ii+a+b})''$	4.38(12)
–$CH_3(4b^{iv})$	3.93(11)
$CH_3(3a)''$–$CH_3(3b^{ii+a+b})''$	4.36(6)
–$CH_3(4a^{iv-c})$	3.92(3)
–$CH_3(4b^{ii+a})$	4.01(4)
$CH_3(3b^{ii+a+b})'$–$CH_3(3a)'$	4.12(11)
–$CH_3(4a^{iv-c})$	4.15(4)
–$CH_3(4b^{iv})$	4.26(4)
$CH_3(3b^{ii+a+b})''$–$CH_3(3a)'$	4.38(12)
–$CH_3(4a^{+a})$	3.71(6)
–$CH_3(4a^{iv-c})$	4.46(6)
–$CH_3(4b^{iv})$	3.41(6)

Table 58A-1-012. $Ca_2Sr(CD_3CD_2COO)_6$ (DDSP). Interatomic distances and angles at $T = 294$ K [88Mac].

Interatomic distances [Å]		Bond angles [°]	
Sr–Ca	3.795(1)	O(11)–C(11)–O(11)^{iii}	121.6(6)
Sr–Ca"	3.969(1)	O(11)–C(11)–C(12)	119.4(6)
Sr–O(11)	2.735(4)	C(11)–C(12)–C(13)	124(1)
Sr–O(12)	2.778(4)	C(13)–C(12)–C(13)^{iii}	112(1)
Sr–O(31)	2.612(3)	O(21)–C(21)–O(21)^{iii}	117.4(6)
Sr–O(41)	3.075(4)	O(21)–C(21)–C(22)	111.5(8)
Sr–O(42)	2.670(3)	C(21)–C(22)–C(23)	121(2)
O(11)–C(11)	1.230(4)	O(31)–C(31)–O(32)	125.6(4)
C(11)–C(12)	1.503(10)	O(31)–C(31)–C(32)	116.3(4)
C(12)–C(13)	1.300(13)	O(32)–C(31)–C(32)	118.1(4)
O(21)–C(21)	1.225(8)	C(31)–C(32)–C(33)'	112(1)
C(21)–C(22)	1.520(12)	C(31)–C(32)–C(33)"	119.9(8)
C(22)–C(23)	1.21(3)	C(33)'–C(32)–C(33)"	64(1)
O(31)–C(31)	1.237(5)	O(41)–C(41)–O(42)	121.0(4)
O(32)–C(31)	1.221(5)	O(41)–C(41)–C(42)	122.0(5)
Ca–O(11)^{iii}	2.318(3)	O(42)–C(41)–C(42)	116.9(4)
Ca–O(21)$^{ii–b}$	2.297(4)	C(41)–C(42)–C(43)	112.7(6)
Ca–O(31)	2.355(4)		
Ca–O(32)$^{iv–b}$	2.265(4)		
Ca–O(41)	2.269(4)		
Ca–O(42)$^{ii–b}$	2.326(4)		
C(31)–C(32)	1.519(5)		
C(32)–C(33)'	1.38(2)		
C(32)–C(33)"	1.33(2)		
C(41)–C(41)	1.219(5)		
C(42)–C(41)	1.230(5)		
C(41)–C(42)	1.518(7)		
C(42)–C(43)	1.464(10)		

Symmetry code: (i) x, y, z; (ii) $1/2 - x$, $1/2 + y$, $1/4 - z$; (iii) y, x, $-z$; (iv) $1/2 - y$, $1/2 + x$, $1/4 + z$.

Table 58A-1-013. $Ca_2Sr(CD_3CD_2COO)_6$ (DDSP). Interatomic distances and angles at T = 258 K [88Mac].

Interatomic distances [Å]			
Sr–Ca(1)	3.795(1)	O(11)–C(11)	1.234(10)
Sr–Ca(1)$^{ii–c}$	3.987(1)	O(12)–C(11)	1.246(10)
Sr–Ca(2)	3.768(1)	C(11)–C(12)	1.505(11)
Sr–Ca(2)^{iii}	3.961(1)	C(12)–C(13)'	1.37(10)
Sr–O(11)	2.768(5)	C(12)–C(13)"	1.43(2)
Sr–O(12)	2.690(6)	O(21)–C(21)	1.227(8)
Sr–O(21)	2.739(5)	O(22)–C(21)	1.231(10)
Sr–O(22)	2.813(6)	C(21)–C(22)	1.516(13)
Sr–O(3a1)	2.608(5)	C(22)–C(23)'	1.17(3)
Sr–O(3b1)	2.603(4)	C(22)–C(23)"	1.12(4)
Sr–O(4a2)	2.648(5)	C(23)'–C(23)"	1.49(6)
Sr–O(4b1)	2.947(7)	O(3a1)–C(3a1)	1.252(8)
Sr–O(4b2)	2.686(5)	O(3a2)–C(3a1)	1.226(9)
Ca(1)–O(12)	2.324(6)	C(3a1)–C(3a2)	1.502(12)
Ca(1)–O(22)$^{iii–b}$	2.302(6)	C(3a2)–C(3a3)"	1.44(2)
Ca(1)–O(3a1)	2.362(5)	O(3b1)–C(3b1)	1.248(8)
Ca(1)–O(3a2)$^{iii–b}$	2.253(6)	O(3b2)–C(3b1)	1.240(9)
Ca(1)–O(4a1)	2.269(5)	C(3b1)–C(3b2)	1.516(12)
Ca(1)–O(4b2)$^{iii–b}$	2.320(5)	C(3b2)–C(3b3)'	1.41(2)
Ca(2)–O(11)	2.312(5)	C(3b2)–C(3a3)"	1.22(7)
Ca(2)–O(21)$^{ii–a–c}$	2.298(6)	C(3b3)'–C(3b3)"	1.52(7)
Ca(2)–O(3b1)	2.355(4)	O(4a1)–C(4a1)	1.227(8)
Ca(2)–O(3b2)$^{ii–b–c}$	2.272(4)	O(4a2)–C(4a1)	1.245(9)
Ca(2)–O(4a2)$^{ii–a–c}$	2.322(5)	C(4a1)–C(4a2)	1.502(12)
Ca(2)–O(4b1)	2.261(5)	C(4a2)–C(4a3)	1.46(2)
		O(4b1)–C(4b1)	1.243(8)
		O(4b2)–C(4b2)	1.236(9)
		C(4b1)–C(4b2)	1.527(13)
		O(4b2)–C(4b3)	1.48(2)

Bond angles [°]			
O(11)–C(11)–O(12)	121.2(7)	C(3a1)–C(3a2)–C(3a3)"	115(1)
O(11)–C(11)–C(12)	120.3(8)	O(3b1)–C(3b1)–O(3b2)	125.2(7)
O(12)–C(11)–C(12)	118.5(8)	O(3b2)–C(3b1)–C(4b2)	117.5(6)
C(11)–C(12)–C(13)'	122(2)	O(3b2)–C(3b1)–C(3b2)	117.2(6)
C(11)–C(12)–C(13)"	118.9(9)	C(3b1)–C(3b2)–C(3b3)'	112(1)
C(13)'–C(12)–C(13)"	118(4)	C(3b1)–C(3b2)–C(3b2)"	123(3)
O(21)–C(21)–O(22)	117.8(6)	C(3b3)'–C(3b2)–C(3b3)"	70(3)
O(21)–C(21)–C(22)	120.7(9)	O(4a1)–C(4a1)–O(4a2)	122.9(8)
O(22)–C(21)–C(22)	121(1)	O(4a1)–C(4a1)–C(4a2)	119.8(8)
C(21)–C(22)–C(23)'	131(3)	O(4a2)–C(4a1)–C(4a2)	117.3(6)
C(21)–C(22)–C(23)"	128(3)	C(4a1)–C(4a2)–C(4a3)	113(1)
C(23)'–C(22)–C(23)"	81(3)	O(4b1)–C(4b1)–C(4b2)	120.3(7)
O(3a1)–C(3a1)–O(3a2)	123.4(7)	O(4b1)–C(4b1)–C(4b2)	122.6(8)
O(3a1)–C(3a1)–C(3a2)	114.5(6)	C(4b2)–C(4b1)–C(4b2)	117.0(7)
O(3a2)–C(3a1)–C(3a2)	122.1(6)	C(4b1)–C(4b2)–C(4b3)	114(1)

Symmetry code: (i) x, y, z; (ii) 1/2 + y, 1/2 – x, 3/4 + z; (iii) 1/2 – y, 1/2 + x, 1/4 + z.

Table 58A-1-014. $Ca_2Sr(CH_3CH_2COO)_6$ (DSP). Occupancies of disordered atoms in phase II [82Mis]. T = –40 °C.

Atom	Difference Fourier map	Least-squares method
C(13)' : C(13)"	0.64 : 0.36	0.81(5) : 0.19
C(23)' : C(23)"	0.53 : 0.47	0.65(10) : 0.35
C(3a3)' : C(3a3)"	0.38 : 0.62	0.19(6) : 0.81
C(3a3)' : C(3b3)"	0.80 : 0.20	0.73(6) : 0.27

Table 58A-1-015. $Ca_2Sr(CD_3CD_2COO)_6$ (DDSP). Occupancies of the disordered C_β atoms (C(i3) for i = 1, 2, 3a and 3b) between the two occupied positions denoted by ' and " below Θ_f [88Mac].

Atom	258 K	184 K	120 K
C(13)"	0.14(8)	0	0
C(13)'	0.86(8)	1	1
C(23)"	0.46(1)	0.37(4)	0.36(5)
C(23)'	0.54(1)	0.63(4)	0.64(5)
C(3a3)"	0	0	0
C(3a3)'	1	1	1
C(3b3)'	0.84(5)	1	1
C(3b3)"	0.16(5)	0	0

Table 58A-1-016. $Ca_2Sr(CH_3CH_2COO)_6$ (DSP). Refractive indices [1882Fit].

λ [nm]	n_o	n_e
535	1.4897	1.4998
589	1.4871	1.4956
671	1.4839	1.4917

Table 58A-1-017. $Ca_2Sr(CH_3CH_2COO)_6$ (DSP). n_o vs. T [71Kin]. n_o: refractive index for ordinary light. λ = 589.3 nm.

T [°C]	n_o	T [°C]	n_o
70	1.4944	–50	1.5045
60	1.4952	–60	1.5054
50	1.4960	–70	1.5062
40	1.4968	–80	1.5069
30	1.4976	–90	1.5077
20	1.4984	–100	1.5084
10	1.4991	–110	1.5091
0	1.4999	–120	1.5098
–10	1.5009	–130	1.5103
–20	1.5019	–140	1.5107
–30	1.5028	–150	1.5113
–40	1.5037		

Table 58A-1-018. $Ca_2Sr(CH_3CH_2COO)_6$ (DSP). Internal mode frequencies [cm^{-1}] obtained from Raman spectra [89Yag]. γ: out-of-plane bend. δ: in-plane bend. ν: stretch. *w*: wag. *tw*: twist. Subscripts s and a denote symmetric and asymmetric vibrations, respectively. Spectral intensities of each mode are expressed by vs (very strong), s (strong), m (medium), w (weak) and vw (very weak).

Mode	*b*(*cc*)*a*	*b*(*cb*)*a*	*b*(*ab*)*a*	*b*(*aa*)c
γ(COO)	508 s	511 m	506 w	511 m
	607 w	601 w	596 w	602 w
δ(COO)	640 m	638 m	635 w	638 w
		820 m	820 w	
ν_s(CC)	896 s	895 m		893 s
	906 vs	904 s	901 w	905 s
		1008 m	1008 w	1008 m
w(CH_3)	1022 m	1021 s	1021 w	1022 m
	1085 s	1082 m	1084 w	1083 s
		1093 w		
	1250 w			
tw(CH_2)	1263 s	1260 m	1266 w	1261 w
w(CH_2)	1315 w	1311 w	1311 vw	1313 w
δ_s(CH_3)	1377 vw	1380 w		1380 vw
ν_s(COO)	1428 m	1426 s	1427 m	1429 m
		1448 s		
	1454 m		1451 m	1453 s
δ_a(CH_3)		1477 m	1470 w	
	1482 m			1480 m
ν_a(COO)	1557 vw	1569 w		
	1588 m	1586 w	1578 vw	1580 w
ν(C=O)		1625 w	1637 w	1638 w
	2740 vw	2735 vw		2738 vw
	2832 vw			
ν_s(CH_2)	2887 w	2886 w		2883 w
ν_s(CH_3)	2917 m	2916 w		2918 m
			2934 w	
ν_a(CH_2)	2949 m	2949 m		2948 w
ν_a(CH_3)	2980 w	2979 m	2978 m	2976 w

Table 58A-1-019. $Ca_2Sr(CD_3CD_2COO)_6$ (DDSP). Internal mode frequencies [cm^{-1}] obtained from Raman spectra [89Yag]. Notations are the same as in Table 58A-1-018.

Mode	*b*(*cc*)*a*	*b*(*cb*)*a*	*b*(*ab*)*a*	*b*(*aa*)*c*
γ(COO)	546 w	523 w	532 w	537 m
δ(COO)	607 s	606 m	605 w	607 m
	617 s			
	666 w	659 m	656 vw	660 w
		684 vw		685 vw
w(CD_3)	790 s	782 m	780 w	780 s
	807 w	803 vw		798 w
	850 vw			
				880 m
ν_s(CC)	889 m	889 m	890 vw	893 m
	900 m			
tw(CD_2)	930 s	922 m	922 m	924 s
w(CD_2)	959 m	952 w	954 w	953 m
	980 w	969 m	972 w	972 w
	1015 w			1009 w
δ_s(CD_3)	1046 w	1051 m	1052 m	1054 m
	1061 m	1058 s	1060 m	1062 m
	1071 m			
δ_a(CH_3)	1101 s	1095 w	1102 vw	1095 s
	1112 m			1106 w
	1160 w	1153 w		1155 vw
	1182 w	1180 w		1182 w
	1221 vw			
	1302 vw	1298 vw		
ν_s(COO)		1425 m	1423 vw	1428 m
		1447 m	1446 w	
	1466 m			1460 m
ν_a(COO)		1559 w	1571 vw	1567 w
	1585 m	1579 w		1578 w
		1600 vw		
		1618 w		
ν(C=O)	1635 vw		1630 w	1632 vw
	2034 vw	2023 vw		
ν_s(CD_2)	2086 s	2079 w		2080 w
				2114 w
	2121 w	2128 w	2134 vw	
ν_s(CD_3)	2148 vs	2142 w		2142 vs
ν_a(CD_2)	2189 s			2184 m
	2226 w	2217 m	2209 w	2218 w
ν_a(CD_3)	2241 s	2234 s	2234 s	2232 m

Table 58A-1-020. $Ca_2Sr(CH_3CH_2COO)_6$ (DSP), $Ca_2Ba(CH_3CH_2COO)_6$ (DBP), $Ca_2Pb(CH_3CH_2COO)_6$ (DLP). Spin Hamiltonian parameters of M^{2+} center [89Mis3].

	T [K]	g_{zz}	g_{xx}	b_2^0	b_2^2	b_4^0	b_4^2	b_4^4	A	B
DSP	295	2.1000	2.0868	0.141	–0.082	0.006	–0.060	–0.353	–0.278	–0.267
DBP	295	2.0090	2.0226	0.391	*	–0.001	*	*	–0.269	–0.285
DLP	373	2.006	2.004	0.697	–0.644	–0.009	–0.284	0.069	–0.270	–0.269

$\mathbf{H} = \mu_B (g_{zz} H_z S_z + g_{xx} H_x S_x) + \frac{1}{3} (b_2^0 O_2^0 + b_2^2 O_2^2) + \frac{1}{60} (b_4^0 O_4^0 + b_4^2 O_4^2 + b_4^4 O_4^4) + A S_z I_z + B(S_x I_x + S_y I_y)$.

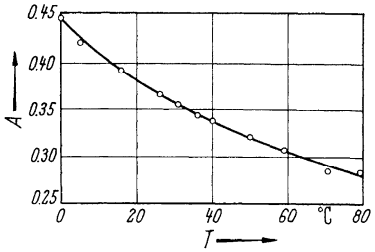

Fig. 58A-1-001. $Ca_2Sr(CH_3CH_2COO)_6$ (DSP). *A* vs. *T* [65Kob]. *A*: solubility in H_2O (solute/solvent in $kg \cdot kg^{-1}$).

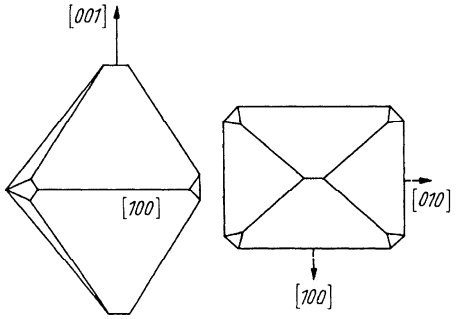

Fig. 58A-1-002. $Ca_2Sr(CH_3CH_2COO)_6$ (DSP). Crystal form [61Kob].

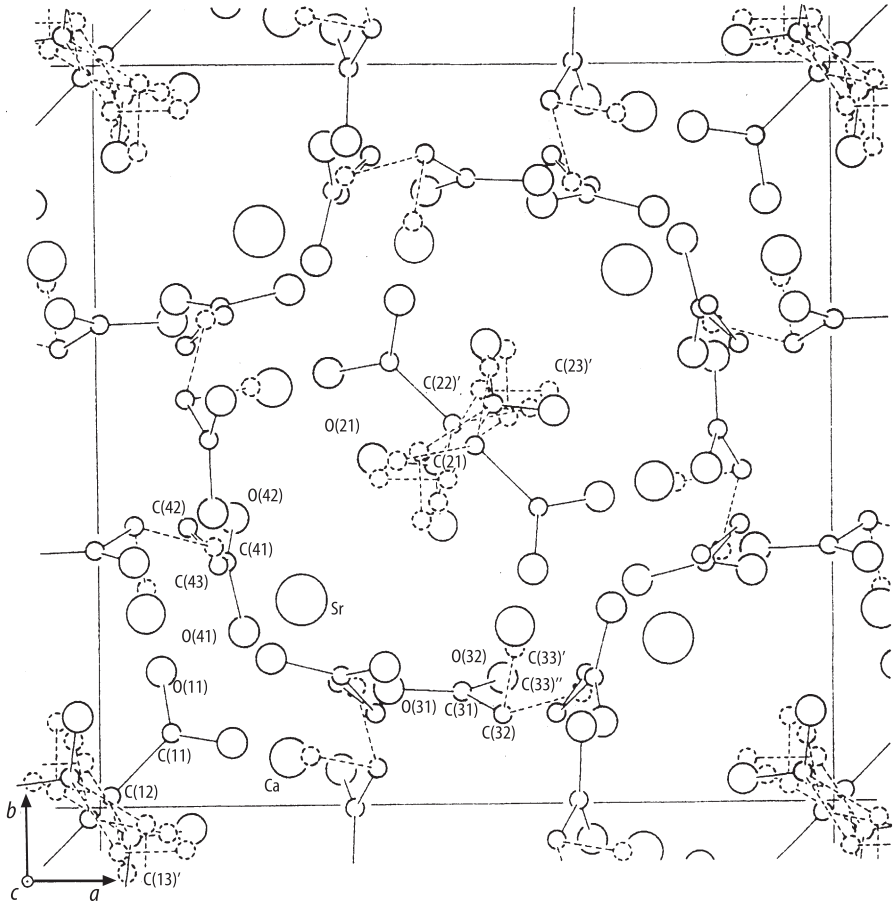

Fig. 58A-1-003. $Ca_2Sr(CH_3CH_2COO)_6$ (DSP). Structure of levorotatory crystal in phase I [81Ito]. Disordered atoms and their bonds are depicted by broken lines.

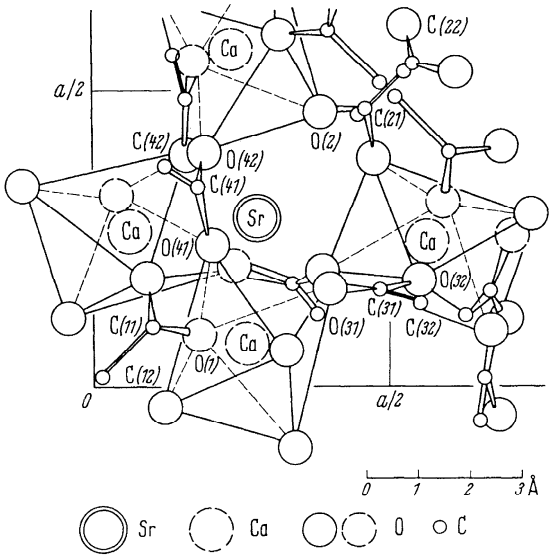

Fig. 58A-1-004. $Ca_2Sr(CH_3CH_2COO)_6$ (DSP). Structure of the phase I projected on (001) plane [67Mar]. Numerals at each of the atoms are the same as in Table 58A-1-002.

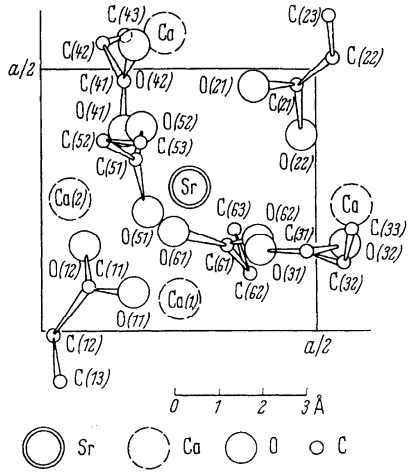

Fig. 58A-1-005. $Ca_2Sr(CH_3CH_2COO)_6$ (DSP). Structure of the phase II projected on (001) plane [67Miz]. Numerals at each of the atoms are the same as in Table 58A-1-003.

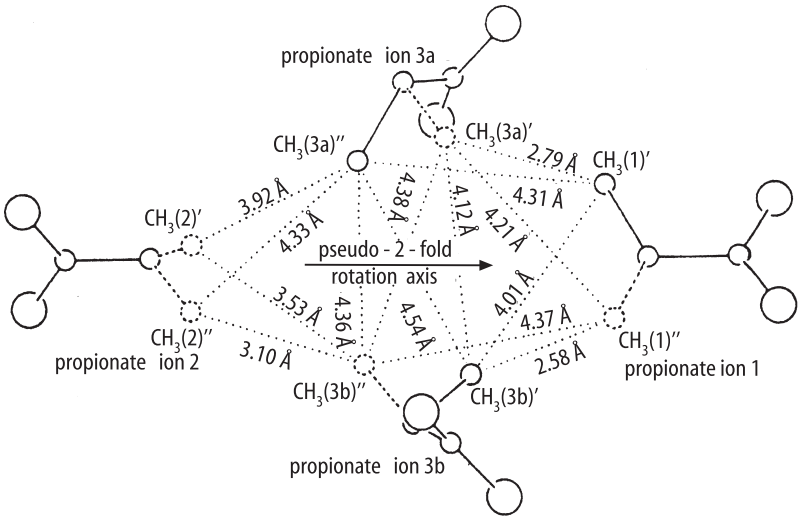

Fig. 58A-1-006. $Ca_2Sr(CH_3CH_2COO)_6$ (DSP). Positions and distances between methyl groups in the phase II (T = –40 °C) [82Mis].

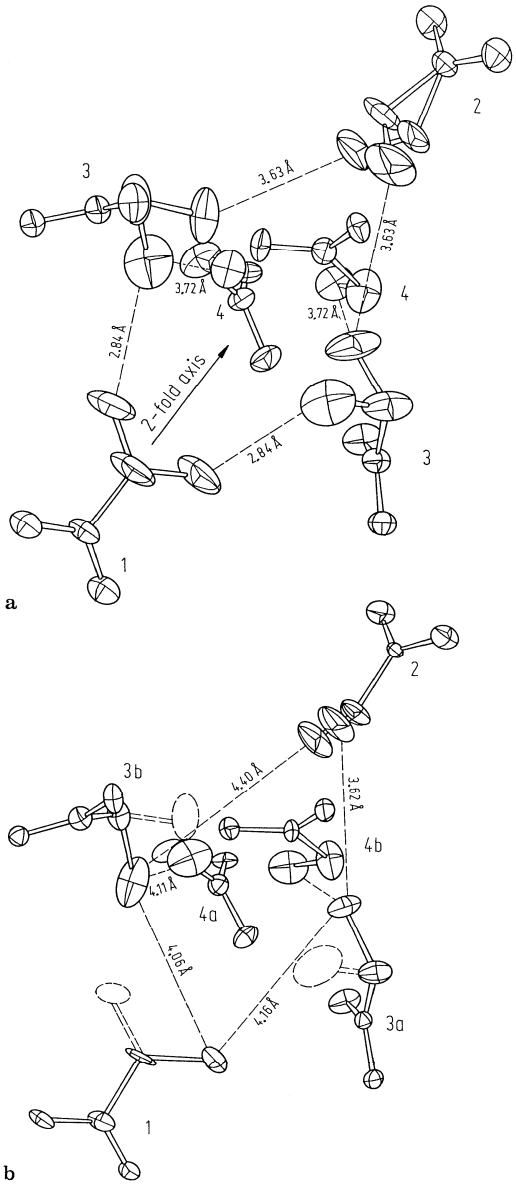

Fig. 58A-1-007. $Ca_2Sr(CD_3CD_2COO)_6$ (DDSP). Views of disordered propionate groups [88Mac]. (**a**) T = 294 K. See Table 58A-1-006 for the numbers of labelled atoms. (**b**) T = 258 K. See Table 58A-1-007 for the numbers of labelled atoms.

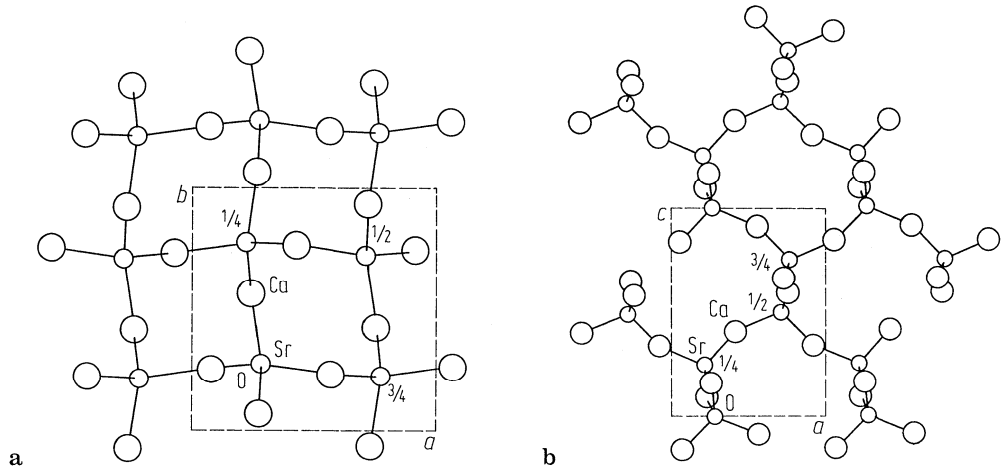

Fig. 58A-1-008. $Ca_2Sr(CD_3CD_2COO)_6$ (DDSP). Cation framework [88Mac]. Fractional values denote the heights of Sr atoms. The dashed lines denote the unit cell. (**a**) Projection on (001). (**b**) Projection on (010).

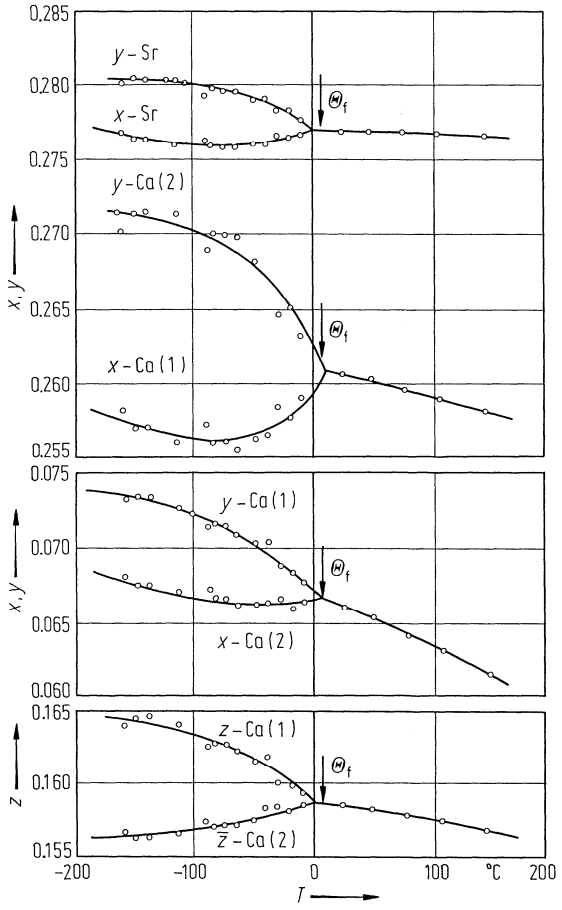

Fig. 58A-1-009. $Ca_2Sr(CH_3CH_2COO)_6$ (DSP). x, y, z vs. T [84Mis]. x, y, z: fractional coordinates of Ca and Sr atoms.

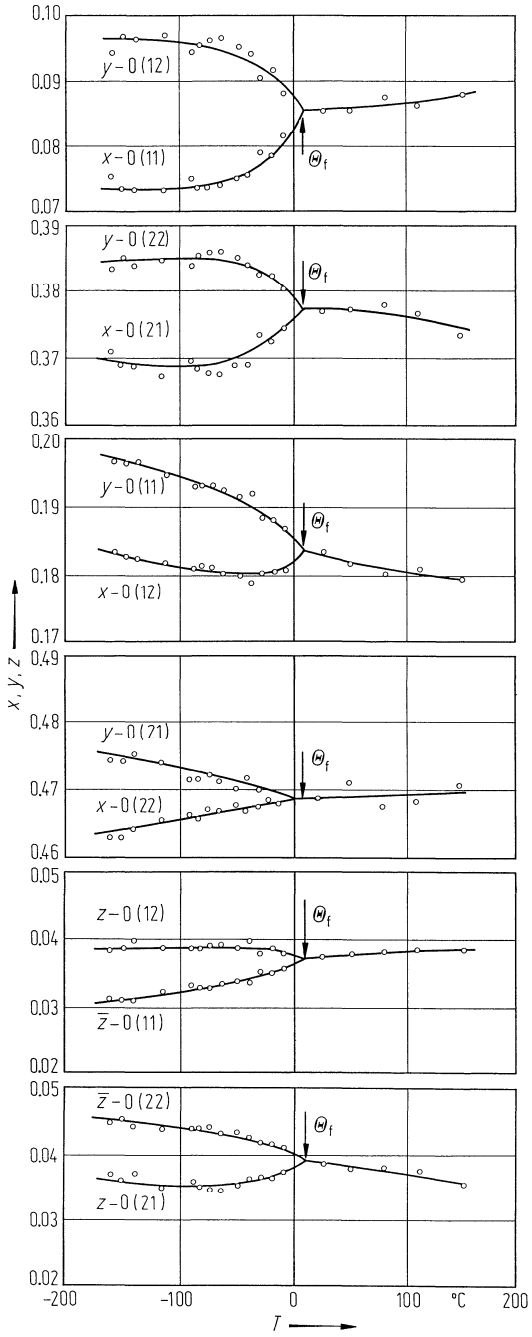

Fig. 58A-1-010. $Ca_2Sr(CH_3CH_2COO)_6$ (DSP). x, y, z vs. T [84Mis]. x, y, z: fractional coordinates of O(11), O(12), O(21), O(22) atoms.

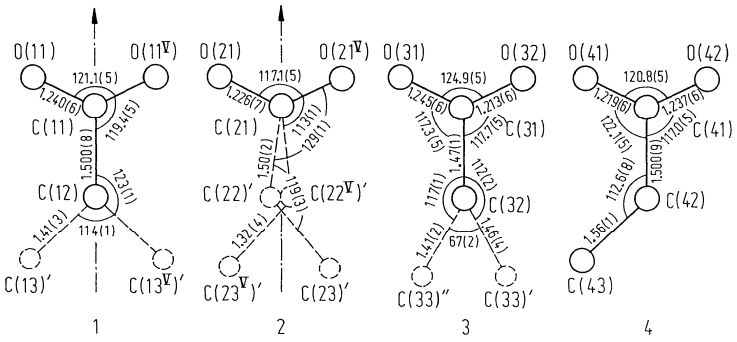

Fig. 58A-1-011. $Ca_2Sr(CH_3CH_2COO)_6$ (DSP). Bond lengths [Å] and angles [°] of propionate groups at 25 °C [81Ito]. Disordered atoms are depicted by dotted lines. Positions of individual atoms; see Table 58A-1-004.

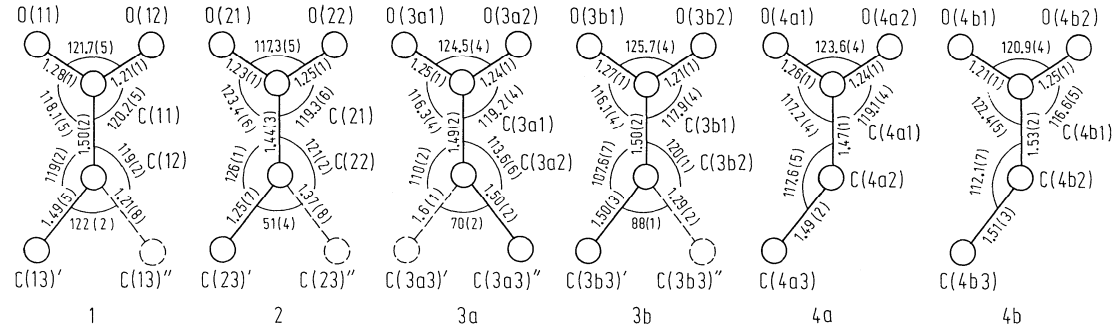

Fig. 58A-1-012. $Ca_2Sr(CH_3CH_2COO)_6$ (DSP). Bond lengths [Å] and angles [°] of propionate groups at –40 °C [82Mis]. Disordered atoms with smaller occupancies are depicted by dotted lines. Positions of individual atoms; see Table 58A-1-005.

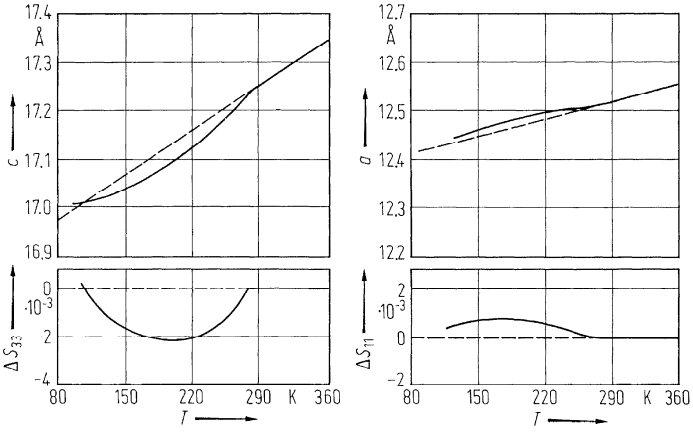

Fig. 58A-1-013. $Ca_2Sr(CH_3CH_2COO)_6$ (DSP). *a*, *c*, ΔS_{33}, ΔS_{11} vs. *T* [71Kob]. ΔS_{ij}: component of spontaneous strain.

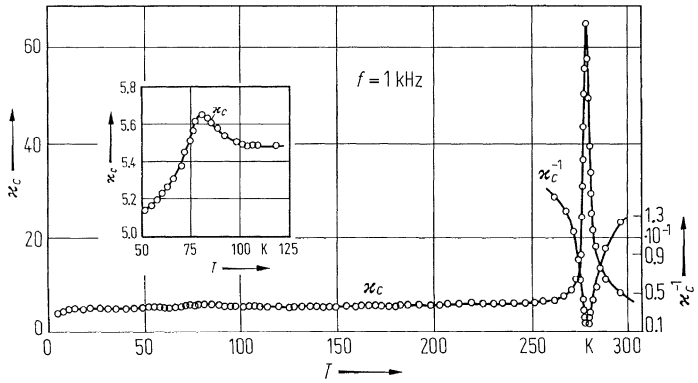

Fig. 58A-1-014. $Ca_2Sr(CH_3CH_2COO)_6$ (DSP). κ_c vs. T [75Var].

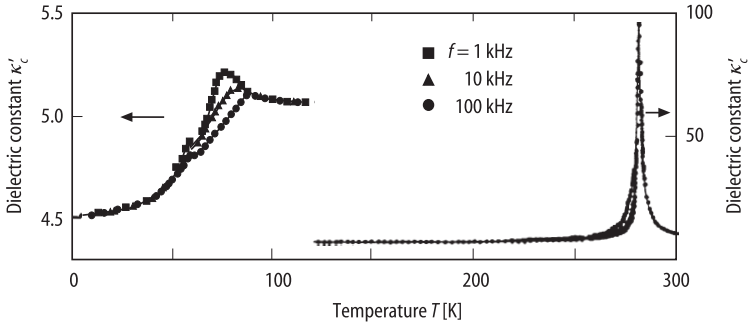

Fig. 58A-1-015. $Ca_2Sr(CH_3CH_2COO)_6$ (DSP). κ'_c vs. T [89Yan]. Parameter: f.

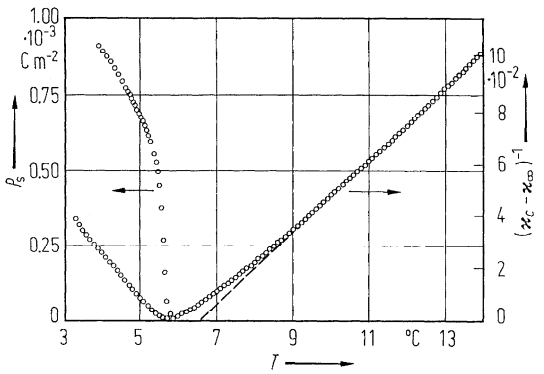

Fig. 58A-1-016. $Ca_2Sr(CH_3CH_2COO)_6$ (DSP). $(\kappa_c - \kappa_\infty)^{-1}$, P_s vs. T in the vicinity of Θ_f for the specimen annealed at 330 °C for 60 h [76Deg]. $\kappa_\infty = 4.0$: microwave dielectric constant.

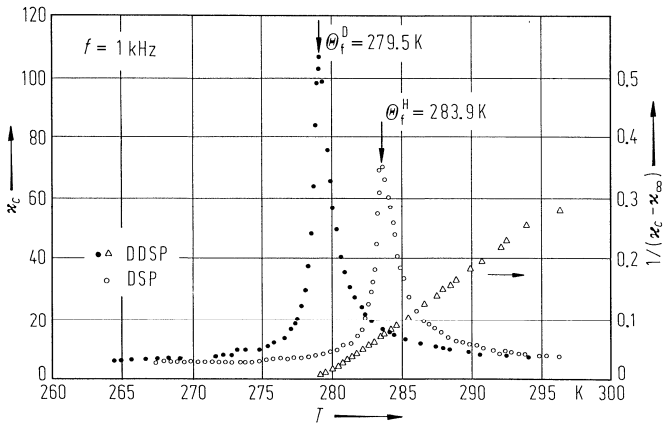

Fig. 58A-1-017. $Ca_2Sr(CH_3CH_2COO)_6$ (DSP), $Ca_2Sr(CD_3CD_2COO)_6$ (DDSP). κ_c, $(\kappa_c - \kappa_\infty)^{-1}$ vs. T [86Yag]. $\kappa_\infty = 3.7$. Θ_f^D, Θ_f^H : Curie temperatures of deuterated and nondeuterated crystals, respectively.

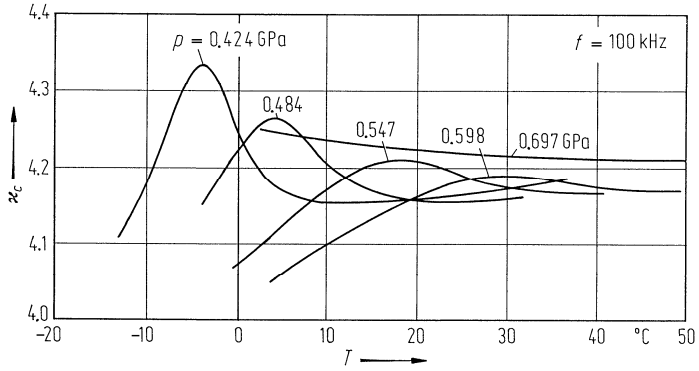

Fig. 58A-1-018. $Ca_2Sr(CH_3CH_2COO)_6$ (DSP). κ_c vs. T [84Ges]. Parameter: p.

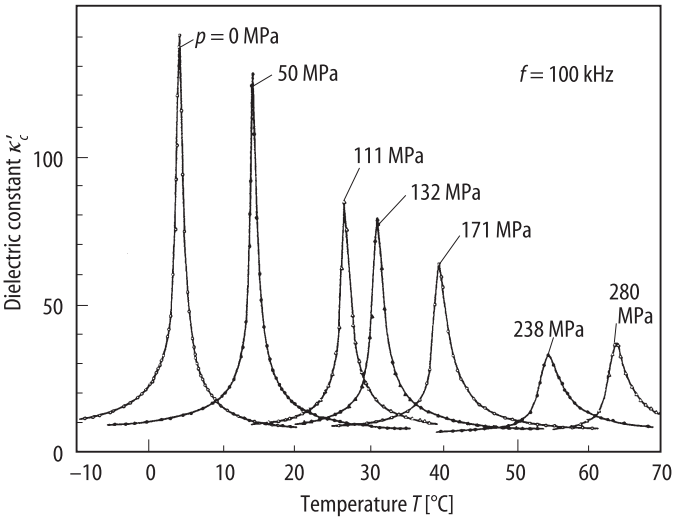

Fig. 58A-1-019. $Ca_2Sr(CD_3CD_2COO)_6$ (DDSP). κ_c' vs. T [90Ges]. Parameter: p.

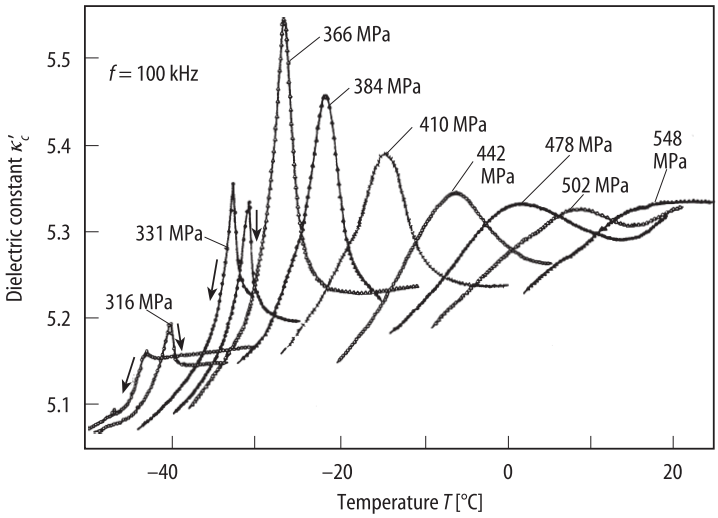

Fig. 58A-1-020. $Ca_2Sr(CD_3CD_2COO)_6$ (DDSP). κ_c' vs. T in the vicinity of Θ_{III-II} [90Ges]. Parameter: p.

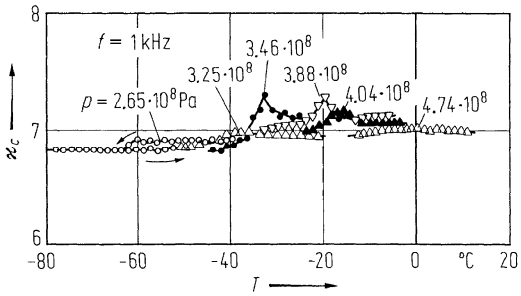

Fig. 58A-1-021. $Ca_2Sr(CH_3CH_2COO)_6$ (DSP). κ_c vs. T in the vicinity of II–III transition [75Ges]. Parameter: p.

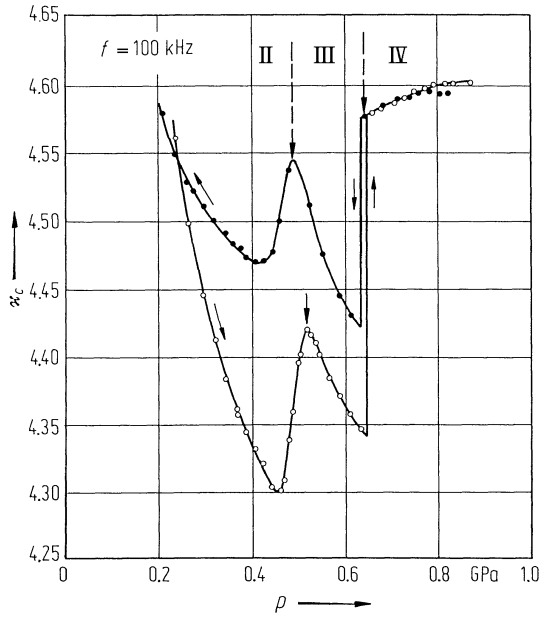

Fig. 58A-1-022. $Ca_2Sr(CH_3CH_2COO)_6$ (DSP). κ_c vs. p at 10.7 °C [84Ges].

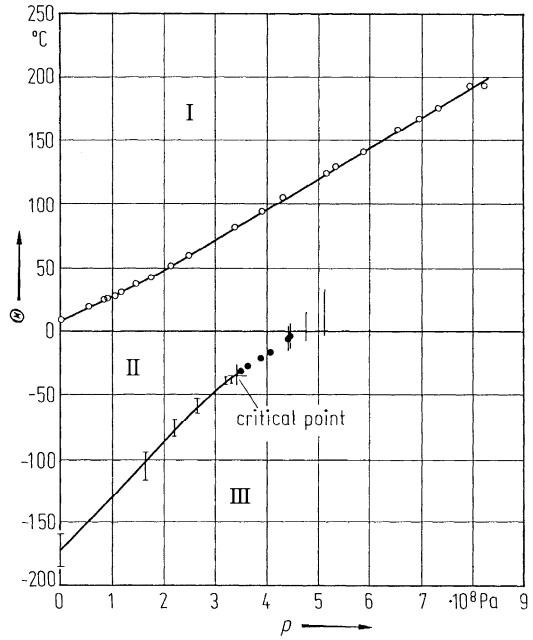

Fig. 58A-1-023. $Ca_2Sr(CH_3CH_2COO)_6$ (DSP). Θ vs. p [75Ges]. Full circles indicate the maximum of dielectric constant in the supercritical region. The first order III–II phase transition terminates at the critical point.

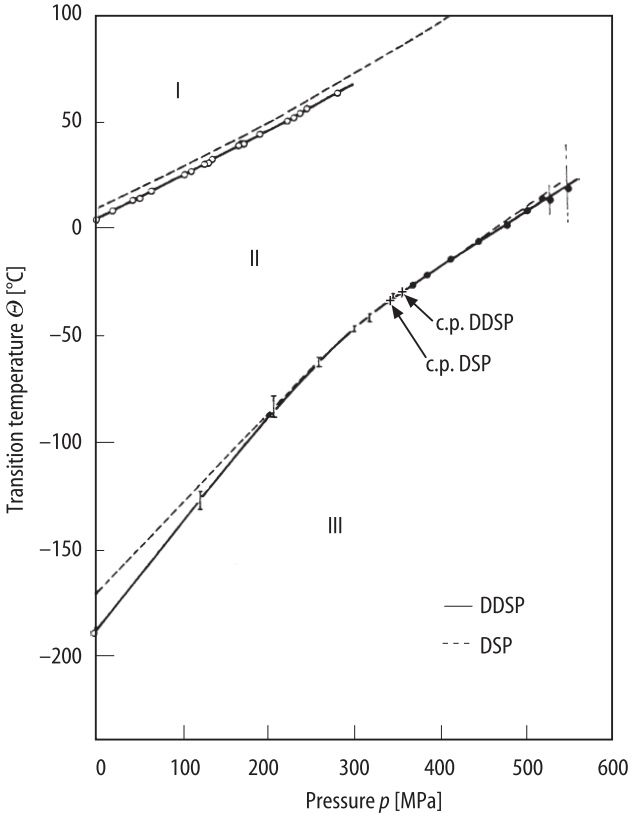

Fig. 58A-1-024. $Ca_2Sr(CH_3CH_2COO)_6$ (DSP), $Ca_2Sr(CD_3CD_2COO)_6$ (DDSP). Θ vs. p [90Ges]. Broken line: DSP. Full line: DDSP. c.p.: critical point of III–II transition.

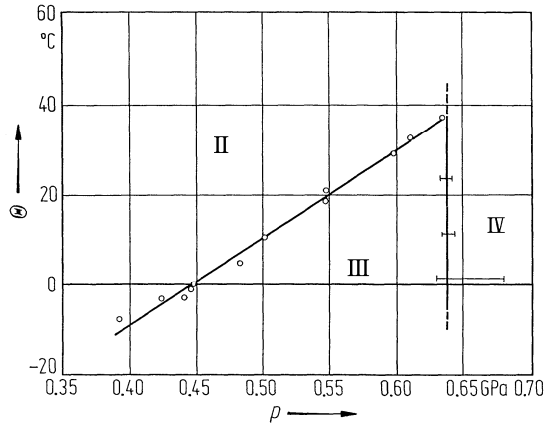

Fig. 58A-1-025. $Ca_2Sr(CH_3CH_2COO)_6$ (DSP). Θ vs. p [84Ges]. Pressure induced phase IV is shown.

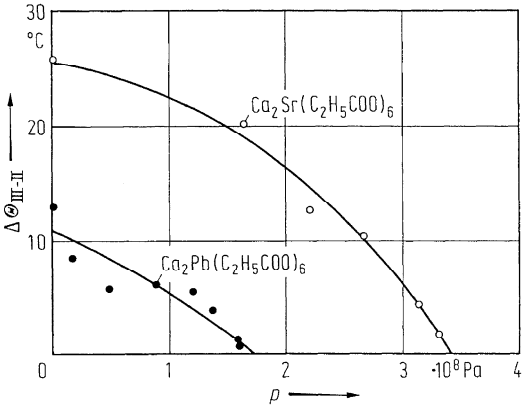

Fig. 58A-1-026. $Ca_2Sr(CH_3CH_2COO)_6$ (DSP), $Ca_2Pb(CH_3CH_2COO)_6$ (DLP). $\Delta\Theta_{III-II}$ vs. p [75Ges]. $\Delta\Theta_{III-II}$: thermal hysteresis of III–II transition determined by measurements of κ_c.

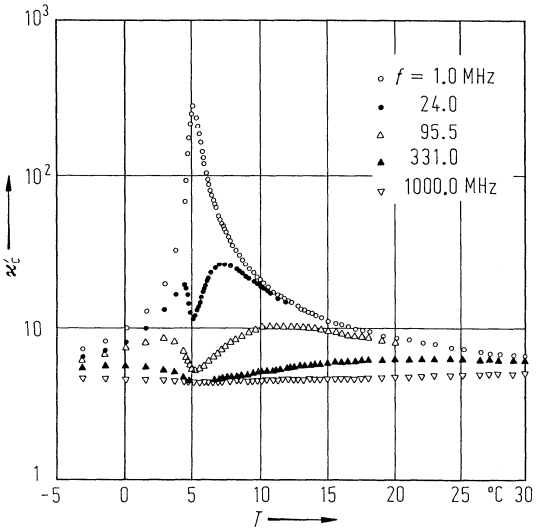

Fig. 58A-1-027. $Ca_2Sr(CH_3CH_2COO)_6$ (DSP). κ'_c vs. T [83Nak]. Parameter: f.

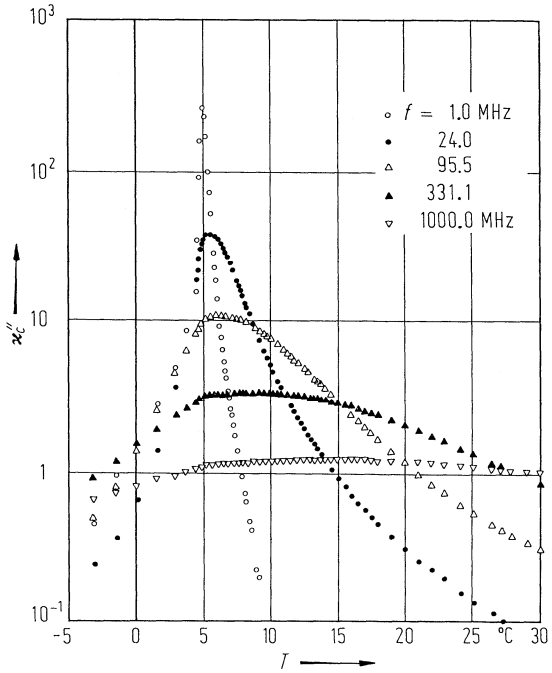

Fig. 58A-1-028. $Ca_2Sr(CH_3CH_2COO)_6$ (DSP). κ_c'' vs. T [83Nak]. Parameter: f.

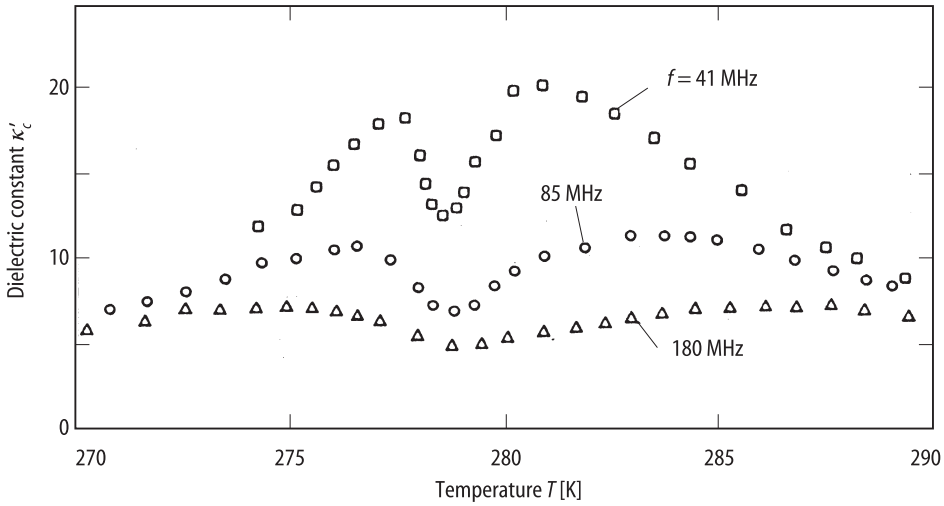

Fig. 58A-1-029. $Ca_2Sr(CD_3CD_2COO)_6$ (DDSP). κ_c' vs. T [92Ban]. Parameter: f.

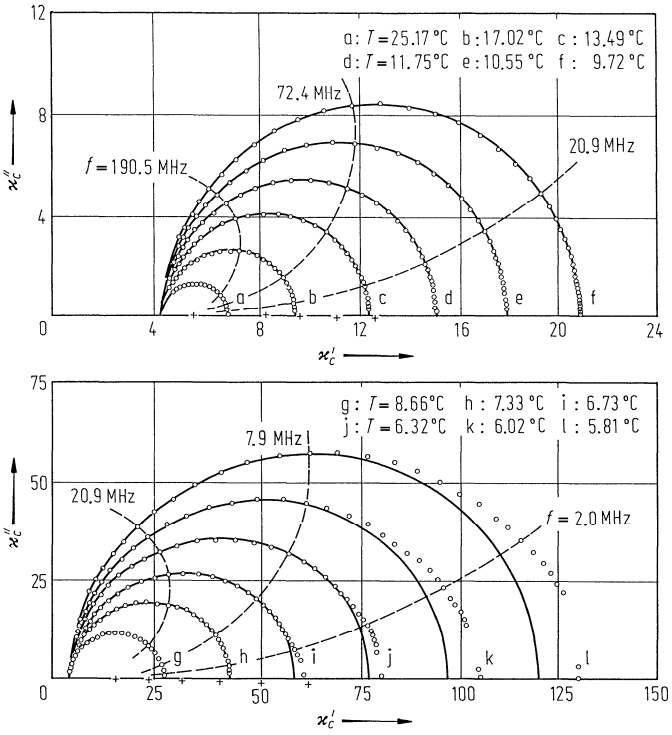

Fig. 58A-1-030. $Ca_2Sr(CH_3CH_2COO)_6$ (DSP). κ_c' vs. κ_c'' above Θ_f [83Nak]. Parameter: *T*.

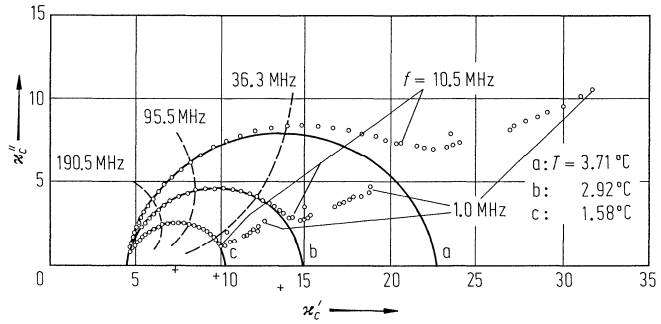

Fig. 58A-1-031. $Ca_2Sr(CH_3CH_2COO)_6$ (DSP). κ_c' vs. κ_c'' below Θ_f [83Nak]. Parameter: *T*.

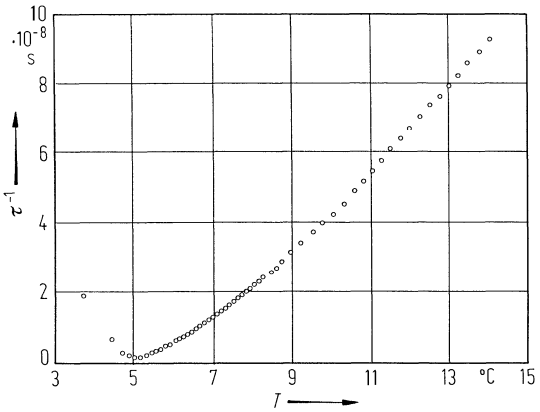

Fig. 58A-1-032. $Ca_2Sr(CH_3CH_2COO)_6$ (DSP). τ^{-1} vs. T [83Nak]. τ: relaxation time of dielectric dispersion.

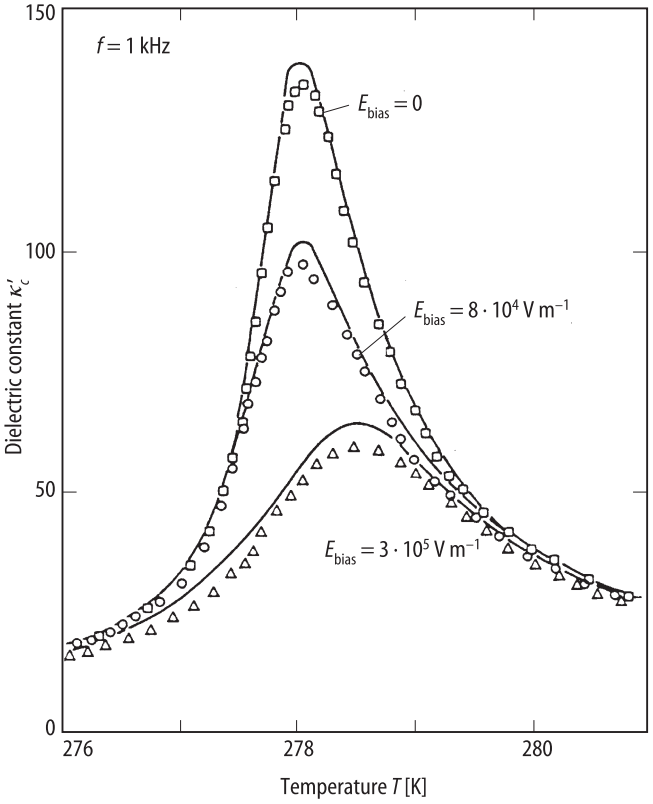

Fig. 58A-1-033. $Ca_2Sr(CD_3CD_2COO)_6$ (DDSP). κ_c' vs. T [92Ban]. Parameter: E_{bias}.

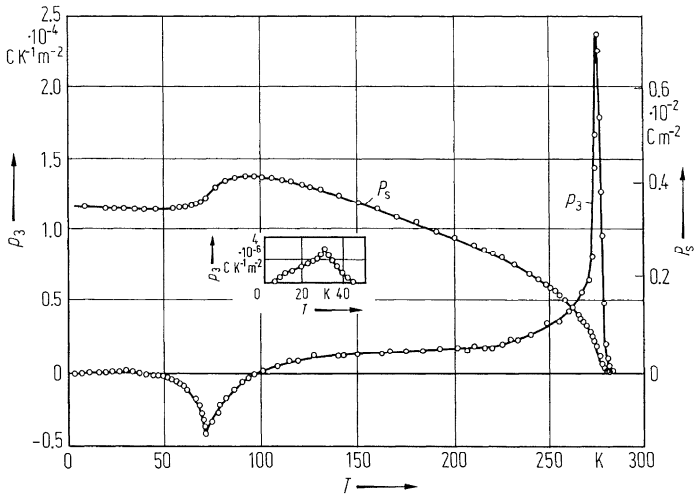

Fig. 58A-1-034. $Ca_2Sr(CH_3CH_2COO)_6$ (DSP). P_s, p_3 vs. T [75Var]. p_3: pyroelectric coefficient.

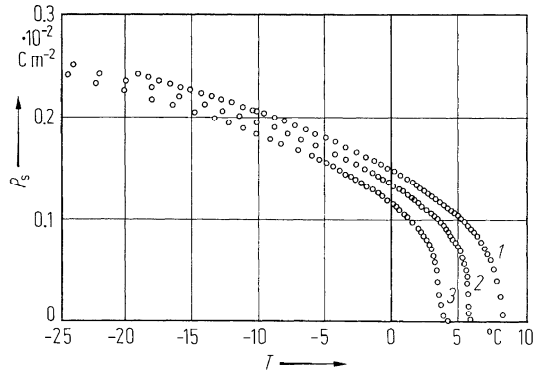

Fig. 58A-1-035. $Ca_2Sr(CH_3CH_2COO)_6$ (DSP). P_s vs. T for various specimens [76Deg]. Curve *1*: unannealed crystal, *2*: annealed at 330 °C for 60 h; *3*: annealed at 330 °C for 60 h and at 390 °C for 5 h.

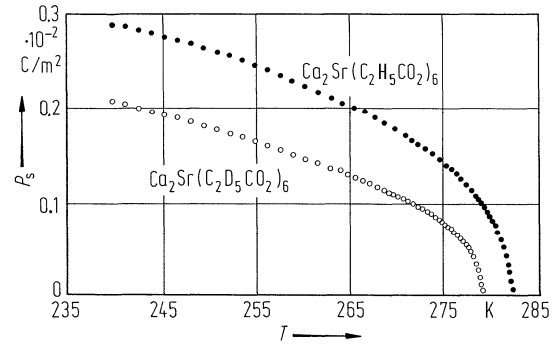

Fig. 58A-1-036. $Ca_2Sr(CH_3CH_2COO)_6$ (DSP), $Ca_2Sr(CD_3CD_2COO)_6$ (DDSP). P_s vs. T [87Yag2].

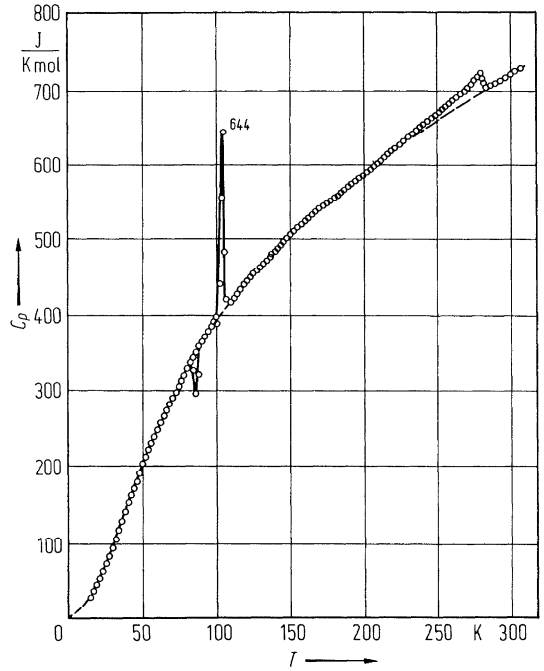

Fig. 58A-1-037. $Ca_2Sr(CH_3CH_2COO)_6$ (DSP). C_p vs. T [65Nak].

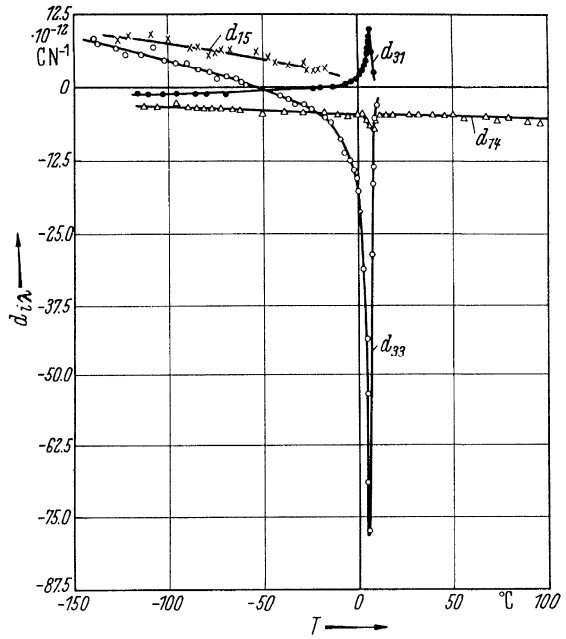

Fig. 58A-1-038. $Ca_2Sr(CH_3CH_2COO)_6$ (DSP). $d_{i\lambda}$ vs. T [66Ham].

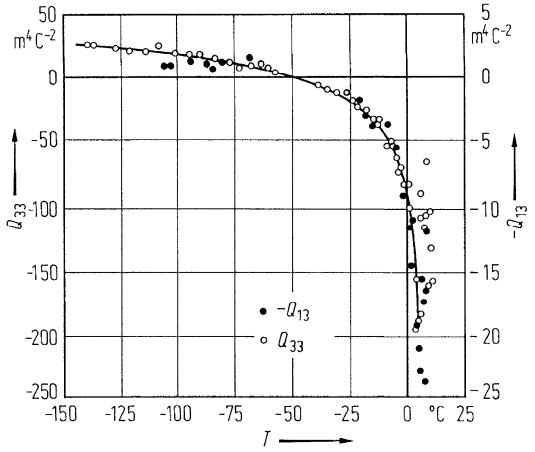

Fig. 58A-1-039. $Ca_2Sr(CH_3CH_2COO)_6$ (DSP). Q_{33}, Q_{13} vs. T [66Ham]. Q_{33}, Q_{13}: electrostrictive constants.

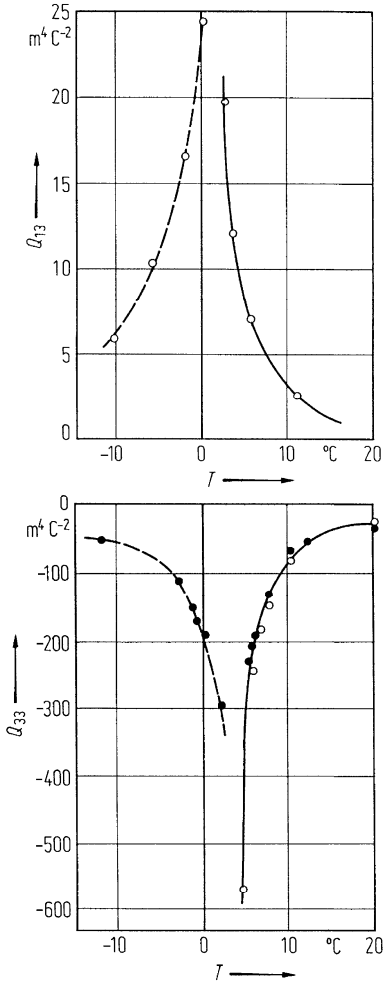

Fig. 58A-1-040. $Ca_2Sr(CH_3CH_2COO)_6$ (DSP). Q_{13}, Q_{33} vs. T [74Sch]. Values above Θ_f were determined from $Q_{\lambda 3} = S_\lambda / D_3^2$ and those below Θ_f by $Q_{\lambda 3} = d_{3\lambda}/2P_s$ ($\lambda = 1, 3$). Dashed line: [66Ham].

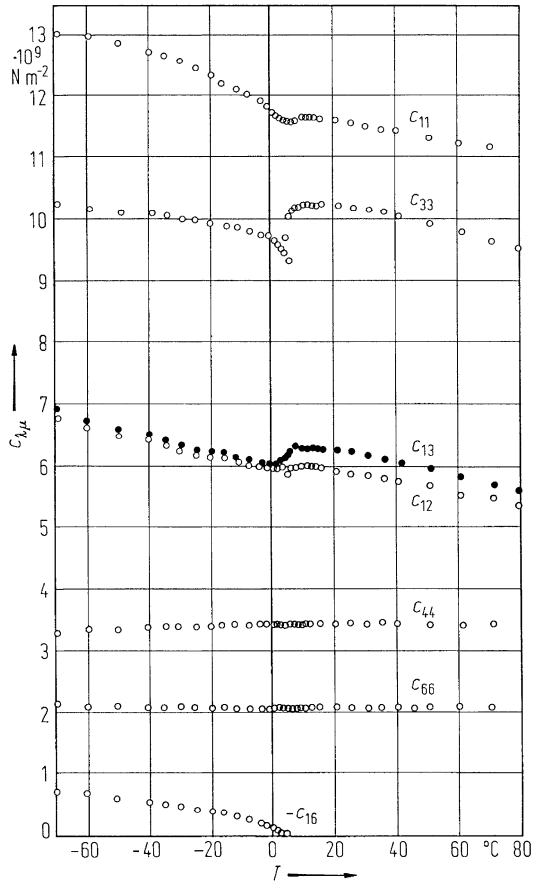

Fig. 58A-1-041. $Ca_2Sr(CH_3CH_2COO)_6$ (DSP). $c_{\lambda\mu}$ vs. T [79Kam2].

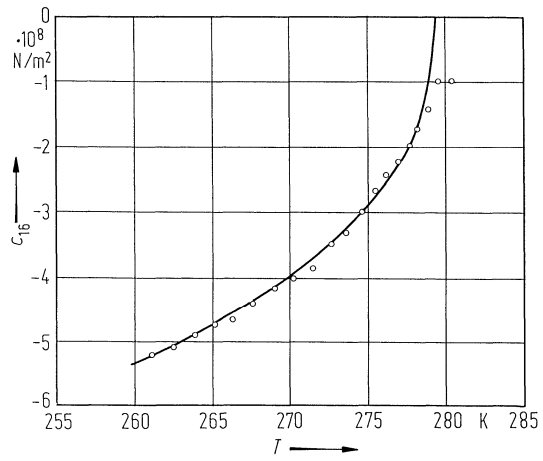

Fig. 58A-1-042. $Ca_2Sr(CD_3CD_2COO)_6$ (DDSP). c_{16} vs. T [87Yag1]. c_{16}: elastic stiffness determined from Brillouin scattering.

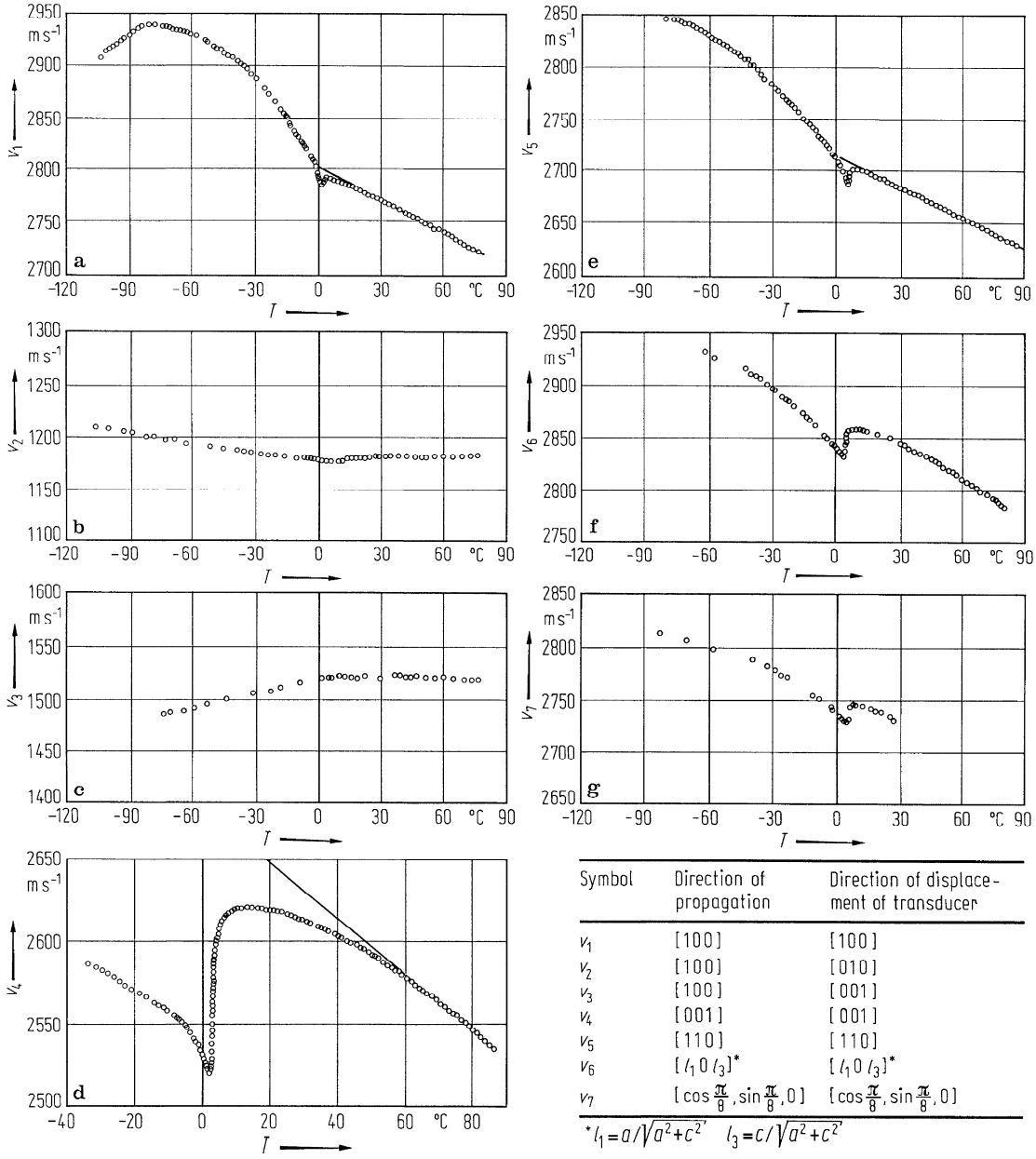

Symbol	Direction of propagation	Direction of displacement of transducer
v_1	[100]	[100]
v_2	[100]	[010]
v_3	[100]	[001]
v_4	[001]	[001]
v_5	[110]	[110]
v_6	$[l_1 0 l_3]^*$	$[l_1 0 l_3]^*$
v_7	$[\cos\frac{\pi}{8}, \sin\frac{\pi}{8}, 0]$	$[\cos\frac{\pi}{8}, \sin\frac{\pi}{8}, 0]$

$^*l_1 = a/\sqrt{a^2+c^2}$ $l_3 = c/\sqrt{a^2+c^2}$

Fig. 58A-1-043. $Ca_2Sr(CH_3CH_2COO)_6$ (DSP). v vs. T [79Kam2]. v: velocity of ultrasonic wave. f = 7 MHz.

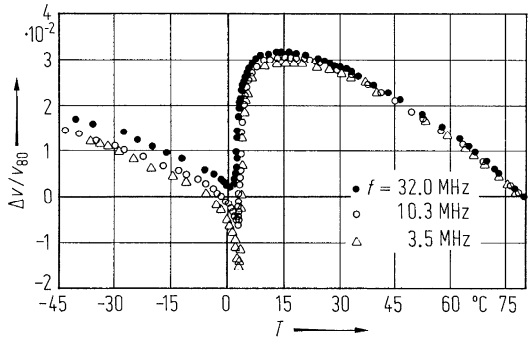

Fig. 58A-1-044. $Ca_2Sr(CH_3CH_2COO)_6$ (DSP). $\Delta v/v_{80}$ vs. T [74Kam]. Parameter: f. $\Delta v = v - v_{80}$. v: longitudinal sound wave velocity propagating along the [001] direction. v_{80}: v at 80 °C.

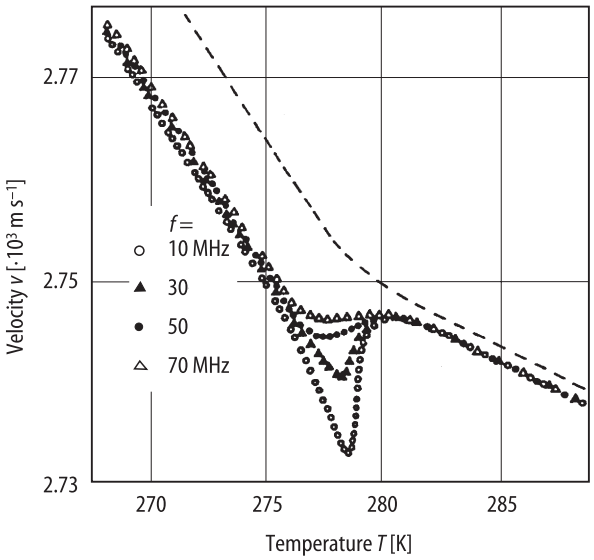

Fig. 58A-1-045. $Ca_2Sr(CD_3CD_2COO)_6$ (DDSP). v vs. T [94Val]. Parameter: f. v: velocity of longitudinal ultrasonic wave propagating along [100]. Dashed line: Brillouin data [87Yag1].

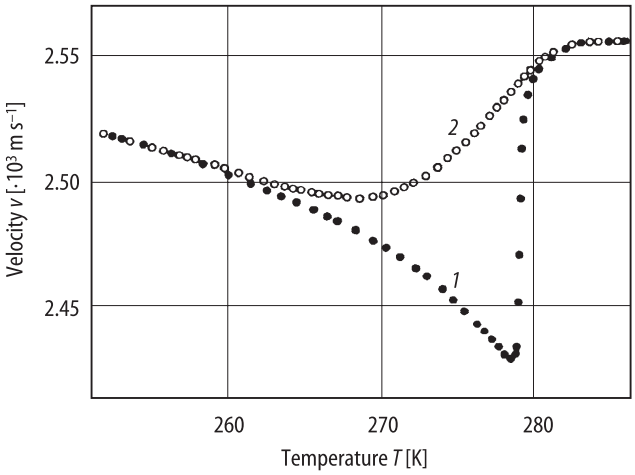

Fig. 58A-1-046. $Ca_2Sr(CD_3CD_2COO)_6$ (DDSP). v vs. T [94Val]. v: velocity of longitudinal ultrasonic wave propagating along [001]. f = 10 MHz. *1*: first cooling run. *2*: second cooling run.

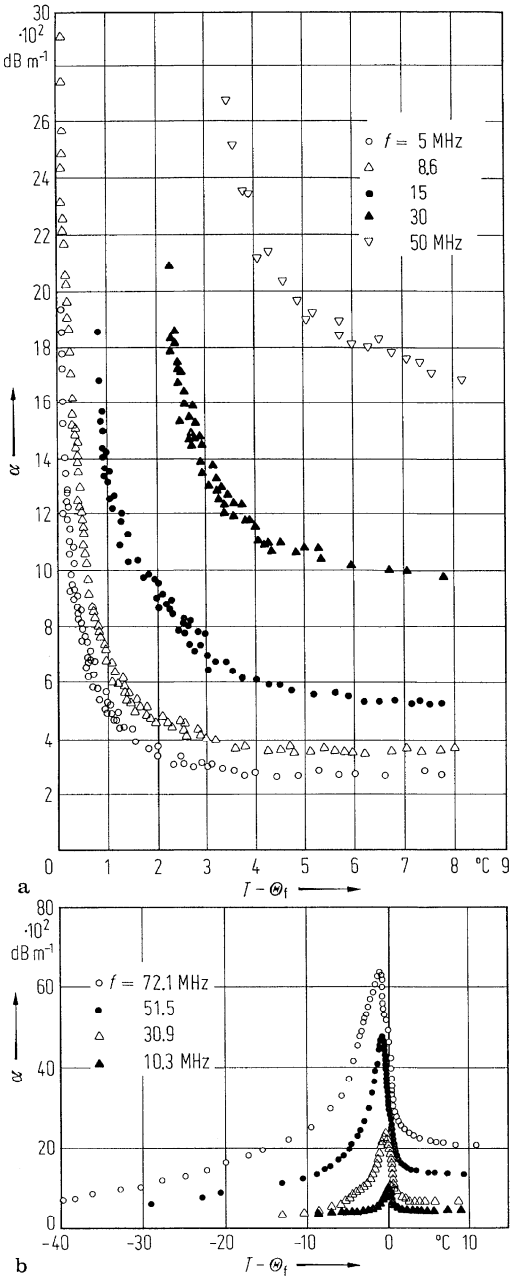

Fig. 58A-1-047. $Ca_2Sr(CH_3CH_2COO)_6$ (DSP). α vs. $T - \Theta_f$. α: attenuation coefficient of longitudinal ultrasonic wave. (**a**) for the wave propagating along the [001] direction [71Tod]. (**b**) for the wave propagating along the [110] direction [79Kam1]. Parameter: *f*.

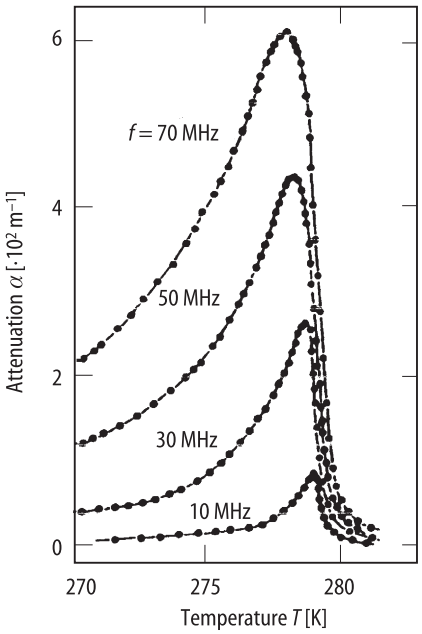

Fig. 58A-1-048. $Ca_2Sr(CD_3CD_2COO)_6$ (DDSP). α vs. T [94Val]. Parameter: f. α: attenuation of longitudinal ultrasonic wave propagating along [100].

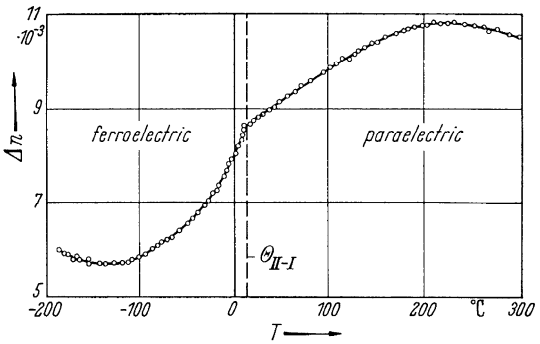

Fig. 58A-1-049. $Ca_2Sr(CH_3CH_2COO)_6$ (DSP). Δn vs. T [63Kob].

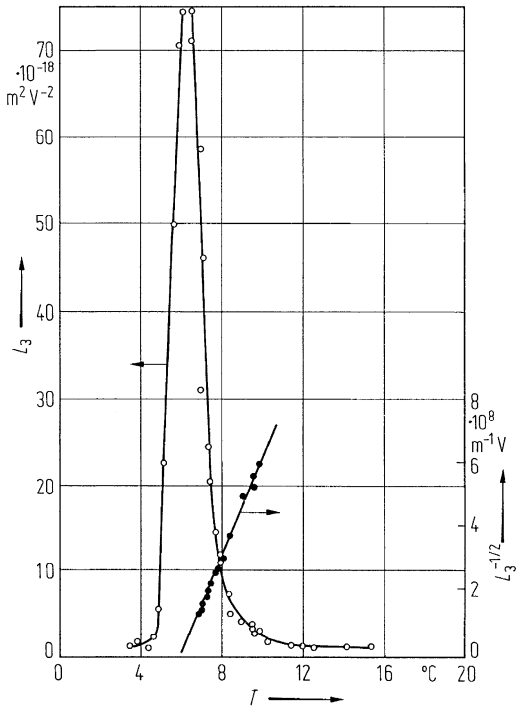

Fig. 58A-1-050. $Ca_2Sr(CH_3CH_2COO)_6$ (DSP). L_3 vs. T [75Ani]. $L_3 = n_1^3 L_{13} - n_3^3 L_{33}$. $L_{\lambda\mu}$: quadratic electrooptic constant. $\lambda = 633$ nm.

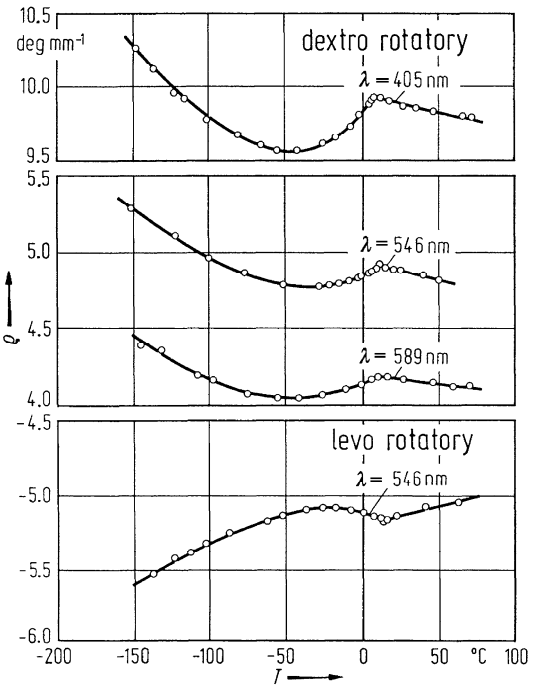

Fig. 58A-1-051. $Ca_2Sr(CH_3CH_2COO)_6$ (DSP). ρ vs. T [71Kob]. ρ: optical rotatory power.

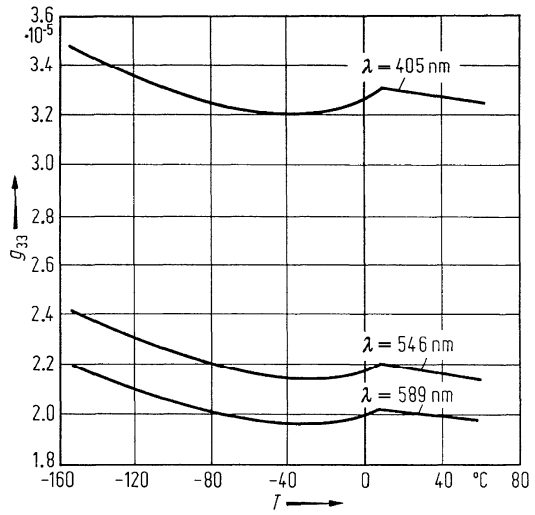

Fig. 58A-1-052. $Ca_2Sr(CH_3CH_2COO)_6$ (DSP). g_{33} vs. T [71Kob]. g_{33}: optical gyration tensor component.

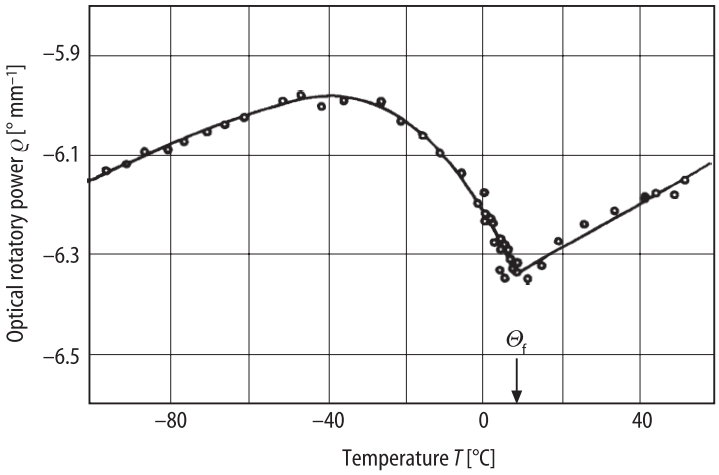

Fig. 58A-1-053. $Ca_2Sr(CD_3CD_2COO)_6$ (DDSP). ρ vs. T [87Ues]. ρ: optical rotatory power. $\lambda = 488$ nm.

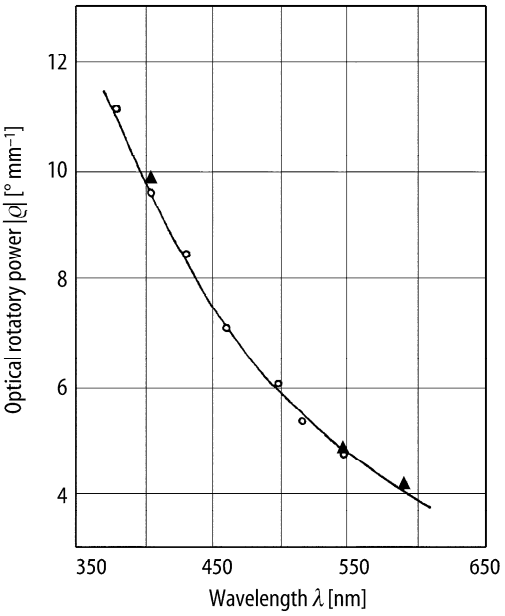

Fig. 58A-1-054. $Ca_2Sr(CH_3CH_2COO)_6$ (DSP), $Ca_2Sr(CD_3CD_2COO)_6$ (DDSP). $|\rho|$ vs. λ [87Ues]. ρ: optical rotatory power. T = 28.2 °C. Open circle: DSP; full triangle: DDSP.

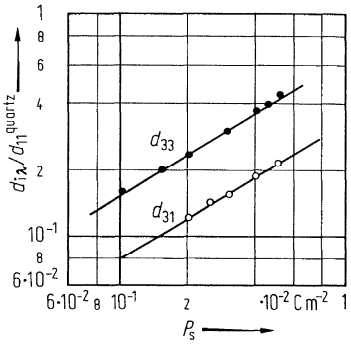

Fig. 58A-1-055. $Ca_2Sr(CH_3CH_2COO)_6$ (DSP). $d_{i\lambda} / d_{11}^{quartz}$ vs. P_s [74Ish]. $d_{i\lambda}$: nonlinear optical susceptibility. λ = 1.06 μm.

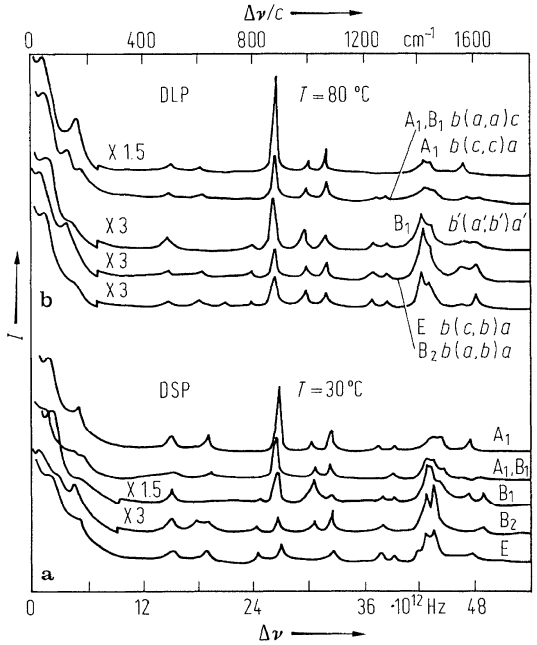

Fig. 58A-1-056. $Ca_2Sr(CH_3CH_2COO)_6$ (DSP), $Ca_2Pb(CH_3CH_2COO)_6$ (DLP). I vs. $\Delta\nu$ [76Nag]. I: Raman scattering intensity. (**a**) DSP at 30 °C. (**b**) DLP at 80 °C. a' and b' denote the Cartesian coordinate in which a and b axes are rotated by 45° around the z axis.

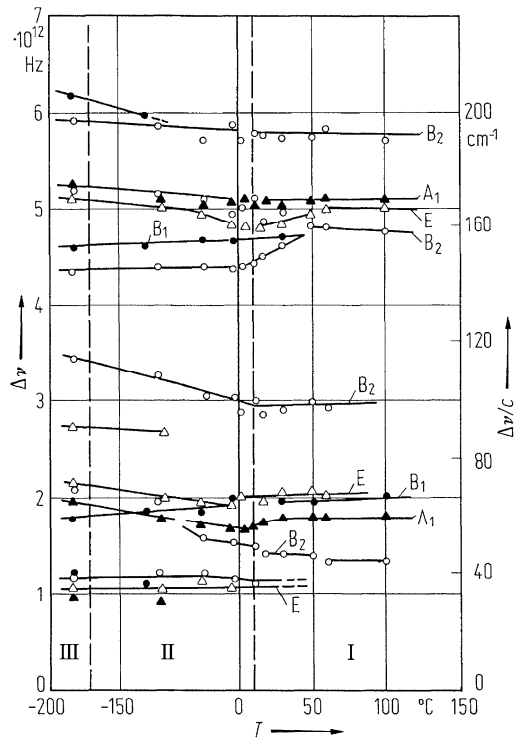

Fig. 58A-1-057. $Ca_2Sr(CH_3CH_2COO)_6$ (DSP). $\Delta\nu$ vs. T [76Nag]. $\Delta\nu$: Raman frequency shift. Successive phases are denoted as I, II, and III.

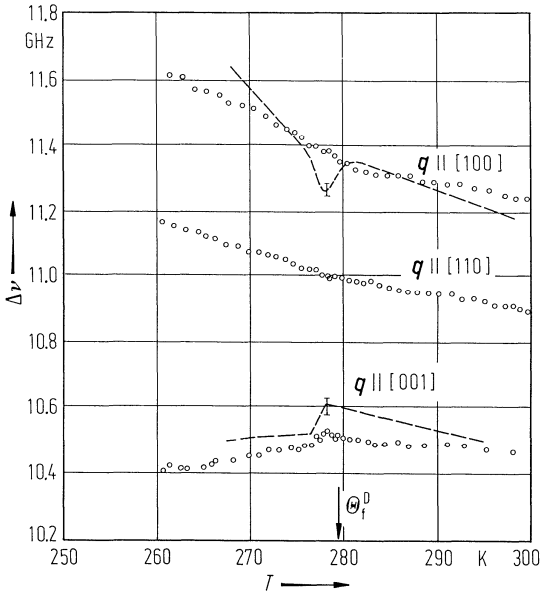

Fig. 58A-1-058. $Ca_2Sr(CD_3CD_2COO)_6$ (DDSP). $\Delta\nu$ vs. T [87Yag1]. Parameter: $\boldsymbol{q}$. $\Delta\nu$: Brillouin shift of longitudinal acoustic wave. $\boldsymbol{q}$: wave vector of the acoustic wave. Dashed lines are the data of $Ca_2Sr(CH_3CH_2COO)_6$ in [73Shi].

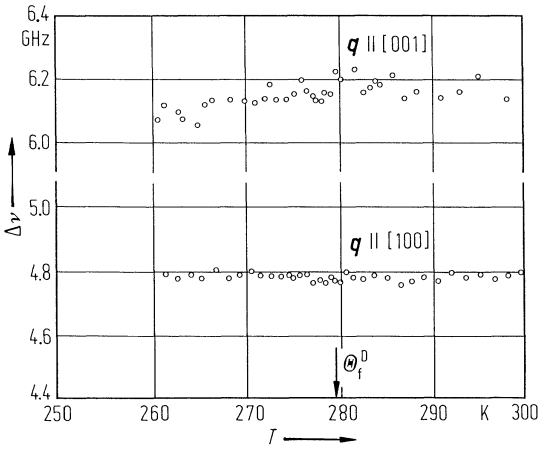

Fig. 58A-1-059. $Ca_2Sr(CD_3CD_2COO)_6$ (DDSP). $\Delta\nu$ vs. T [87Yag1]. Parameter: $\boldsymbol{q}$. $\Delta\nu$: Brillouin shift of transverse acoustic wave. $\boldsymbol{q}$: wave vector of the acoustic wave.

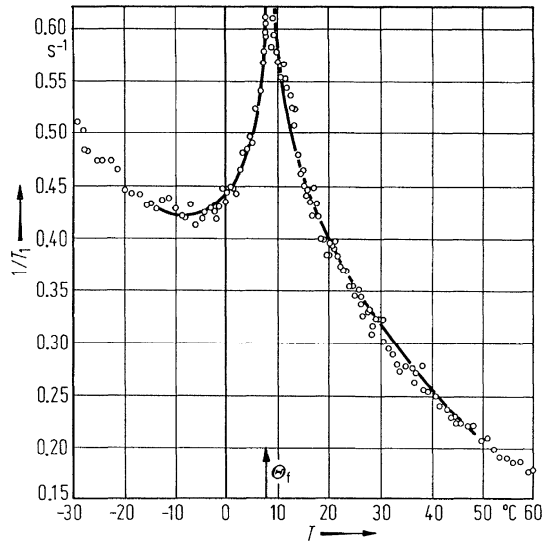

Fig. 58A-1-060. $Ca_2Sr(CH_3CH_2COO)_6$ (DSP). $1/T_1$ vs. T near Θ_f [73Hik]. T_1: proton spin-lattice relaxation time.

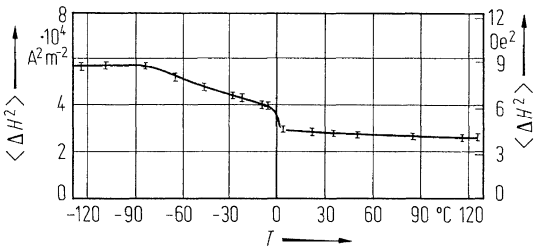

Fig. 58A-1-061. $Ca_2Sr(CH_3CH_2COO)_6$ (DSP). $\langle \Delta H^2 \rangle$ vs. T [67Ale]. $\langle \Delta H^2 \rangle$: second moment of proton.

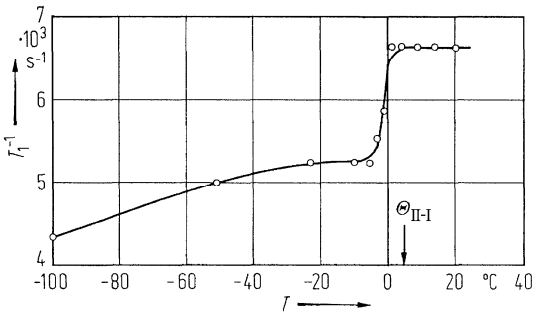

Fig. 58A-1-062. $Ca_2Sr(CH_3CH_2COO)_6$ (DSP). T_1^{-1} vs. T [74Vol]. T_1: electron spin-lattice relaxation time of radical produced by X-irradiation.

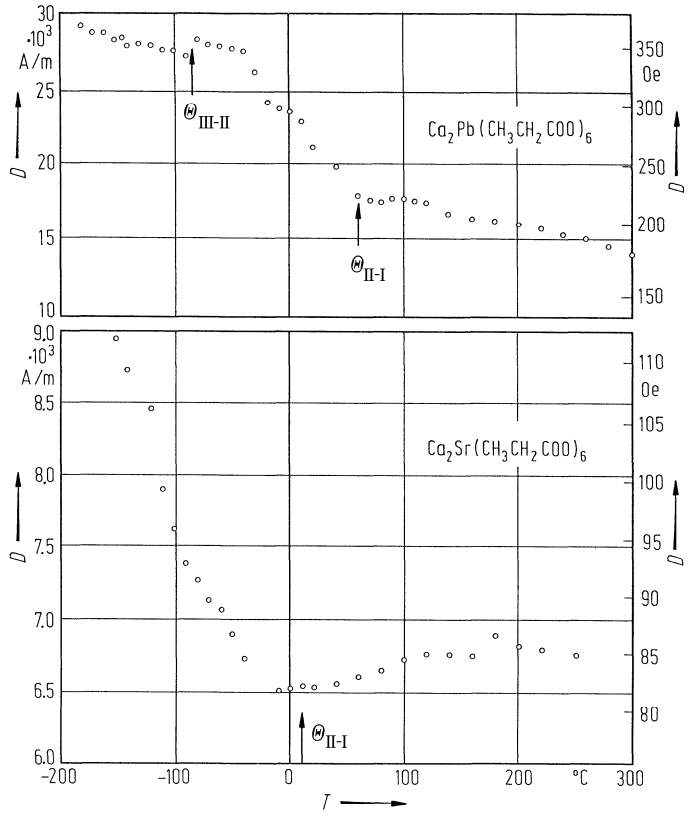

Fig. 58A-1-063. $Ca_2Sr(CH_3CH_2COO)_6$ (DSP), $Ca_2Pb(CH_3CH_2COO)_6$ (DLP). *D* vs. *T* [82Bha]. *D*: FS parameter of Mn^{2+} centers.

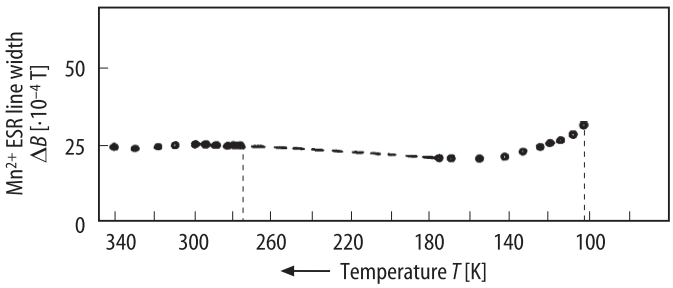

Fig. 58A-1-064. $Ca_2Sr(CH_3CH_2COO)_6$ (DSP). ΔB vs. *T* [89Mis3]. ΔB: Mn^{2+} ESR line width. *B* at 30° from [001] in (100) plane.

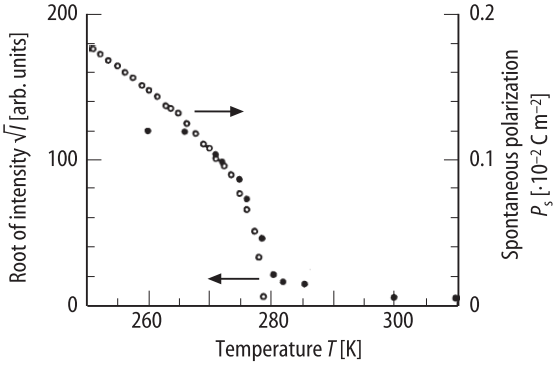

Fig. 58A-1-065. $Ca_2Sr(CD_3CD_2COO)_6$ (DDSP). $\sqrt{I}$, P_s vs. T [90Yag]. I: intensity of neutron (5, 0, 0) reflection which is forbidden in the paraelectric phase. Spontaneous polarization obtained by dielectric measurement is indicated for comparison. Full circle: $\sqrt{I}$. Open circle: P_s.

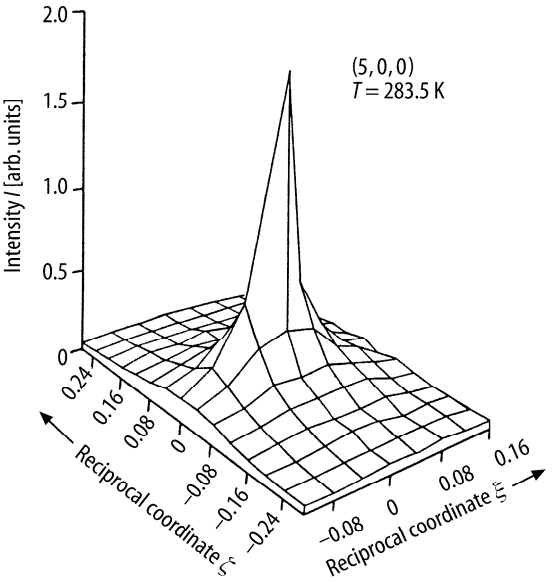

Fig. 58A-1-066. $Ca_2Sr(CD_3CD_2COO)_6$ (DDSP). I vs. ξ, ζ [90Yag]. I: critical neutron scattering intensity around (5, 0, 0) in reciprocal space. T = 283.5 K.

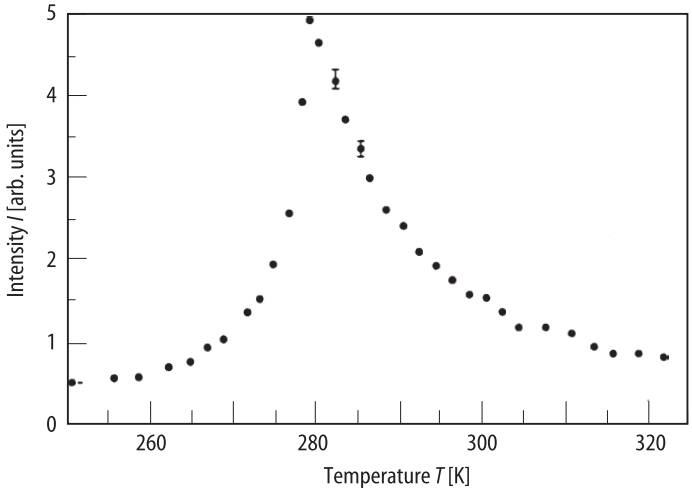

Fig. 58A-1-067. $Ca_2Sr(CD_3CD_2COO)_6$ (DDSP). I vs. T [90Yag]. I: neutron scattering intensity at (4.94, 0, 0) in reciprocal space.

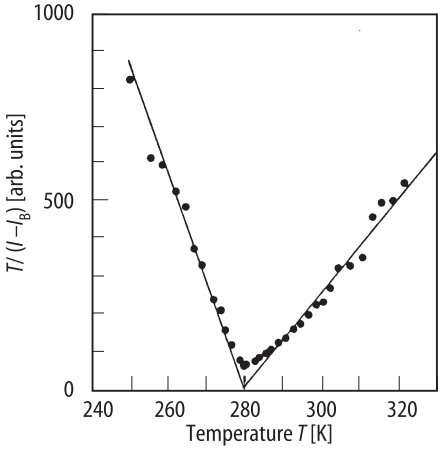

Fig. 58A-1-068. $Ca_2Sr(CD_3CD_2COO)_6$ (DDSP). $T/(I - I_B)$ vs. T [90Yag]. I: neutron scattering intensity at (4.94, 0, 0) in reciprocal space. I_B: background intensity of I.

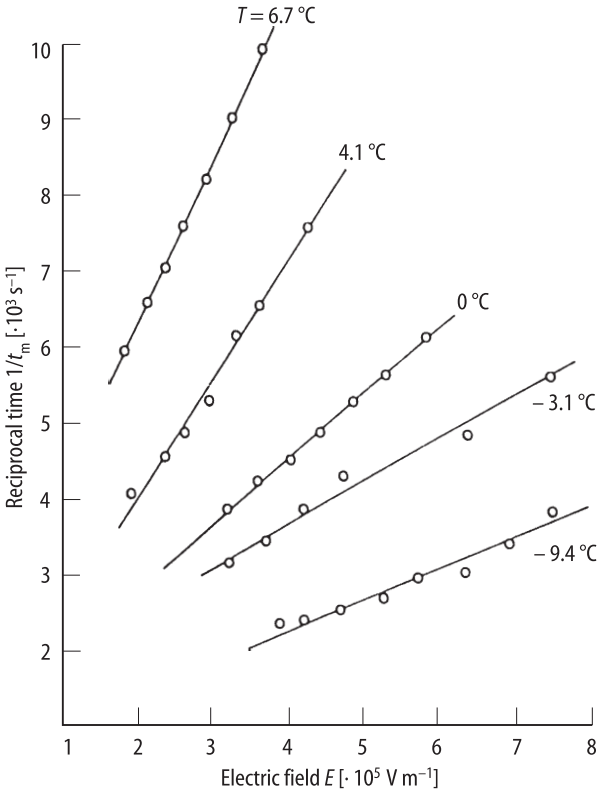

Fig. 58A-1-069. $Ca_2Sr(CH_3CH_2COO)_6$ (DSP). $1/t_m$ vs. E [82Rav]. Parameter: T. t_m: time corresponding to the maximum switching current.

References

1882Fit Fitz, A., Sanson, F.: Z. Kristallogr. **6** (1882) 67.
57Mat Matthias, B.T., Remeika, J.P.: Phys. Rev. **107** (1957) 1727.
61Kob Kobayashi, J., Yamada, N.: Bull. Sci. Eng. Res. Lab., Waseda Univ. **18** (1961) 35.
63Kob Kobayashi, J., Yamada, N.: J. Phys. Soc. Jpn. **18** (1963) 324.
65Kob Kobayashi, J.: Butsuri (Proc. Phys. Soc. Jpn.) **20** (1965) 203.
65Nak Nakamura, N., Suga, H., Chihara, H., Seki, S.: Bull. Chem. Soc. Jpn. **38** (1965) 1779.
66Ham Hamano, K.: Jpn. J. Appl. Phys. **5** (1966) 865.
67Ale Aleksandrova, I.P., Zherebtsova, L.I., Aleksandrov, K.S.: Kristallografiya **12** (1967) 894; Sov. Phys. Crystallogr. (English Transl.) **12** (1968) 780.
67Mar Maruyama, H., Tomiie, Y., Mizutani, I., Yamazaki, Y., Kobayashi, J.: J. Phys. Soc. Jpn. **23** (1967) 899.
67Miz Mizutani, I., Yamazaki, Y., Uesu, Y., Yamada, N., Kobayashi, J., Maruyama, H., Tomiie, Y.: J. Phys. Soc. Jpn. **23** (1967) 900.
67Moc Mochizuki, J., Futama, H.: J. Phys. Soc. Jpn. **23** (1967) 127.
67Nak Nakamura, E., Hosoya, M.: J. Phys. Soc. Jpn. **23** (1967) 844.
68Nak Nakamura, N., Suga, H., Chihara, H., Seki, S.: Bull. Chem. Soc. Jpn. **41** (1968) 291.
69Nak Nakamura, E., Nagai, T., Hashimoto, S., Hosoya, M.: J. Phys. Soc. Jpn. **26** (1969) 979.
71Kin Kind, R.: Phys. Kondens. Mater. **13** (1971) 217.
71Kob Kobayashi, J., Bouillot, J., Kinoshita, K.: Phys. Status Solidi (b) **47** (1971) 619.
71Shi Shiraki, H., Tatsuzaki, I., Yagi, T.: Phys. Status Solidi (a) **7** (1971) 227.
71Som Someya, T., Kobayashi, J.: Phys. Status Solidi (a) **4** (1971) K161.
71Tod Todo, I., Tatsuzaki, I.: J. Phys. Soc. Jpn. **31** (1971) 1479.
73Hik Hikita, T., Sakata, K., Tatsuzaki, I.: J. Phys. Soc. Jpn. **34** (1973) 1248.
73Ram Ramani, K., Srinivasan, R.: Indian J. Pure Appl. Phys. **11** (1973) 223.
73Shi Shimizu, H., Umeno, M., Wakita, K., Kameyama, H., Ishibashi, Y.: J. Phys. Soc. Jpn. **4** (1973) 983.
74Ish Ishidate, T., Inoue, K., Kameyama, H., Ishibashi, I.: J. Phys. Soc. Jpn. **37** (1974) 1176.
74Kam Kameyama, H., Ishibashi, Y., Takagi, Y.: J. Phys. Soc. Jpn. **36** (1974) 614.
74Sch Schmidt, G., Warnstorff, K.: Phys. Status Solidi (a) **24** (1974) K137.
74Vol Volkel, G., Bartuch, V., Brunner, W., Windsch, W.: Phys. Status Solidi (a) **25** (1974) 591.
75Ani Anistratov, A.T., Mel'nikova, S.V., Komogortsev, S.V.: Kristallografiya **20** (1975) 848; Sov. Phys. Crystallogr. (English Transl.) **20** (1976) 522.
75Ges Gesi, K., Ozawa, K.: J. Phys. Soc. Jpn. **39** (1975) 1026.
75Var Varikash, V.M., Drozhdin, S.N., Zarembovskaya, T.A., Novik, V.K.: Kristallografiya **20** (1975) 435; Sov. Phys. Crystallogr. (English Transl.) **20** (1975) 267.
76Deg Deguchi, K., Nakamura, E.: J. Phys. Soc. Jpn. **40** (1976) 478.
76Nag Nagae, Y., Wada, M., Ishibashi, Y., Takagi, Y.: J. Phys. Soc. Jpn. **41** (1976) 1659.
77Saw Sawada, A., Ishibashi, Y., Takagi, Y.: J. Phys. Soc. Jpn. **43** (1977) 195.
78Hos Hosokawa, T., Kobayashi, J., Uesu, Y., Miyazaki, H.: Ferroelectrics **20** (1978) 201.
79Kam1 Kameyama, H., Ishibashi, Y., Takagi, Y.: J. Phys. Soc. Jpn. **47** (1979) 559.
79Kam2 Kameyama, H., Ishibashi, Y., Takagi, Y.: J. Phys. Soc. Jpn. **46** (1979) 566.
81Bha Bhalla, A.S., Cross, L.E.: Ferroelectrics **38** (1981) 935.
81Gla Glazer, A.M., Stadnicka, K., Singh, S.: J. Phys. C **14** (1981) 5011.
81Ito Itoh, K., Mishima, N., Nakamura, E.: J. Phys. Soc. Jpn. **50** (1981) 2029.
82Bha Bhat, S.V., Dhar, V., Srinivasan, R.: Ferroelectrics **40** (1982) 49.
82Mis Mishima, N., Itoh, K., Nakamura, E.: J. Phys. Soc. Jpn. **51** (1982) 3958.
82Rav Ravi, R., Narayanan, P.S.: Ferroelectrics **45** (1982) 179.
83Nak Nakamura, E., Deguchi, K., Shimakawa, K., Fujimoto, Y.: J. Phys. Soc. Jpn. **52** (1983) 288.
83Shi Shimakawa, K., Deguchi, K., Nakamura, E., Motegi, H., Mishima, N.: J. Phys. Soc. Jpn. **52** (1983) 2246.
84Ges Gesi, K.: J. Phys. Soc. Jpn. **53** (1984) 1602.
84Mis Mishima, N.: J. Phys. Soc. Jpn. **53** (1984) 1062.

86Yag Yagi, T.: J. Phys. Soc. Jpn. **55** (1986) 1822.
87Ues Uesu, Y., Sekiguchi, M., Inoue, M., Yagi, T.: J. Phys. C **20** (1987) 5877.
87Yag1 Yagi, T., Fujisaki, H., Sakai, A.: J. Phys. Soc. Jpn. **56** (1987) 2535.
87Yag2 Yagi, T., Fujisaki, H., Sakai, A.: J. Phys. Soc. Jpn. **56** (1987) 1649.
88Cha Chaudhari, R.M., Krishnakumar, R.: Bull. Mater. Sci. **11** (1988) 43.
88Mac Machida, M., Yagi, T.: J. Phys. Soc. Jpn. **57** (1988) 1291.
89Mis1 Misra, S.K., Jerzak, S.: Solid State Commun. **69** (1989) 325.
89Mis2 Misra, S.K., Jerzak, S.: Phys. Rev. B **39** (1989) 2041.
89Mis3 Misra, S.K., Jerzak, S.: Acta Phys. Pol. A **76** (1989) 943.
89Yag Yagi, T., Sasaki, A.: Ferroelectrics **89** (1989) 61.
89Yan Yano, S., Sahara, M., Iwauchi, K.: J. Phys. Soc. Jpn. **58** (1989) 577.
90Ges Gesi, K., Yagi, T.: J. Phys. Soc. Jpn. **59** (1990) 4155.
90Yag Yagi, T., Chou, H., Shapiro, S.M.: J. Phys. Soc. Jpn. **59** (1990) 2387.
92Ban Banys, J., Grigas, J., Lapinskas, S., Lileikis, Z., Yagi, T.: Phys. Status Solidi (a) **132** (1992) 191.
94Val Valevicius, V., Samulionis, V., Banys, J., Grigas, J., Yagi, T.: Ferroelectrics **156** (1994) 365.

No. 58A-2 $Ca_2Ba(CH_3CH_2COO)_6$, Dicalcium barium propionate (DBP)

(M = 655.91)

1a Pressure-induced ferroelectricity in DBP was reported by Sawada et al. in 1979. 79Saw

b

phase	III [b])	II [a])	I [a])
crystal system			cubic [c])
space group			$Fd3m-O_h^{7}$ [c])
Θ [K]	204 [b])	266.9 [a])	

[a]) 55Sek
[b]) 68Nak
[c]) 35Nit

Under hydrostatic pressure of $p = 0.90 \cdot 10^8$ Pa:

phase	V	IV
state	F	P
crystal system	tetragonal	tetragonal
space group	$P4_1-C_4^2$ or $P4_3-C_4^4$	$P4_12_12-D_4^4$ or $P4_32_12-D_4^8$
Θ_f [°C]	–6.5	

79Saw

Pressure-induced phases: see Fig. 58A-2-008 in subsection 5a.

$\rho = 1.44 \cdot 10^3 \cdot$ kg m^{-3} at 27 °C. 35Bie

$\rho_X = 1.450 \cdot 10^3$ kg m^{-3} at RT. 80Sta

Transparent, colorless.

2a Crystal growth: evaporation method from aqueous solution. 35Bie

3a Unit cell parameter: a = 18.178(1) Å at RT. 80Sta

b Z = 8 in phase I. 35Bie

Crystal structure: Table 58A-2-001; Fig. 58A-2-001, Fig. 58A-2-002.

4 Thermal expansion: Fig. 58A-2-003.

5a Dielectric constant in phase IV: Fig. 58A-2-004.

$\kappa_{(100)} - \kappa_\infty = C/(T - \Theta_p)$ with κ_∞ = 5.5, C = 49 K, Θ_p = –6.5 °C at 90 MPa. 79Saw

Effect of p on $\kappa_{(100)}$ vs. T: Fig. 58A-2-005, Fig. 58A-2-006, Fig. 58A-2-007.

Phase diagram in regard to p: Fig. 58A-2-008.

c Remanent polarization and coercive field: Fig. 58A-2-009.

6a Transition heat and transition entropy at III–II phase transition: ΔQ_m = 7277 J mol^{-1}, ΔS_m = 27.4 J mol^{-1} K^{-1}. 65Nak

8a Elastic stiffness: Fig. 58A-2-010.

Sound velocity: Fig. 58A-2-011, Fig. 58A-2-012, Fig. 58A-2-013.

11 Electrical conductivity and thermoelectric power of pure and Cu^{2+}, Fe^{3+} doped single crystals: see 81Mad

13a NMR of proton: Fig. 58A-2-014, Fig. 58A-2-015; see also 71Shi

b ESR of Mn^{2+}: Fig. 58A-2-016, Fig. 58A-2-017;

see also Table 58A-1-020 in No. 58A-1 and 89Mis1

14b X-ray diffuse scattering: Fig. 58A-2-018.

Table 58A-2-001. $Ca_2Ba(CH_3CH_2COO)_6$ (DBP). Structure of phase I [80Sta]. T = RT. (**a**) fractional coordinates. Asterisks indicate atoms with half site-occupancy factor. (**b**) anisotropic temperature parameters [Å^2] defined by Eq. (d) in Introduction. (**c**) bond distances [Å] and angles [°].

(**a**)

	Site	Point symmetry	x	$y = z$
Ba	8(a)	$\bar{4}3$ m	0	0
Ca	16(c)	$\bar{3}$ m	1/8	1/8
O	96(g)	m	0.1532(3)	0.0397(1)
C(1)	48(f)	mm	0.1886(4)	0
C(2)*	96(g)	m	0.2714(7)	0.0175(7)
C(3)*	96(g)	m	0.3191(9)	–0.0233(7)

(**b**)

	U_{11}	$U_{22} = U_{33}$	U_{23}	$U_{13} = U_{12}$
Ba	0.0456(2)	0.0456(2)	0	0
Ca	0.0924(7)	0.0924(7)	–0.0281(6)	–0.0281(6)
O	0.124(3)	0.188(3)	–0.113(3)	–0.006(2)
C(1)	0.068(4)	0.155(5)	–0.042(6)	0
C(2)	0.068(5)	0.308(9)	–0.136(9)	0.009(6)
C(3)	0.108(7)	0.328(9)	–0.083(9)	0.058(7)

(**c**)

Distances [Å]		Angles [°]	
Ba–O	2.965(5)	Ca–O–Ba	97.0(2)
Ca–O	2.253(4)	C(2)–C(1)–O	105.6(7)
O–O′	2.039(8)	C(2)–C(1)–O′	139.0(8)
O–C(1)	1.205(5)	C(3)–C(2)–C(1)	113(1)
C(1)–C(2)	1.57(2)	O–C(1)–O′	115.5(8)
C(2)–C(3)	1.36(2)		

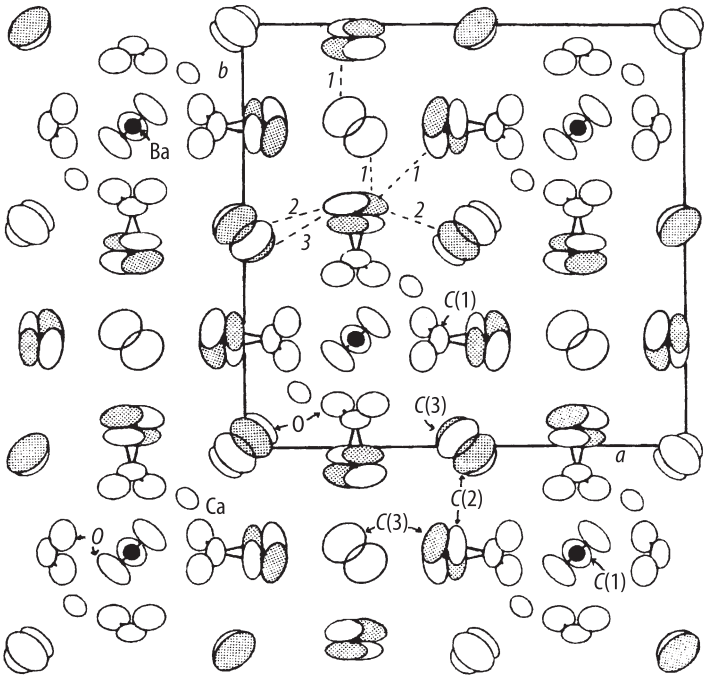

Fig. 58A-2-001. $Ca_2Ba(CH_3CH_2COO)_6$ (DBP). Structure of phase I [80Sta]. T = RT. Projection of a section onto (001) with $z = 0.175 \pm 0.125$. The shading indicates one ordered arrangement of C(3) and C(2) when intermolecular C(3) – C(2) contacts are maximized. The distances marked are (*1*) 4.052 Å, (*2*) 4.195 Å , (*3*) 4.395 Å.

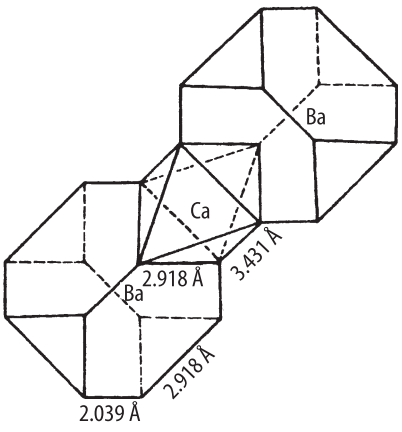

Fig. 58A-2-002. $Ca_2Ba(CH_3CH_2COO)_6$ (DBP). Coordination polyhedra of O atoms around Ba and Ca [80Sta]. T = RT (phase I).

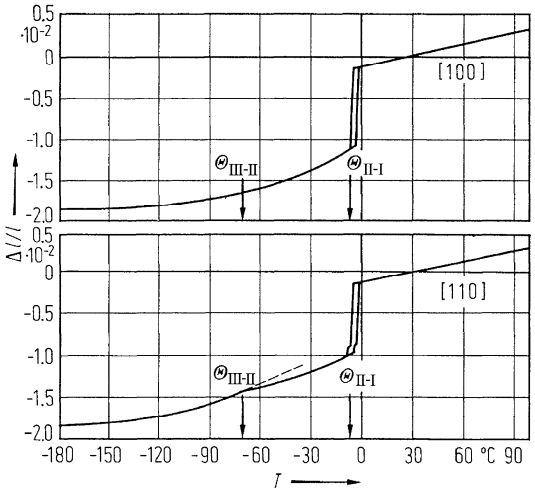

Fig. 58A-2-003. $Ca_2Ba(CH_3CH_2COO)_6$ (DBP). $\Delta l/l$ vs. T [75Kam].

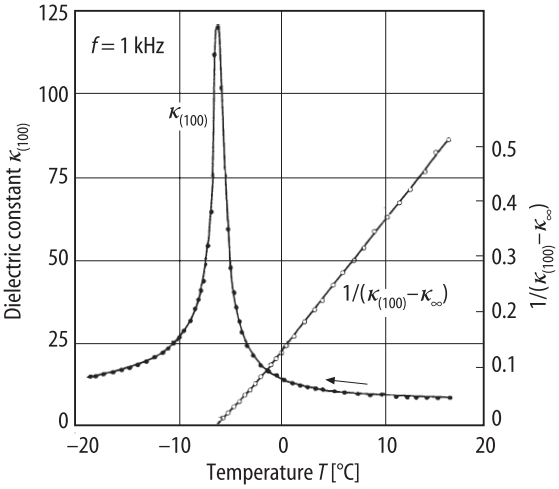

Fig. 58A-2-004. $Ca_2Ba(CH_3CH_2COO)_6$ (DBP). $\kappa_{(100)}$, $1/(\kappa_{(100)} - \kappa_\infty)$ vs. T at 90 MPa [79Saw]. The specimen was annealed at 270 °C for 9 h prior to the measurement. $\kappa_\infty = 5.5$.

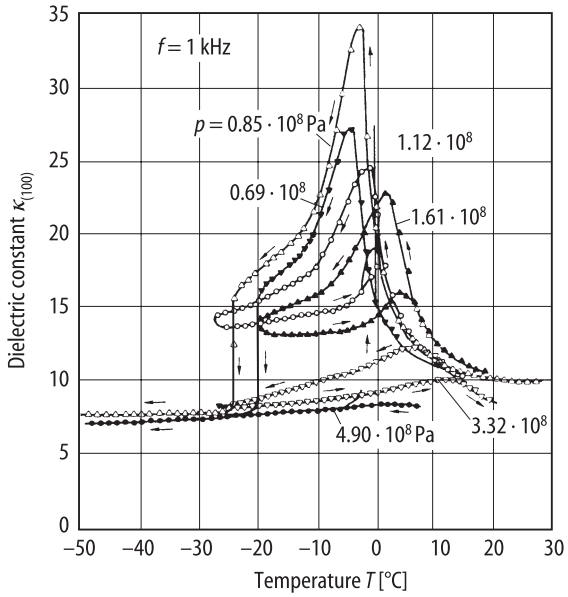

Fig. 58A-2-005. $Ca_2Ba(CH_3CH_2COO)_6$ (DBP). $\kappa_{(100)}$ vs. T [75Ges]. Parameter: p.

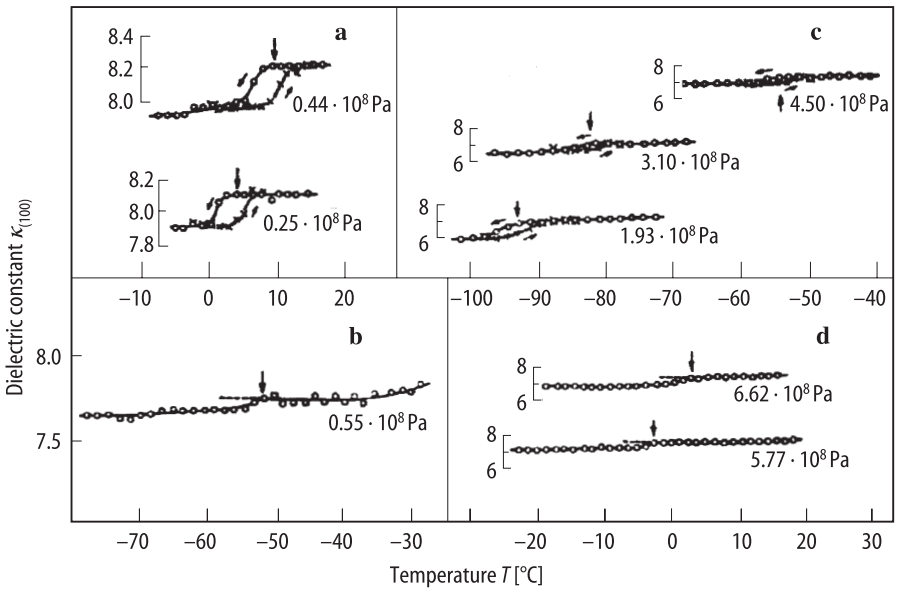

Fig. 58A-2-006. $Ca_2Ba(CH_3CH_2COO)_6$ (DBP). $\kappa_{(100)}$ vs. T [75Ges]. Parameter: p. (**a**) I–II transition. (**b**) II–III transition. (**c**) V–VI transition. (**d**) IV–VII transition. The transition points are indicated by vertical arrows. f = 1 kHz.

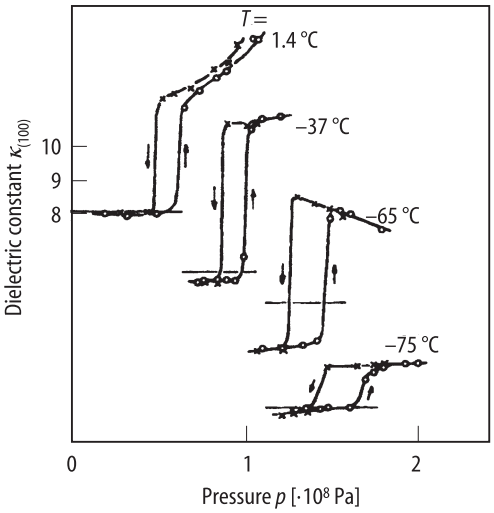

Fig. 58A-2-007. $Ca_2Ba(CH_3CH_2COO)_6$ (DBP). $\kappa_{(100)}$ vs. p at II–V and III–V transitions [75Ges]. Parameter: T. f = 1 kHz. Thin horizontal line: level of $\kappa_{(100)}$ = 8.0.

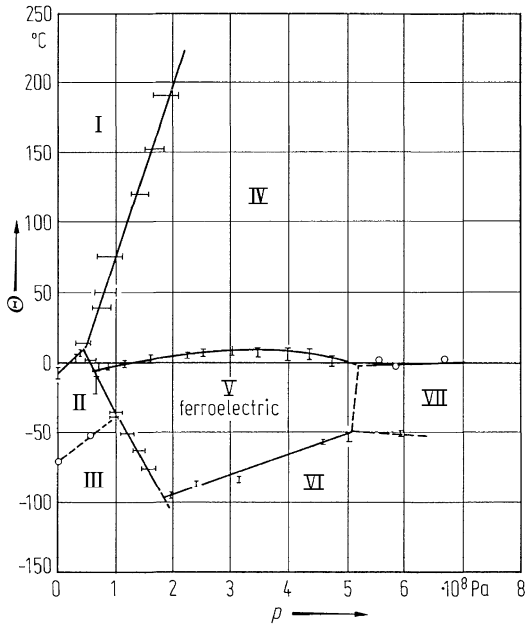

Fig. 58A-2-008. $Ca_2Ba(CH_3CH_2COO)_6$ (DBP). Phase diagram [75Ges].

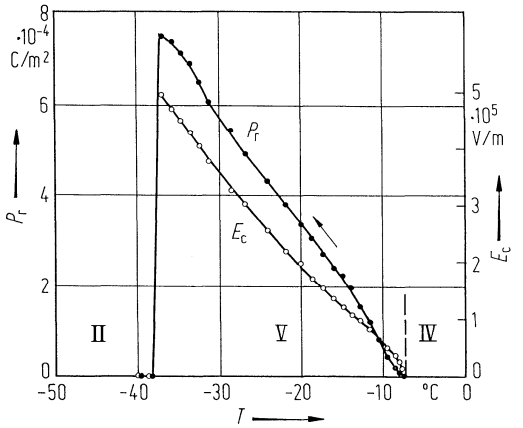

Fig. 58A-2-009. $Ca_2Ba(CH_3CH_2COO)_6$ (DBP). P_r, E_c vs. T at p = 85 MPa [79Saw]. The specimen was annealed at 270 °C for 17 h prior to the measurement.

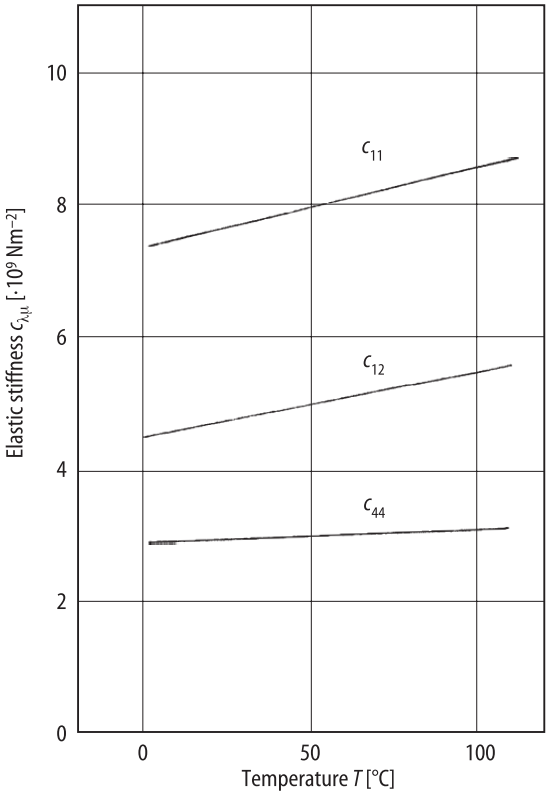

Fig. 58A-2-010. $Ca_2Ba(CH_3CH_2COO)_6$ (DBP). $c_{\lambda\mu}$ vs. T [75Kam].

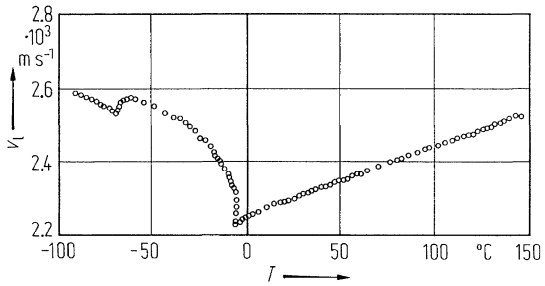

Fig. 58A-2-011. $Ca_2Ba(CH_3CH_2COO)_6$ (DBP). v_l vs. T [75Kam]. v_l: velocity of the longitudinal sound wave propagating along the [100] direction.

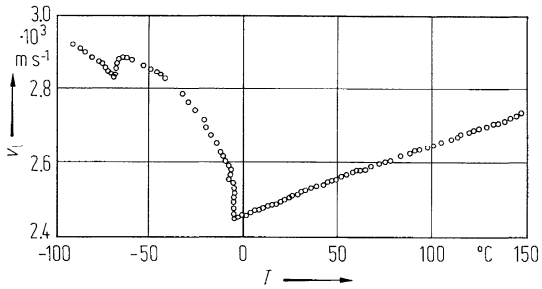

Fig. 58A-2-012. $Ca_2Ba(CH_3CH_2COO)_6$ (DBP). v_l vs. T [75Kam]. v_l: velocity of the longitudinal sound wave propagating along the [110] direction.

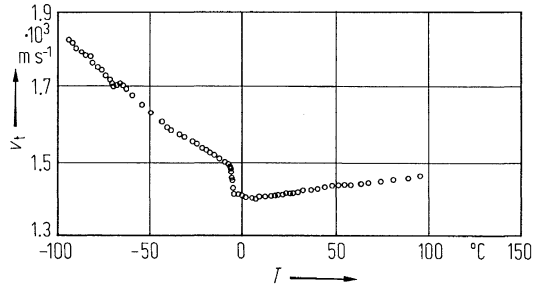

Fig. 58A-2-013. $Ca_2Ba(CH_3CH_2COO)_6$ (DBP). v_t vs. T [75Kam]. v_t: velocity of the transverse sound wave polarized along [010] propagating along the [100] direction.

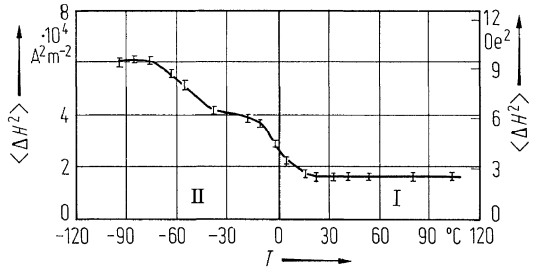

Fig. 58A-2-014. $Ca_2Ba(CH_3CH_2COO)_6$ (DBP). $\langle \Delta H^2 \rangle$ vs. T [67Ale]. $\langle \Delta H^2 \rangle$: second moment for proton NMR line.

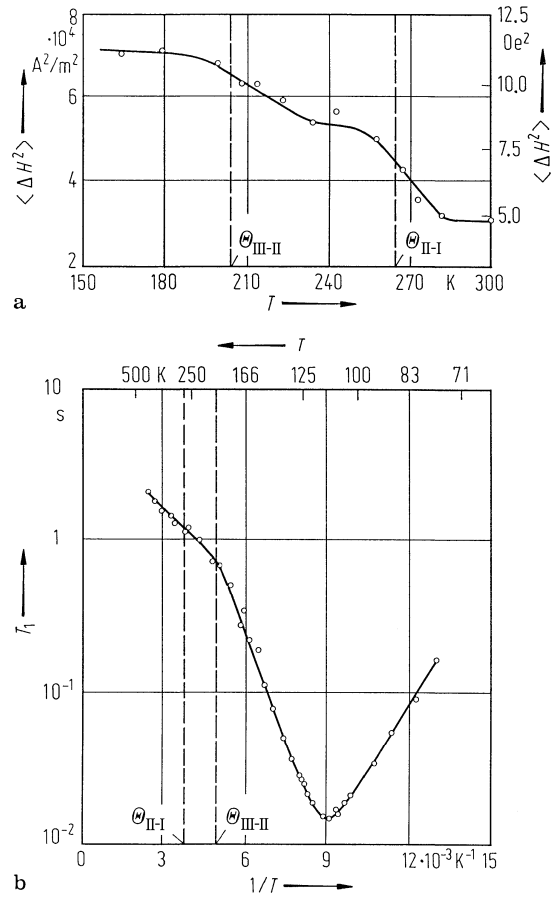

Fig. 58A-2-015. $Ca_2Ba(CH_3CH_2COO)_6$ (DBP). Proton NMR [85Sun]. (**a**) $\langle \Delta H^2 \rangle$ vs. T. $\langle \Delta H^2 \rangle$: second moment of NMR line for powdered sample. (**b**) T_1 vs. T^{-1}. T_1: spin-lattice relaxation time.

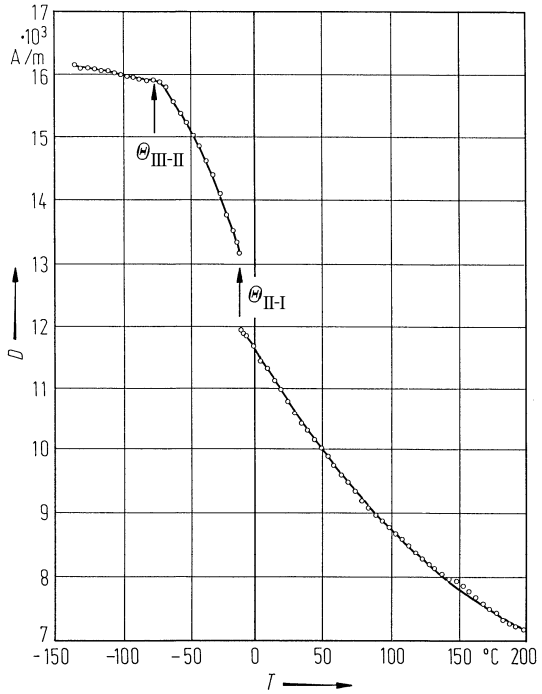

Fig. 58A-2-016. $Ca_2Ba(CH_3CH_2COO)_6$ (DBP). D vs. T [81Bha]. D: FS parameter of Mn^{2+}.

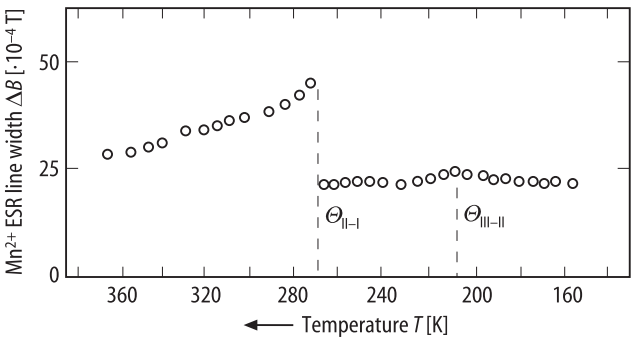

Fig. 58A-2-017. $Ca_2Ba(CH_3CH_2COO)_6$ (DBP). ΔB vs. T [89Mis2]. ΔB: Mn^{2+} ESR line width. $\boldsymbol{B} \perp$ (100) plane. $\boldsymbol{B} \parallel \boldsymbol{b} + 25°$.

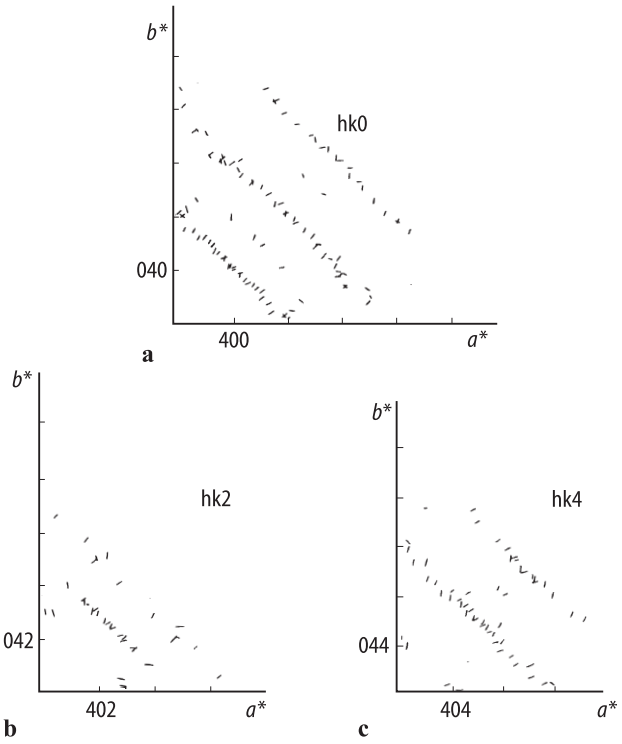

Fig. 58A-2-018. $Ca_2Ba(CH_3CH_2COO)_6$ (DBP). Distribution of X-ray diffuse scattering in reciprocal lattice sections [80Sta]. T = RT. (**a**) hk0 section. (**b**) hk2 section. (**c**) hk4 section.

References

35Bie Biefeld, L.P., Harris, P.M.: J. Am. Chem. Soc. **57** (1935) 396.
35Nit Nitta, I., Watanabe, T.: Sci. Pap. Inst. Phys. Chem. Res. **26** (1935) 164.
55Sek Seki, S., Momotani, M., Nakatsu, K., Oshima, T.: Bull. Chem. Soc. Jpn. **28** (1955) 411.
65Nak Nakamura, N., Suga, H., Chihara, H., Seki, S.: Bull. Chem. Soc. Jpn. **38** (1965) 1779.
67Ale Aleksandrova, I.P., Zherebtsova, L.I., Aleksandrov, K.S.: Kristallografiya **12** (1967) 894; Sov. Phys. Crystallogr. (English Transl.) **12** (1968) 780.
68Nak Nakamura, N., Suga, H., Chihara, H., Seki, S.: Bull. Chem. Soc. Jpn. **41** (1968) 291.
71Shi Shiraki, H., Tatsuzaki, I., Yagi, T.: Phys. Status Solidi (a) **7** (1971) 227.
75Ges Gesi, K., Ozawa, K.: J. Phys. Soc. Jpn. **38** (1975) 467.
75Kam Kameyama, H., Ishibashi, Y., Takagi, Y.: J. Phys. Soc. Jpn. **38** (1975) 1703.
79Saw Sawada, A., Kikugawa, T., Ishibashi, Y.: J. Phys. Soc. Jpn. **46** (1979) 871.
80Sta Stadnicka, K., Glazer, A.M.: Acta Crystallogr. Sect. B **36** (1980) 2977.
81Bha Bhat, S.V., Dhar, V., Srinivasan, R.: J. Phys. Soc. Jpn. **50** (1981) 2312.
81Mad Madhusudan, V., Sathyanarayan, S.G., Sivarama Sastry, G.: Phys. Status Solidi (a) **66** (1981) 371.
85Sun Sundaram, C.S., Ganesan, K., Ramakrishna, J., Chandrasekhar, K., Sastry, V.S.S.: Phase Transitions **5** (1985) 169.
89Mis1 Misra, S.K., Jerzak, S.: Phys. Rev. B **39** (1989) 2041.
89Mis2 Misra, S.K., Jerzak, S.: Acta Phys. Pol. A **76** (1989) 943.

No. 58A-3 $Ca_2Pb(CH_3CH_2COO)_6$, Dicalcium lead propionate (DLP)

(M = 725.8)

1a Ferroelectricity in DLP was discovered by Takashige et al. in 1975. 75Tak

b

phase	III [a])	II [a])	I [a])
state	(F) [b])	F [c])	P [c])
crystal system		tetragonal [c])	tetragonal [c])
space group		$P4_1 - C_4^2$ or $P4_3 - C_4^4$ *)	$P4_12_12 - D_4^4$ or $P4_32_12 - D_4^8$ *)
Θ [°C]		– 82 [a])	60 [a])

[a]) 65Nak
[b]) 75Osa
[c]) 75Tak

*) Space group of dextrorotatory crystal: Phase I: $P4_32_12 - D_4^8$, Phase II: $P4_3 - C_4^4$. 90Kas

Transition temperature Θ_{II-I} increases with increasing concentration of Mn^{2+} impurity. 84Bad
Θ–p phase diagram: see Fig. 58A-3-016 in subsection 5a.
P_s || [001]. 75Tak
Transparent, colorless.
$\rho = 1.76 \cdot 10^3$ kg m^{-3} in phase II; 59Fer
$\rho = 1.785(8) \cdot 10^3$ kg m^{-3} at RT. 84Sin

2a Evaporation method from aqueous solution. 72Tat

3a Unit cell parameters: a = 12.50 Å, c = 17.26 Å at RT, 59Fer
a = 12.538(2) Å, c = 17.364(3) Å at T = 70 °C (phase I), 90Kas
a = 12.533(6) Å, c = 17.344(6) Å at T = 45 °C (phase II),
a = 12.476(8) Å, c = 17.108(7) Å at T = –80 °C (phase III).

b Z = 4. 59Fer
Crystal structure: Fig. 58A-3-001, Fig. 58A-3-002.
Fractional coordinates and temperature parameters: Table 58A-3-001, Table 58A-3-002, Table 58A-3-003; Fig. 58A-3-003.
Interatomic distances and angles: Table 58A-3-004, Table 58A-3-005; Fig. 58A-3-004, Fig. 58A-3-005.
Occupancies of disordered atoms: Table 58A-3-006; Fig. 58A-3-006.
Mean-square displacement of atoms: Fig. 58A-3-007.

4 Thermal expansion: Fig. 58A-3-008, Fig. 58A-3-009.

5a κ vs. T: Fig. 58A-3-010, Fig. 58A-3-011.
Dielectric dispersion: Fig. 58A-3-012, Fig. 58A-3-013, Fig. 58A-3-014.
Effect of hydrostatic pressure: Fig. 58A-3-015.
Phase diagram in regard to p: Fig. 58A-3-016.
Thermal hysteresis of III–II transition: see Fig. 58A-1-026 in No. 58A-1.

b Effect of E_{bias} on κ: Fig. 58A-3-017.

c Spontaneous polarization and coercive field: Fig. 58A-3-018.

d Pyroelectric charge: Fig. 58A-3-019.

6a Heat capacity: Fig. 58A-3-020.
Transition heat and transition entropy at Θ_{II-II}: ΔQ_m = 4850 J mol^{-1}, 65Nak
ΔS_m = 24 J mol^{-1} K^{-1}.

7a Piezoelectric constant: Fig. 58A-3-021.

8a	Elastic compliance: Fig. 58A-3-022. Sound velocity: Fig. 58A-3-023. Ultrasonic attenuation: see	72Tod
9a	Birefrengence: Fig. 58A-3-024; see also	89Vlo
b	Electrooptic constant: Fig. 58A-3-025.	
d	Rotatory power: Fig. 58A-3-026; see also	89Vlo
	Rotatory strength: see	88Ues, 90Ues
	Circular dichroism: see	89Ues
	The crystal of space group $P4_1$ is levorotatory; see subsection 1b.	84Sin
e	Second harmonic generation: see	91Ara
10a	Raman scattering: Fig. 58A-3-027; see also Fig. 58A-1-056 in No. 58A-1.	
b	Brillouin scattering: Fig. 58A-3-028.	
13a	NMR: Fig. 58A-3-029, Fig. 58A-3-030, Fig. 58A-3-031.	
b	ESR of Mn^{2+}: Fig. 58A-3-032; see also Table 58A-1-020 and Fig. 58A-1-063 in No. 58A-1 and	89Mis1
14b	Inelastic neutron scattering: see	75Dim

Table 58A-3-001. $Ca_2Pb(CH_3CH_2COO)_6$ (DLP). Fractional coordinates and temperature parameters U_{ij} [$\cdot 10^{-2}$ Å^2] of phase I [90Kas]. Dextrorotatory crystal. T = 70 °C. U_{ij} is defined by Eq. (d) in Introduction. Prime and double prime indicate disordered atoms with occupancy 0.5.

Atom	x	y	z	U_{11}	U_{22}	U_{33}	U_{12}	U_{13}	U_{23}
Pb	0.72352(5)	0.72352(5)	0.0	4.24(2)	4.24(2)	4.22(2)	–0.21(3)	0.06(4)	–0.06(4)
Ca	0.7430(2)	0.9372(2)	–0.1581(1)	7.3(2)	4.2(1)	5.9(1)	–0.16(9)	0.9(1)	1.52(9)
O(11)	0.8206(7)	0.9142(7)	–0.0390(5)	13.3(7)	12.9(8)	9.9(6)	–5.3(6)	–3.7(5)	3.7(5)
O(21)	0.6149(7)	0.5242(7)	–0.0382(5)	11.7(8)	10.0(7)	15.5(8)	2.9(5)	6.1(6)	–2.7(6)
O(31)	0.6081(5)	0.8496(6)	–0.0901(4)	5.8(4)	8.3(5)	8.9(5)	–0.8(4)	2.1(4)	1.6(4)
O(32)	0.4626(7)	0.8278(8)	–0.0270(4)	13.1(7)	16.7(9)	7.1(5)	–2.7(7)	3.6(5)	1.6(5)
O(41)	0.8007(7)	0.7643(5)	–0.1704(6)	12.6(7)	4.9(5)	18.3(8)	2.0(4)	3.0(6)	1.1(5)
O(42)	0.8073(6)	0.6125(5)	–0.1193(4)	14.0(8)	5.4(4)	6.5(4)	0.0(4)	2.3(5)	0.1(4)
C(11)	0.9031(15)	0.9031(15)	0.0	10.8(17)	10.8(17)	9.8(12)	–5.8(10)	–4.7(19)	4.7(19)
C(12)	0.9814(18)	0.9814(18)	0.0	24.9(48)	24.9(48)	33.5(41)	–22.2(26)	–18.2(57)	18.2(57)
C(13)'	0.9695(31)	1.0674(33)	–0.0194(26)	18.0(38)	31.1(56)	19.5(44)	–9.4(36)	–6.2(34)	3.7(38)
C(21)	0.5375(14)	0.5375(14)	0.0	6.7(12)	6.7(12)	11.6(13)	–1.6(7)	2.8(16)	–2.8(16)
C(22)'	0.4684(25)	0.4244(30)	–0.0040(42)	9.0(26)	16.9(39)	37.6(50)	–3.8(26)	10.6(37)	–19.9(42)
C(23)'	0.4183(39)	0.3908(33)	–0.0373(31)	27.4(65)	10.6(27)	38.6(90)	–5.1(30)	–2.5(45)	–16.5(44)
C(31)	0.5109(8)	0.8474(8)	–0.0850(5)	7.9(8)	6.3(7)	5.9(6)	–0.1(6)	0.8(6)	2.1(5)
C(32)	0.4516(14)	0.8746(18)	–0.1558(10)	12.9(14)	32.2(27)	15.1(14)	–0.8(15)	–5.5(12)	12.0(17)
C(33)'	0.4292(39)	0.8078(34)	–0.2088(20)	42.0(69)	20.9(46)	16.4(30)	–5.4(44)	–21.0(39)	0.8(31)
C(33)"	0.3463(35)	0.8515(45)	–0.1437(31)	18.7(42)	41.4(72)	33.6(63)	–8.7(49)	–10.6(44)	25.2(57)
C(41)	0.8208(8)	0.6711(7)	–0.1741(6)	9.2(8)	4.5(6)	7.6(7)	0.4(5)	2.5(6)	0.1(5)
C(42)	0.8724(13)	0.6204(10)	–0.2412(8)	22.9(17)	11.4(11)	7.4(8)	2.7(10)	7.1(10)	1.6(8)
C(43)	0.8316(19)	0.6540(22)	–0.3151(11)	27.5(27)	37.4(32)	11.1(13)	6.9(37)	–1.2(15)	–2.0(16)

Table 58A-3-002. $Ca_2Pb(CH_3CH_2COO)_6$ (DLP). Fractional coordinates, temperature parameters U_{ij} [$\cdot 10^{-2}$ Å^2] and mean square displacements $\overline{u^2}$ [Å^2] of phase II [90Kas]. Dextrorotatory crystal. T = 45 °C. U_{ij} is defined by Eq. (d) in Introduction. Prime and double prime indicate disordered atoms.

Atom	x	y	z	U_{11}, $\overline{u^2}$	U_{22}	U_{33}	U_{12}	U_{13}	U_{23}	Atom above Θ_{II-I}
Pb	0.72395(3)	0.72290(3)	0.0	4.24(3)	4.17(3)	4.08(2)	–0.22(2)	0.11(2)	–0.09(2)	Pb
Ca(1)	0.7451(2)	0.9357(2)	–0.1586(2)	7.1(2)	4.4(1)	5.5(2)	–0.3(1)	1.1(1)	1.6(1)	Ca
Ca(2)	0.9366(2)	0.7407(2)	0.1584(2)	3.9(1)	7.3(2)	5.7(2)	–0.2(1)	–1.3(1)	–1.1(1)	Ca^{v}
O(11)	0.8236(10)	0.9090(11)	–0.0400(7)	12.7(10)	16.1(12)	8.7(8)	–6.2(9)	–3.8(8)	3.7(8)	O(11)
O(12)	0.9177(10)	0.8194(9)	0.0384(7)	14.2(10)	11.2(9)	8.8(8)	–4.6(8)	–2.9(7)	3.0(7)	O(11^{v})
O(21)	0.6157(9)	0.5254(9)	–0.0360(8)	10.6(9)	9.2(8)	15.2(12)	1.7(7)	6.2(8)	–2.1(8)	O(21)
O(22)	0.5232(10)	0.6129(10)	0.0385(8)	11.6(9)	12.3(10)	14.8(12)	3.9(8)	2.8(8)	–7.8(9)	O(21^{v})
O(3a1)	0.6086(7)	0.8487(7)	–0.0894(6)	5.2(5)	7.9(7)	10.0(8)	–0.7(5)	1.7(5)	2.0(6)	O(31)
O(3a2)	0.4645(11)	0.8246(11)	–0.0271(7)	12.3(10)	17.2(13)	8.3(9)	–2.5(9)	4.6(7)	1.8(8)	O(32)
O(3b1)	0.8495(7)	0.6063(7)	0.0921(6)	8.1(7)	5.9(6)	8.8(7)	–0.6(5)	–3.1(6)	–1.6(5)	O(31^{v})
O(3b2)	0.8279(11)	0.4587(10)	0.0282(7)	17.3(12)	12.3(10)	7.5(8)	–2.5(9)	–2.8(8)	–2.8(7)	O(32^{v})
O(4a1)	0.8045(10)	0.7642(8)	–0.1694(8)	11.3(9)	5.6(6)	15.6(12)	1.0(6)	1.6(8)	0.8(7)	O(41)
O(4a2)	0.8122(9)	0.6119(7)	–0.1159(6)	13.1(9)	4.5(5)	7.6(7)	0.3(5)	3.9(7)	–0.1(5)	O(42)
O(4b1)	0.7640(7)	0.8023(9)	0.1701(9)	4.2(6)	10.8(9)	19.7(14)	1.4(6)	–1.2(7)	–4.8(9)	O(41^{v})
O(4b2)	0.6109(8)	0.8061(9)	0.1195(6)	7.2(7)	12.5(9)	7.2(7)	–0.8(6)	–1.7(6)	–3.6(7)	O(42^{v})
C(11)	0.9047(14)	0.8978(13)	–0.0034(13)	13.4(14)	9.5(12)	7.3(10)	–6.3(10)	–2.5(12)	0.5(10)	C(11)
C(12)	0.9878(18)	0.9742(18)	–0.0046(23)	13.5(17)	12.5(17)	21.6(26)	–6.8(13)	–1.1(21)	–1.2(22)	C(12)
C(13)'	1.0876(43)	0.9509(49)	0.0009(52)	11.9(48)	17.5(61)	23.2(79)	–5.1(39)	–7.3(51)	12.5(61)	
C(13)"	0.9397(53)	1.0380(48)	0.0329(59)	30.3(81)	18.9(56)	46(14)	0.6(51)	–15.2(87)	–8.8(72)	
C(21)	0.5365(10)	0.5349(10)	–0.0013(12)	5.2(8)	6.0(8)	10.5(11)	–1.2(6)	2.3(10)	–2.8(10)	C(21)
C(22)	0.4553(20)	0.4356(25)	–0.0086(32)	13.3(19)	22.8(27)	44.4(57)	–12.8(19)	–4.9(28)	17.7(35)	C(22)
C(23)'	0.4003(47)	0.4067(53)	0.0346(82)	17.3(44)	33.6(73)	59(17)	–21.7(50)	–12.0(78)	22.9(92)	
C(23)"	0.3676(59)	0.4276(80)	–0.0227(42)	9.9(50)	24.0(88)	12.9(72)	–1.3(59)	–9.8(46)	–0.2(57)	

(continued)

Table 58A-3-002 (continued)

Atom	x	y	z	U_{11}, $\overline{u^2}$	U_{22}	U_{33}	U_{12}	U_{13}	U_{23}	Atom above Θ_{II-I}
C(3a1)	0.5113(12)	0.8494(11)	–0.0841(8)	8.0(10)	7.2(10)	6.7(10)	–0.7(8)	1.8(8)	1.6(8)	C(31)
C(3a2)	0.4465(20)	0.8854(22)	–0.1538(16)	13.4(20)	26.9(32)	17.6(24)	4.2(20)	–7.0(18)	9.8(24)	C(32)
C(3a3)′	0.4542(85)	0.8187(62)	–0.2134(53)	20.1(49)						
C(3a3)″	0.3476(40)	0.8500(47)	–0.1623(39)	13.2(44)	28.9(61)	31.0(78)	–3.9(39)	–8.3(47)	19.4(57)	
C(3b1)	0.8476(11)	0.5074(12)	0.0870(8)	6.5(9)	8.4(10)	6.4(9)	–0.2(7)	–2.8(8)	–0.4(8)	C(31^{v})
C(3b2)	0.8686(28)	0.4418(18)	0.1613(16)	46.4(50)	8.8(15)	17.8(24)	–5.0(22)	–20.8(31)	6.0(16)	C(32^{v})
C(3b3)′	0.8035(56)	0.3949(99)	0.2022(44)	29.4(64)	77(14)	19.2(52)	–3.7(83)	0.2(50)	37.5(75)	
C(3b3)″	0.850(11)	0.348(11)	0.152(11)	11.6(80)						
C(4a1)	0.8268(13)	0.6695(10)	–0.1728(9)	10.2(12)	4.0(8)	9.3(12)	0.9(7)	2.7(9)	–0.7(8)	C(41)
C(4a2)	0.8814(19)	0.6182(14)	–0.2404(12)	27.3(27)	9.6(13)	6.7(12)	3.3(14)	5.9(17)	0.1(12)	C(42)
C(4a3)	0.8343(27)	0.6503(27)	–0.3136(19)	27.3(37)	23.5(33)	14.7(26)	1.4(28)	0.4(26)	0.6(23)	C(43)
C(4b1)	0.6699(10)	0.8202(13)	0.1729(9)	4.5(8)	10.7(12)	7.9(11)	–0.4(8)	1.5(8)	–3.1(9)	C(41^{v})
C(4b2)	0.6209(16)	0.8698(20)	0.2432(12)	12.3(16)	24.3(25)	7.1(13)	3.2(15)	1.4(13)	–4.9(16)	C(42^{v})
C(4b3)	0.6476(34)	0.8308(26)	0.3162(19)	40.0(49)	22.7(33)	13.5(25)	7.6(34)	2.4(29)	–0.3(23)	C(43^{v})

Symmetry code: v: y, x, – z.

Table 58A-3-003. $Ca_2Pb(CH_3CH_2COO)_6$ (DLP). Fractional coordinates, temperature parameters U_{ij} [$\cdot 10^{-2}$ Å^2] and mean square displacements $\overline{u^2}$ [Å^2] of phase III [90Kas]. Dextrorotatory crystal. $T = -80$ °C. U_{ij} is defined by Eq. (d) in Introduction. Prime and double prime indicate disordered atoms.

Atom	x	y	z	U_{11}, $\overline{u^2}$	U_{22}	U_{33}	U_{12}	U_{13}	U_{23}	Atom above Θ_{II-I}
Pb	0.72582(3)	0.72053(3)	0.0	2.84(2)	2.74(2)	2.92(1)	–0.13(2)	0.10(2)	–0.16(2)	Pb
Ca(1)	0.7525(2)	0.9303(2)	–0.1613(1)	4.7(2)	2.8(1)	4.1(1)	0.0(1)	0.5(1)	0.7(1)	Ca
Ca(2)	0.9352(2)	0.7297(2)	0.1600(1)	2.9(1)	5.3(2)	4.5(1)	–0.0(1)	–1.0(1)	–1.4(1)	Ca^{v}
O(11)	0.8249(9)	0.8983(9)	–0.0392(5)	7.2(7)	8.0(8)	5.5(6)	–3.7(6)	–2.1(5)	2.0(5)	O(11)
O(12)	0.9332(7)	0.8031(8)	0.0362(5)	5.7(6)	6.1(7)	5.7(6)	–1.3(5)	–0.8(4)	2.1(5)	$O(11^{v})$
O(21)	0.6289(8)	0.5248(9)	–0.0343(6)	5.1(7)	6.6(7)	10.4(8)	0.3(5)	3.6(6)	–2.0(6)	O(21)
O(22)	0.5257(7)	0.6026(9)	0.0445(7)	8.6(9)	7.1(8)	9.8(8)	1.2(6)	3.1(7)	–2.8(6)	$O(21^{v})$
O(3a1)	0.6137(7)	0.8419(7)	–0.0952(5)	3.8(5)	5.3(6)	6.4(6)	0.0(4)	0.9(4)	1.0(4)	O(31)
O(3a2)	0.4634(9)	0.8107(10)	–0.0336(6)	7.8(9)	11.3(10)	5.3(6)	–1.3(7)	2.9(5)	1.2(6)	O(32)
O(3b1)	0.8458(7)	0.5937(7)	0.0933(5)	5.0(6)	4.3(5)	5.2(5)	–1.1(4)	–0.7(4)	–0.7(4)	$O(31^{v})$
O(3b2)	0.8352(10)	0.4399(9)	0.0323(5)	12.8(11)	8.7(9)	4.6(6)	–2.3(8)	–0.7(6)	–2.0(5)	$O(32^{v})$
O(4a1)	0.8096(10)	0.7610(7)	–0.1802(7)	10.7(9)	2.5(5)	9.6(8)	1.0(5)	1.2(7)	0.3(5)	O(41)
O(4a2)	0.8220(7)	0.6123(7)	–0.1107(5)	6.0(6)	3.9(5)	4.3(5)	–0.1(4)	1.5(4)	–0.4(4)	O(42)
O(4b1)	0.7637(7)	0.8010(8)	0.1566(6)	3.0(5)	7.2(7)	8.7(7)	1.2(5)	–0.8(5)	–0.8(5)	$O(41^{v})$
O(4b2)	0.6033(7)	0.8080(9)	0.1167(5)	3.5(5)	9.6(8)	6.4(6)	0.3(5)	–1.2(4)	–3.7(6)	$O(42^{v})$
C(11)	0.9138(10)	0.8835(9)	–0.0033(10)	5.5(8)	6.8(9)	5.1(7)	–2.3(7)	–0.9(7)	–0.4(8)	C(11)
C(12)	0.9985(15)	0.9715(17)	–0.0126(12)	10.3(14)	10.8(16)	9.9(16)	–7.8(12)	–4.4(11)	2.7(12)	C(12)
C(13)	1.1016(14)	0.9488(17)	0.0171(12)	7.9(13)	12.7(17)	12.3(18)	–4.3(11)	–4.0(12)	4.2(15)	C(13)
C(21)	0.5425(9)	0.5277(8)	0.0005(10)	4.5(7)	2.2(6)	7.7(8)	–0.5(5)	0.1(8)	–1.1(7)	C(21)
C(22)	0.4690(16)	0.4270(18)	–0.0097(22)	8.8(16)	9.6(17)	25.1(29)	–5.5(13)	–4.9(19)	3.6(19)	C(22)
C(23)'	0.3656(20)	0.4315(24)	–0.0078(39)	2.3(14)	9.5(23)	48.2(77)	1.0(13)	1.0(31)	–0.0(38)	
C(23)"	0.4304(52)	0.4001(47)	–0.0624(32)	5.0(21)						

(continued)

Table 58A-3-003 (continued)

Atom	x	y	z	U_{11}, $\overline{u^2}$	U_{22}	U_{33}	U_{12}	U_{13}	U_{23}	Atom above Θ_{II-I}
C(3a1)	0.5143(9)	0.8450(9)	–0.0890(7)	3.8(7)	3.6(7)	4.7(7)	–0.9(5)	0.1(5)	1.2(5)	C(31)
C(3a2)	0.4573(13)	0.8934(15)	–0.1578(11)	6.0(11)	11.3(16)	9.5(12)	–0.3(10)	–2.2(9)	6.2(11)	C(32)
C(3a3)	0.3410(17)	0.8620(20)	–0.1639(14)	7.0(14)	15.6(22)	15.9(21)	–0.5(14)	–4.8(14)	6.0(17)	C(33)
C(3b1)	0.8396(10)	0.4939(10)	0.0930(7)	4.8(8)	3.6(7)	5.0(7)	0.1(6)	–0.3(6)	–0.1(5)	C(31^{v})
C(3b2)	0.8424(19)	0.4366(17)	0.1726(10)	16.3(21)	10.9(16)	5.8(10)	1.2(15)	–0.1(12)	5.0(11)	C(32^{v})
C(3b3)	0.7528(22)	0.4502(30)	0.2136(15)	12.2(24)	31.9(45)	13.1(21)	–1.7(25)	3.9(16)	10.4(25)	C(33^{v})
C(4a1)	0.8413(10)	0.6682(10)	–0.1737(8)	4.2(8)	3.6(7)	6.0(8)	0.5(5)	0.8(6)	1.3(6)	C(41)
C(4a2)	0.9010(14)	0.6129(12)	–0.2365(7)	12.0(14)	7.0(10)	2.5(7)	2.6(9)	2.4(8)	0.6(6)	C(42)
C(4a3)	0.8669(22)	0.6505(17)	–0.3198(10)	22.2(27)	9.5(16)	4.5(10)	2.5(17)	3.0(13)	1.3(9)	C(43)
C(4b1)	0.6690(11)	0.8139(11)	0.1701(8)	5.1(9)	5.5(9)	5.3(8)	0.0(7)	1.3(6)	–2.6(6)	C(41^{v})
C(4b2)	0.6234(21)	0.8461(21)	0.2518(13)	18.7(25)	19.4(26)	7.8(13)	4.6(19)	–3.1(17)	–8.3(17)	C(42^{v})
C(4b3)	0.6723(30)	0.8138(26)	0.3149(14)	27.8(39)	21.8(35)	7.6(17)	5.7(31)	–2.3(20)	0.7(18)	C(43^{v})

Symmetry code: v: y, x, – z.

Table 58A-3-004. $Ca_2Pb(CH_3CH_2COO)_6$ (DLP). Interatomic distances [Å] around Pb and Ca [90Kas].

	–80 °C	45 °C	70 °C		–80 °C	45 °C	70 °C
Pb–Ca(1)	3.818(3)	3.841(3)	>3.844(2)	Pb–Ca(1^{iv-a+b})	4.001(3)	3.965(3)	>3.951(2)
Pb–Ca(2)	3.785(3)	3.834(3)		Pb–Ca($2^{iii+a-b+c}$)	3.918(3)	3.950(3)	
Pb–O(11)	2.625(11)	2.734(15)	>2.767(9)	Pb–O(21)	2.787(11)	2.891(14)	>2.923(9)
Pb–O(12)	2.853(9)	2.794(12)		Pb–O(22)	2.997(12)	2.946(14)	
Pb–O(3a1)	2.627(9)	2.642(11)	>2.654(7)	Pb–O(3a2)	3.509(12)	3.524(14)	>3.554(10)
Pb-O(3b1)	2.700(9)	2.676(11)		Pb–O(3b2)	3.799(13)	3.592(13)	
Pb–O(4a1)	3.294(12)	3.149(14)	>3.155(10)	Pb–O(4a2)	2.617(9)	2.684(11)	>2.707(8)
Pb–O(4b1)	2.900(11)	3.154(16)		Pb–O(4b2)	2.741(11)	2.718(11)	
Ca(1)–O(11)	2.312(11)	2.304(14)	>2.304(9)	Ca(1)–O($22^{iii+a-c}$)	2.294(13)	2.282(15)	>2.287(9)
Ca(2)–O(12)	2.307(10)	2.314(12)		Ca(2)–O(21^{iv+b})	2.296(11)	2.326(15)	
Ca(1)–O(3a1)	2.345(9)	2.357(11)	>2.337(7)	Ca(1)–O($3a2^{iii+a-c}$)	2.273(12)	2.263(14)	>2.269(10)
Ca(2)–O(3b1)	2.329(9)	2.313(11)		Ca(2)–O($3b2^{iv+b}$)	2.246(14)	2.266(14)	
Ca(1)–O(4a1)	2.253(13)	2.283(15)	>2.295(10)	Ca(1)–O($4b2^{iv+b}$)	2.336(11)	2.339(11)	>2.335(7)
Ca(2)–O(4b1)	2.318(11)	2.305(16)		Ca(2)–O($4a2^{iii+a-c}$)	2.328(9)	2.334(11)	

Symmetry code:

(i) x, y, z; (v) $y, x, -z$;
(ii) $-x, -y, 1/2 + z$; (vi) $-y, -x, 1/2 - z$;
(iii) $1/2 - y, 1/2 + x, 3/4 + z$; (vii) $1/2 - x, 1/2 + y, 3/4 - z$;
(iv) $1/2 + y, 1/2 - x, 1/4 + z$; (viii) $1/2 + x, 1/2 - y, 1/4 - z$.

The translation operation by a cell constant is denoted by $\pm a, \pm b, \pm c$.
For simplicity the code (i) is omitted throughout.

Table 58A-3-005. $Ca_2Pb(CH_3CH_2COO)_6$ (DLP). Distances [Å] between methyl groups shorter than 4.5 Å [90Kas]. $CH_3(1)'$ means $C(13')H_3$ and so on. Symmetry codes are the same as those of Table 58A-3-004.

70 °C	$CH_3(1)'$	$-CH_3(2^{iv+b})'$	4.15(7)	45 °C	$CH_3(2)'$	$-CH_3(1^{iv-a+b})'$	3.81(17)
		$-CH_3(2^{vii+a-c})'$	4.26(7)			$-CH_3(1^{iii+a-b})''$	4.45(17)
		$-CH_3(3^{iv+b})'$	4.37(7)			$-CH_3(3a^{iv-a})''$	3.38(16)
		$-CH_3(3^{vii+a-c})'$	3.29(7)			$-CH_3(3a^{iii-b-c})'$	4.17(19)
		$-CH_3(4^{vii+a-c})$	4.19(5)			$-CH_3(3b^{iii-b-c})''$	3.93(24)
	$CH_3(2)'$	$-CH_3(3^{iv-a})'$	4.46(7)		$CH_3(2)''$	$-CH_3(1^{iii+a-b-c})''$	3.58(14)
		$-CH_3(3^{vii-b-c})'$	4.48(7)			$-CH_3(3a^{iv-a})''$	3.95(12)
		$-CH_3(3^{iv\,a})''$	3.97(8)			$-CH_3(3b^{iii-b-c})'$	3.67(16)
		$-CH_3(3^{vii-b-c})''$	3.56(8)			$-CH_3(3b^{iii-b-c})''$	3.16(22)
		$-CH_3(4^{vi+a+b-c})$	3.89(6)		$CH_3(1)'$	$-CH_3(3a^{+a})''$	4.50(11)
	$CH_3(3)'$	$-CH_3(3^{vi+a+b-c})'$	4.40(7)		$CH_3(1)''$	$-CH_3(3b^{iii+a-c})'$	4.16(16)
		$-CH_3(3^{iii+a-c})''$	4.26(7)		$CH_3(3a)''$	$-CH_3(3a^{iv-a+b})'$	4.25(13)
		$-CH_3(4^{viii-a+b-c})$	4.14(6)			$-CH_3(3b^{ii+a+b-c})'$	4.30(14)
	$CH_3(3)''$	$-CH_3(4^{iv-a+b})$	3.60(6)		$CH_3(3b)'$	$-CH_3(3a^{ii+a+b})'$	4.44(16)
45 °C	$CH_3(4a)$	$-CH_3(1^{iii+a-b-c})'$	3.83(9)	–80 °C	$CH_3(1)$	$-CH_3(3a^{+a})$	4.44(3)
		$-CH_3(2^{ii+a+b-c})'$	4.01(15)			$-CH_3(3b^{iii+a-c})$	3.95(4)
		$-CH_3(2^{iii+a-c})''$	4.10(10)			$-CH_3(4a^{iv+b})$	4.25(3)
		$-CH_3(3a^{iii+a-c})''$	3.79(8)		$CH_3(3a)$	$-CH_3(2^{iii-c})'$	3.76(7)
		$-CH_3(3b^{iv+b-c})'$	4.17(13)			$-CH_3(2^{iii-c})''$	4.03(7)
		$-CH_3(3b^{vii+a-c})''$	3.72(19)			$-CH_3(4a^{iv-a+b})$	4.05(4)
	$CH_3(4b)$	$-CH_3(1^{iv-a+b})''$	3.70(11)		$CH_3(3b)$	$-CH_3(4a^{iii+a-b})$	4.03(5)
		$-CH_3(2^{ii+a+b})''$	4.28(11)			$-CH_3(4b^{iii+a-b-c})$	4.38(5)
		$-CH_3(3a^{iii+a})$	4.15(11)		$CH_3(4a)$	$-CH_3(2^{ii+a+b-c})'$	4.45(7)
		$-CH_3(3b^{iv+b})'$	4.24(13)			$-CH_3(2^{iii+a-c})'$	3.83(7)
		$-CH_3(3b^{iv+b})''$	3.69(19)		$CH_3(4b)$	$-CH_3(2^{ii+a+b})'$	4.33(8)
						$-CH_3(2^{ii+a+b})''$	3.63(7)

Table 58A-3-006. $Ca_2Pb(CH_3CH_2COO)_6$ (DLP). Occupancies of disordered atoms in phase II and phase III [90Kas].

Atom	45 °C	–80 °C
C(13)'	0.41(6)	1
C(13)''	0.59	0
C(23)'	0.66(10)	0.76(5)
C(23)''	0.34	0.24*
C(3a3)'	0.38*	0
C(3a3)''	0.62(6)	1
C(3b3)'	0.83(10)	1
C(3b3)''	0.17*	0

* Determined with isotropic thermal parameters.

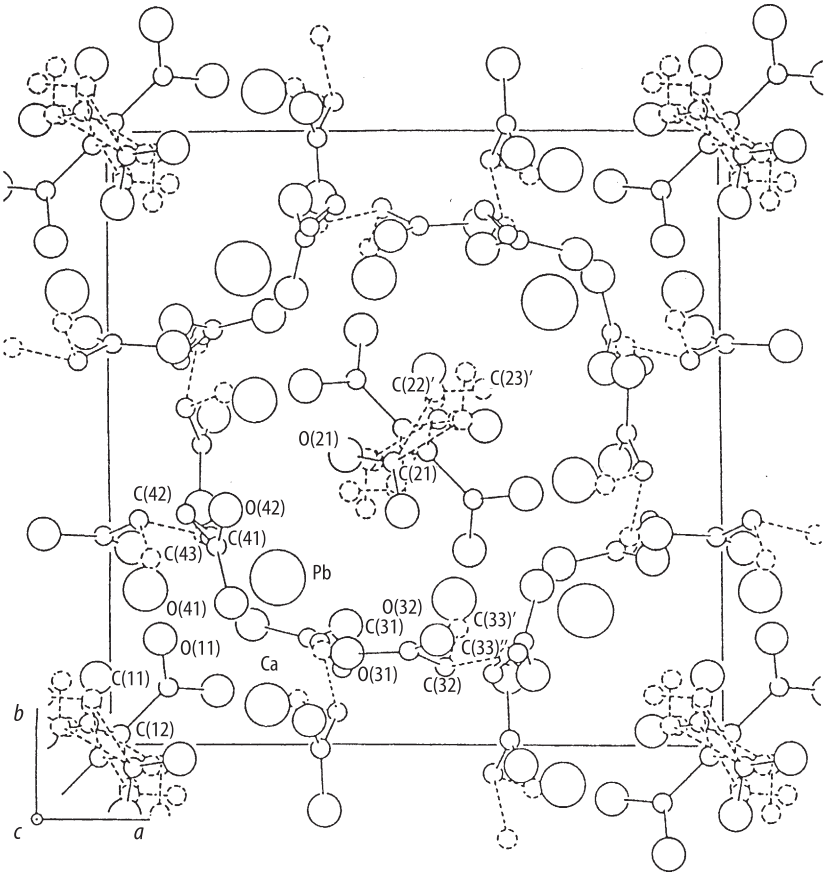

Fig. 58A-3-001. $Ca_2Pb(CH_3CH_2COO)_6$ (DLP). Structure of phase I [90Kas]. Projection on (001). Disordered atoms and their bonds are depicted by broken lines.

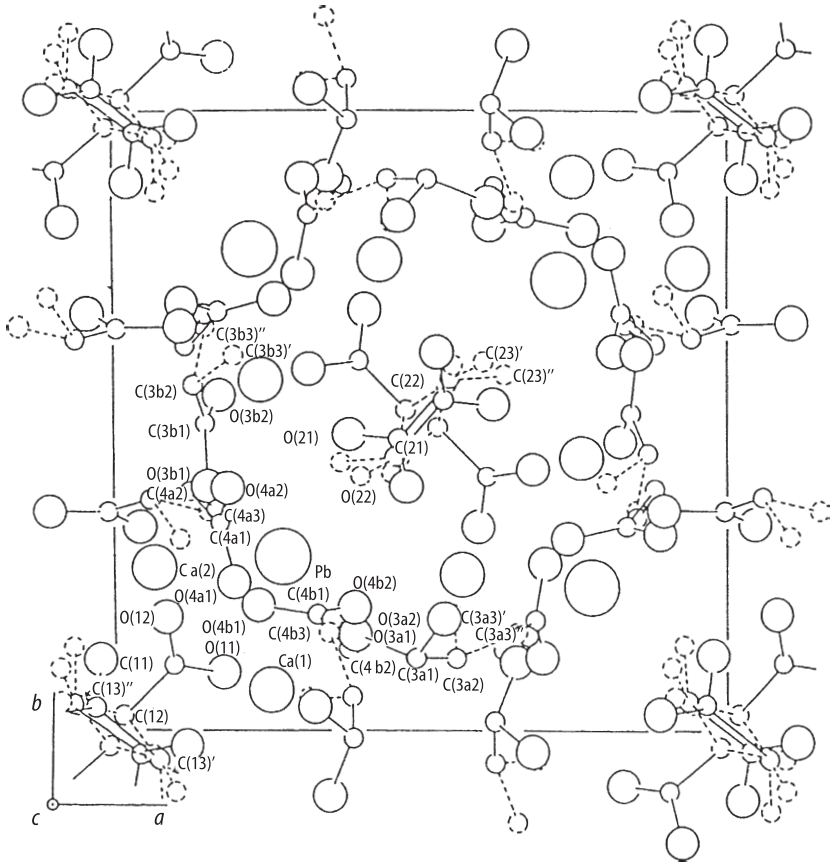

Fig. 58A-3-002. $Ca_2Pb(CH_3CH_2COO)_6$ (DLP). Structure of phase II [90Kas]. Projection on (001). Disordered atoms and their bonds are depicted by broken lines.

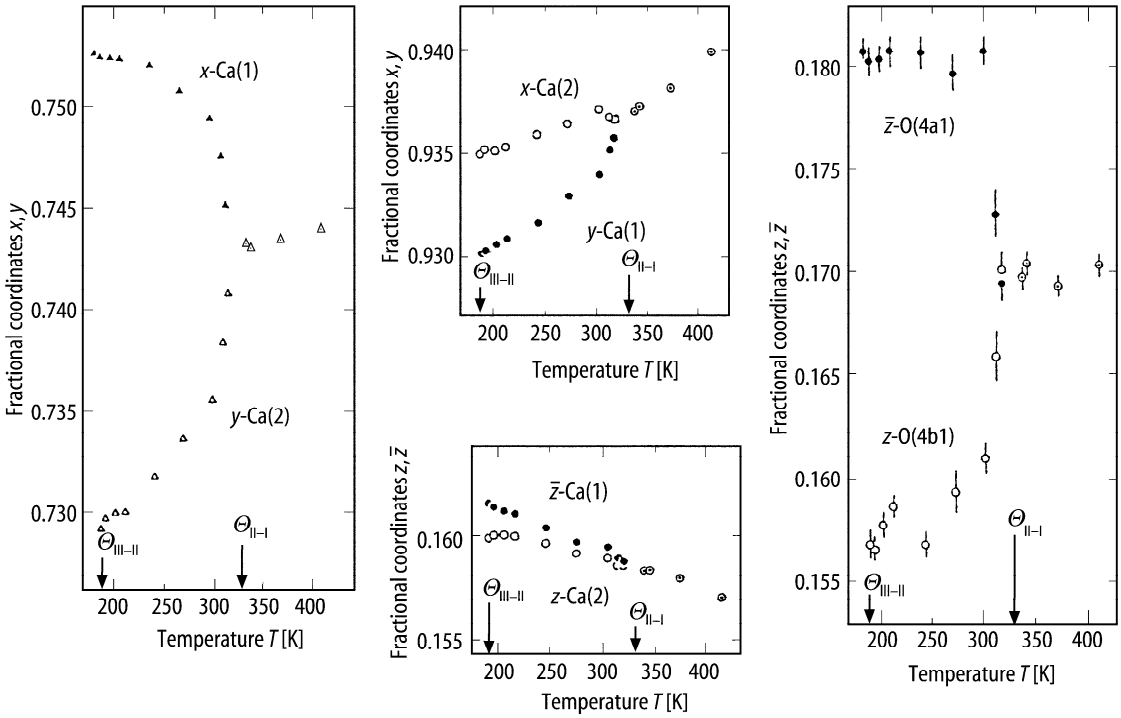

Fig. 58A-3-003. $Ca_2Pb(CH_3CH_2COO)_6$ (DLP). x, y, z, $\bar{z}$ vs. T [92Ito]. x, y, z: fractional coordinates. $\bar{z} = -z$. In phase II, z of Pb atom is fixed to 0.

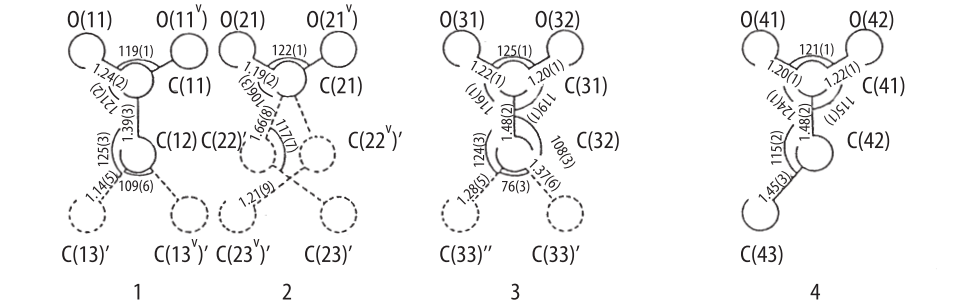

a

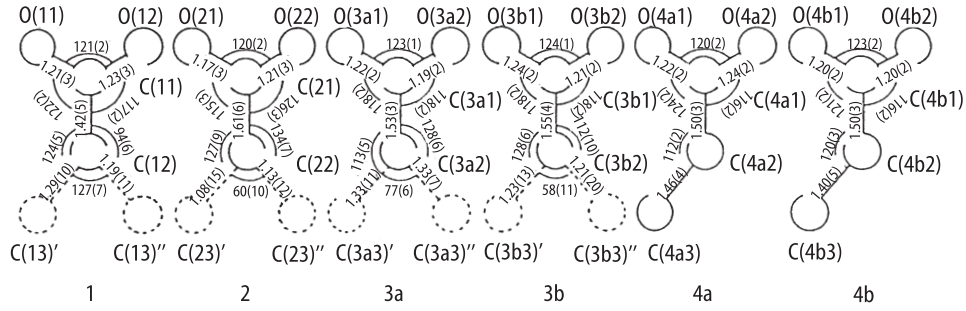

b

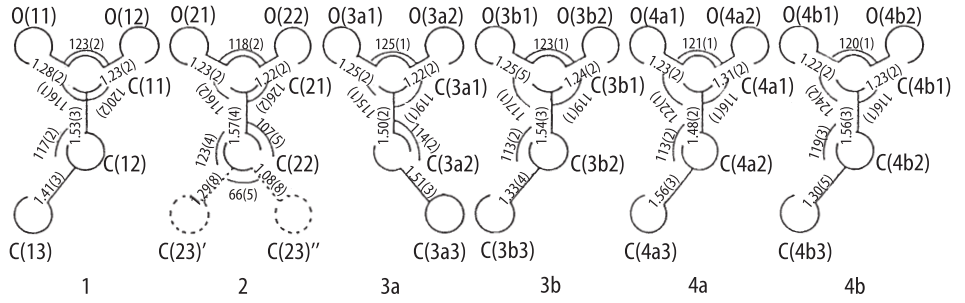

c

Fig. 58A-3-004. $Ca_2Pb(CH_3CH_2COO)_6$ (DLP). Interatomic distances [Å] and angles [°] [90Kas]. (**a**) 70 °C, (**b**) 45 °C, (**c**) –80 °C. Disordered atoms and their bonds are depicted by broken lines. ^{v}: symmetry code, see Table 58A-3-002.

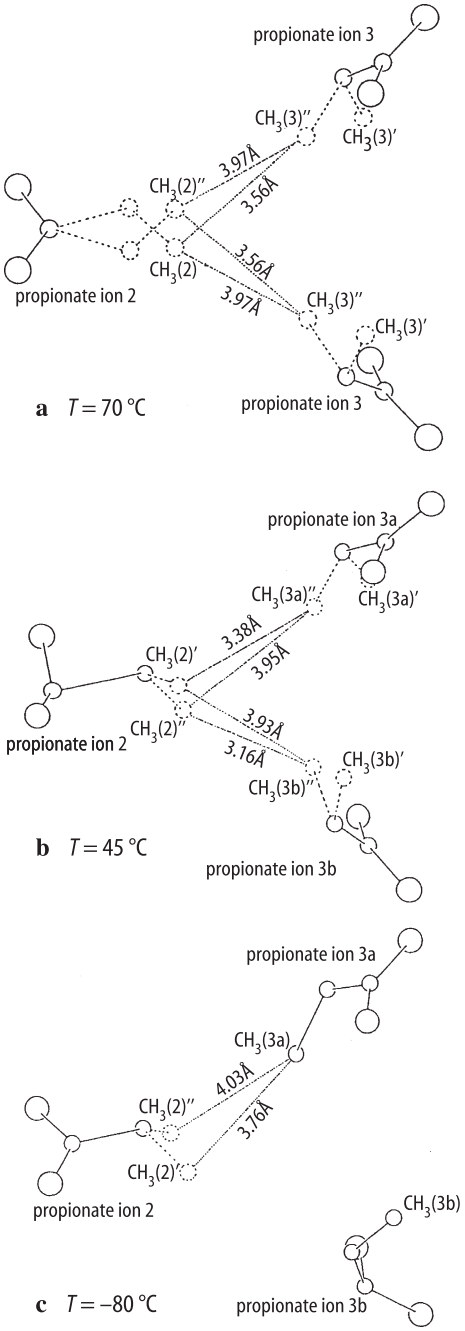

Fig. 58A-3-005. $Ca_2Pb(CH_3CH_2COO)_6$ (DLP). Positions and distances between methyl groups of the propionate ions 2, 3a and 3b viewed along [001] [90Kas]. (**a**) 70 °C, (**b**) 45 °C, (**c**) –80 °C. Disordered atoms and their bonds are depicted by broken lines.

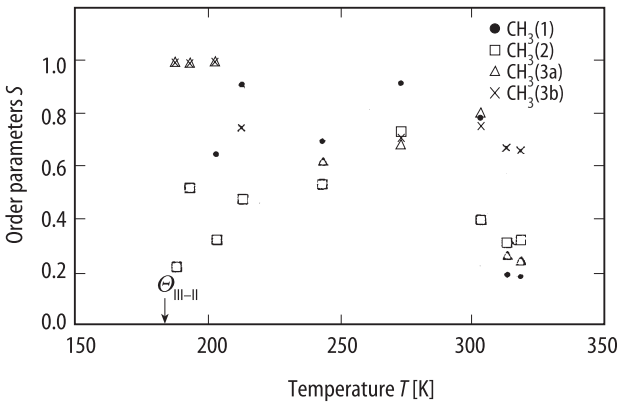

Fig. 58A-3-006. $Ca_2Pb(CH_3CH_2COO)_6$ (DLP). S vs. T [92Ito]. S: order parameters of disordered methyl groups.

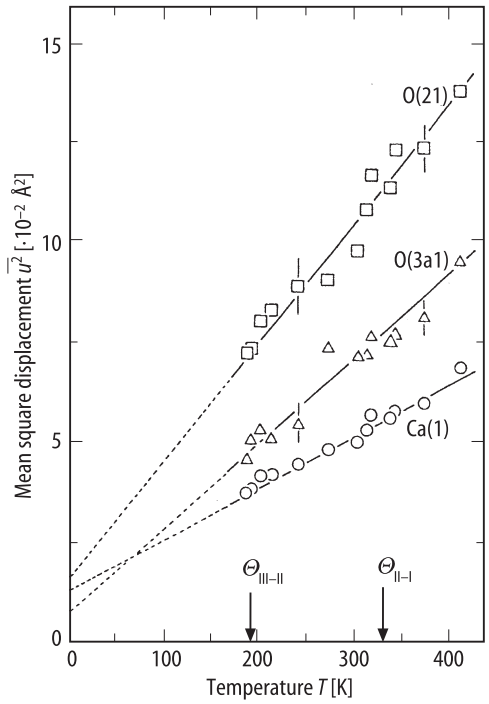

Fig. 58A-3-007. $Ca_2Pb(CH_3CH_2COO)_6$ (DLP). $\overline{u^2}$ vs. T [92Ito]. $\overline{u^2}$: mean square displacement.

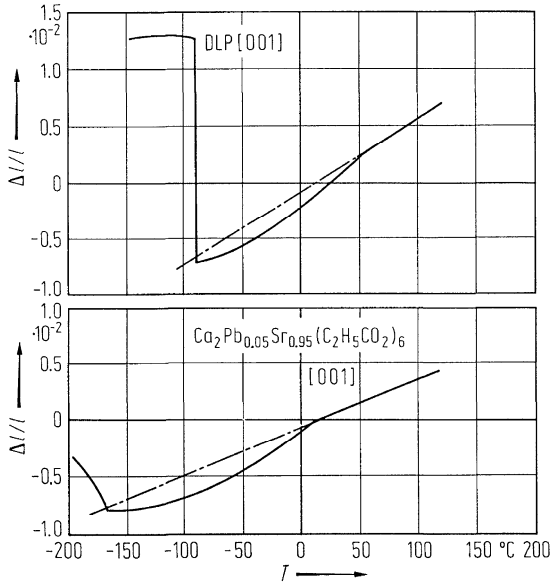

Fig. 58A-3-008. $Ca_2Pb(CH_3CH_2COO)_6$ (DLP), $Ca_2Pb_{0.05}Sr_{0.95}(CH_3CH_2COO)_6$. $\Delta l/l$ vs. T along [001] direction [76Nag1].

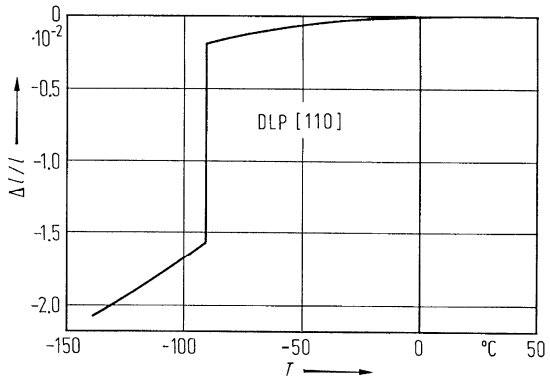

Fig. 58A-3-009. $Ca_2Pb(CH_3CH_2COO)_6$ (DLP). $\Delta l/l$ vs. T along [110] direction [76Nag1].

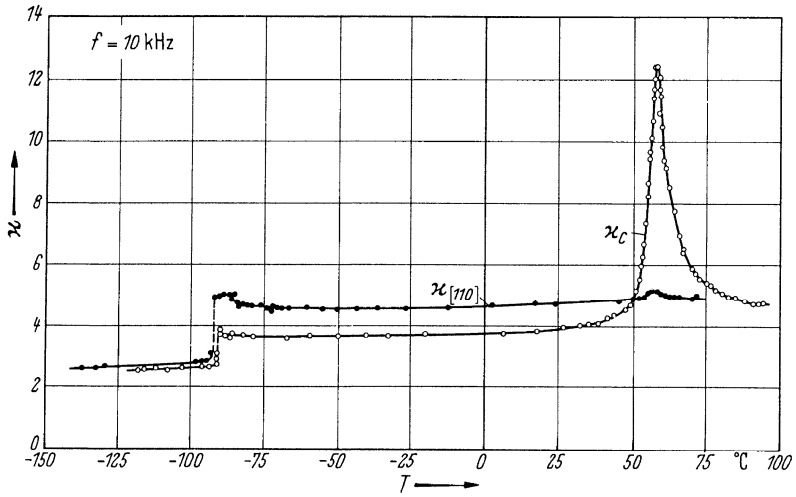

Fig. 58A-3-010. $Ca_2Pb(CH_3CH_2COO)_6$ (DLP). $\varkappa_c$, $\varkappa_{[110]}$ vs. T [65Nak].

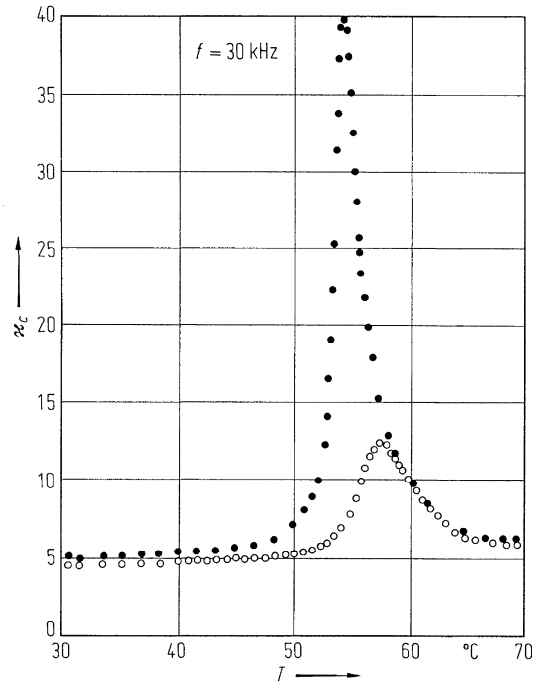

Fig. 58A-3-011. $Ca_2Pb(CH_3CH_2COO)_6$ (DLP). κ_c vs. T [76Tak]. Open circles: as-grown crystal; full circles: annealed crystal.

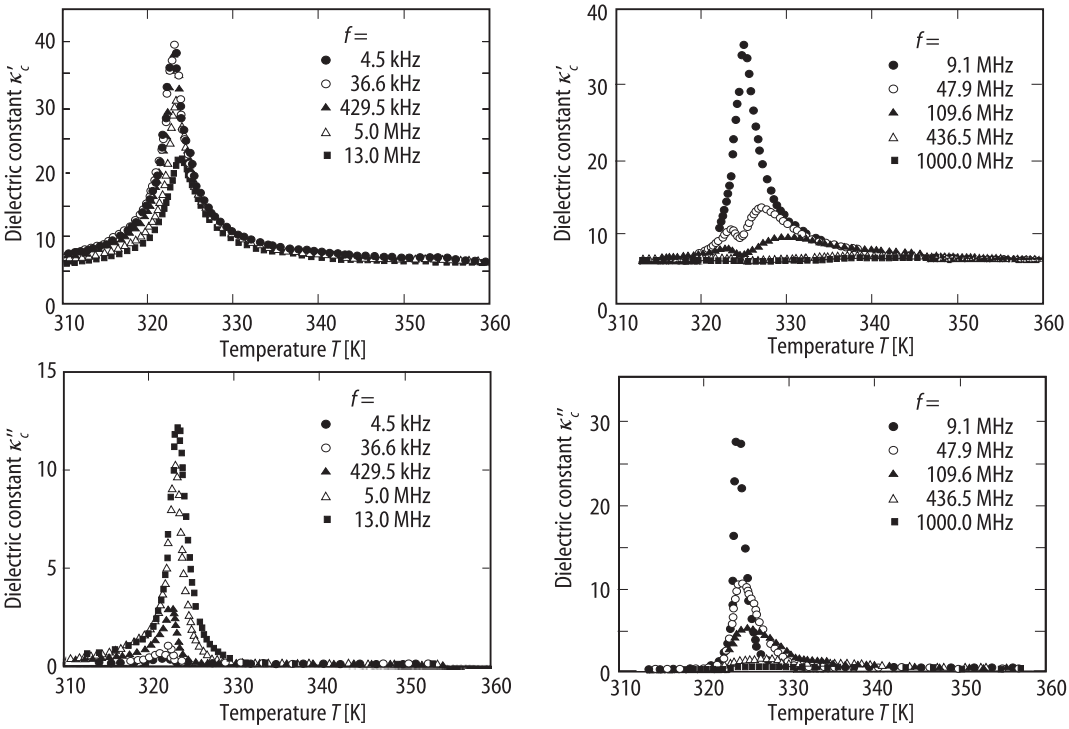

Fig. 58A-3-012. $Ca_2Pb(CH_3CH_2COO)_6$ (DLP). κ_c', κ_c'' vs. T [92Deg]. Parameter: f. Specimen was annealed at 270 °C for 15 h prior to measurements.

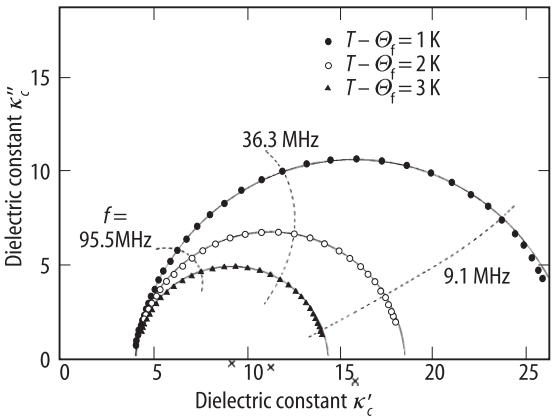

Fig. 58A-3-013. $Ca_2Pb(CH_3CH_2COO)_6$ (DLP). κ_c' vs. κ_c'' [92Deg]. Parameter: *T*. Cross: center of Cole-Cole arc. Specimen was annealed at 270 °C for 15 h.

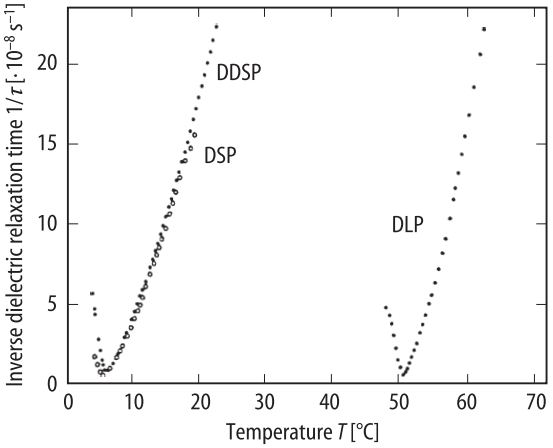

Fig. 58A-3-014. $Ca_2Pb(CH_3CH_2COO)_6$ (DLP), $Ca_2Sr(CH_3CH_2COO)_6$ (DSP), $Ca_2Sr(CD_3CD_2COO)_6$ (DDSP). $1/\tau$ vs. *T* [92Deg]. τ: dielectric relaxation time.

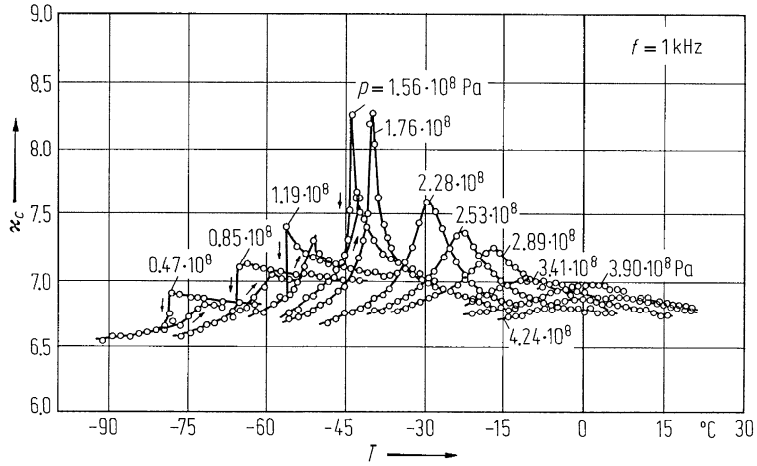

Fig. 58A-3-015. $Ca_2Pb(CH_3CH_2COO)_6$ (DLP). κ_c vs. *T* in the vicinity of III–II transition [75Ges]. Parameter: *p*.

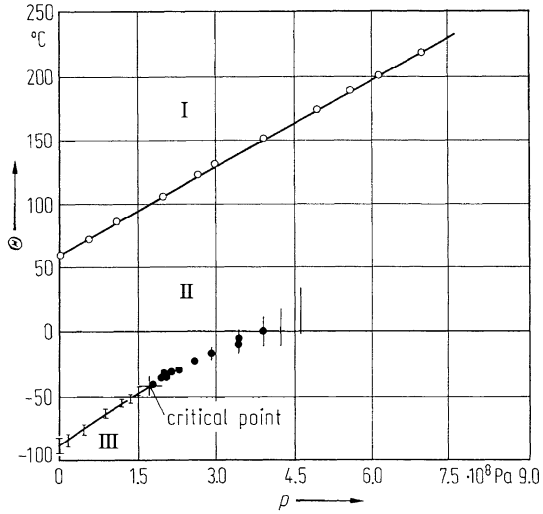

Fig. 58A-3-016. $Ca_2Pb(CH_3CH_2COO)_6$ (DLP). Phase diagram Θ vs. p [75Ges].

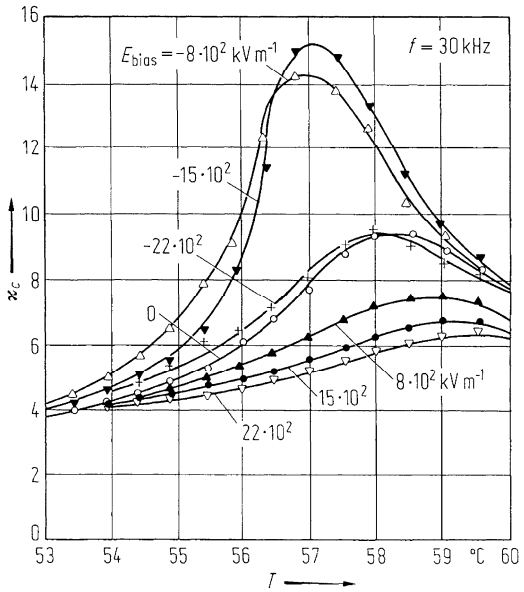

Fig. 58A-3-017. $Ca_2Pb(CH_3CH_2COO)_6$ (DLP). ε_c vs. T of as-grown crystal [76Tak]. Parameter: E_{bias}.

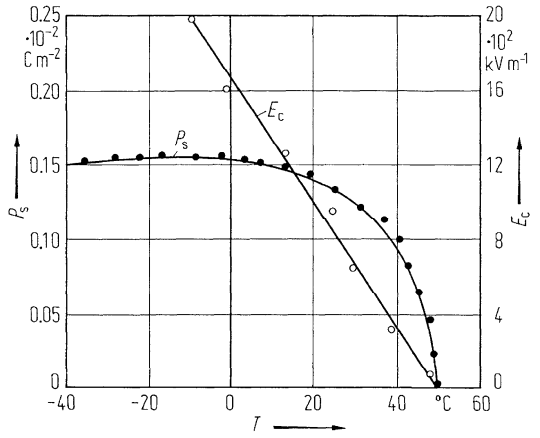

Fig. 58A-3-018. $Ca_2Pb(CH_3CH_2COO)_6$ (DLP). P_s, E_c vs. T [76Tak].

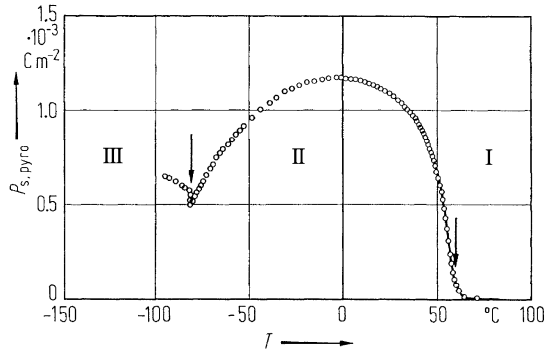

Fig. 58A-3-019. $Ca_2Pb(CH_3CH_2COO)_6$ (DLP). $P_{s,\,pyro}$ vs. T [75Osa]. $P_{s,\,pyro}$: spontaneous polarization obtained by pyroelectric measurement. Arrows point to transition temperatures.

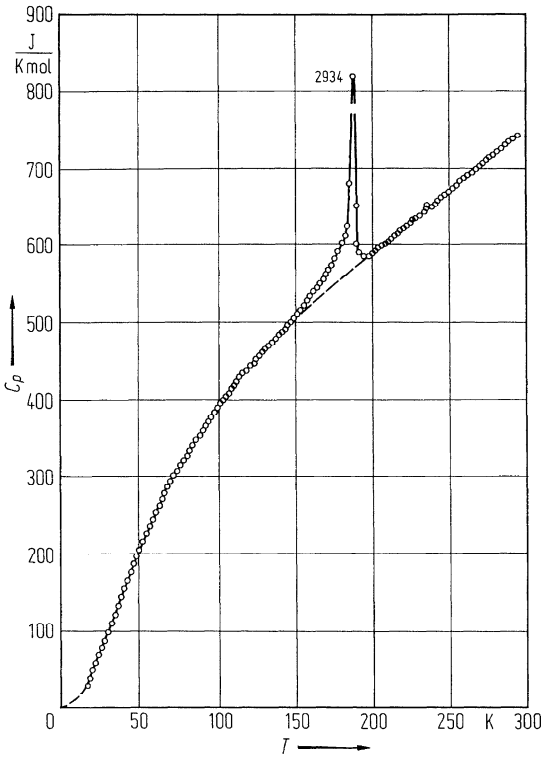

Fig. 58A-3-020. $Ca_2Pb(CH_3CH_2COO)_6$ (DLP). C_p vs. T [65Nak].

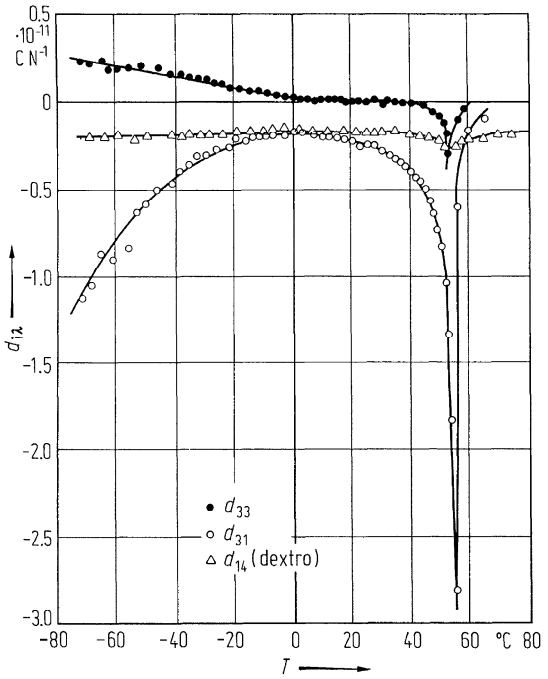

Fig. 58A-3-021. $Ca_2Pb(CH_3CH_2COO)_6$ (DLP). $d_{i\lambda}$ vs. T [78Tak]. Annealed specimen. Quasistatic method.

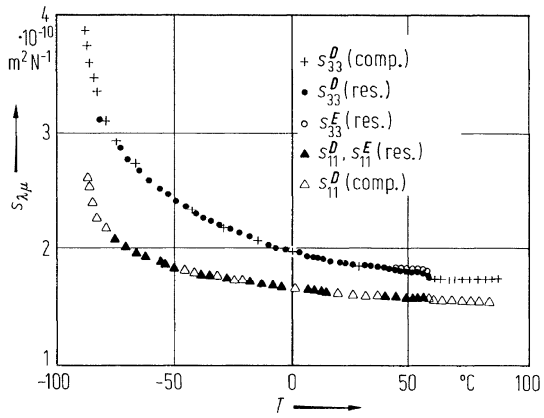

Fig. 58A-3-022. $Ca_2Pb(CH_3CH_2COO)_6$ (DLP). $s_{\lambda\mu}$ vs. T [78Tak]. res.: resonance method; comp.: composite bar method.

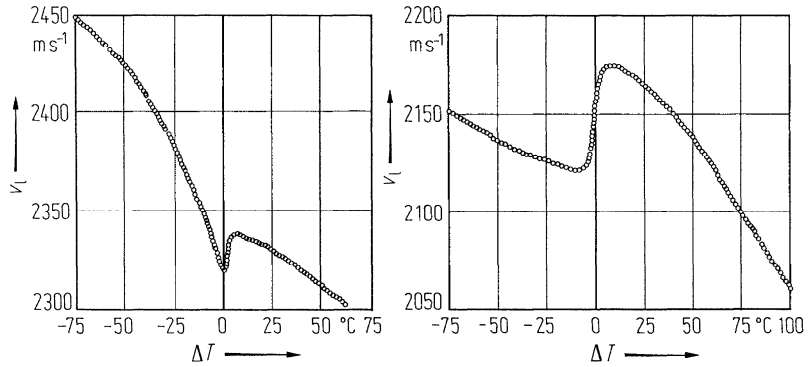

Fig. 58A-3-023. $Ca_2Pb(CH_3CH_2COO)_6$ (DLP). v_l vs. ΔT [74Tod]. v_l: sound velocity of the longitudinal wave. Left hand figure along the *a* axis; right hand figure along the *c* axis. $\Delta T = T - \Theta_{II-I}$.

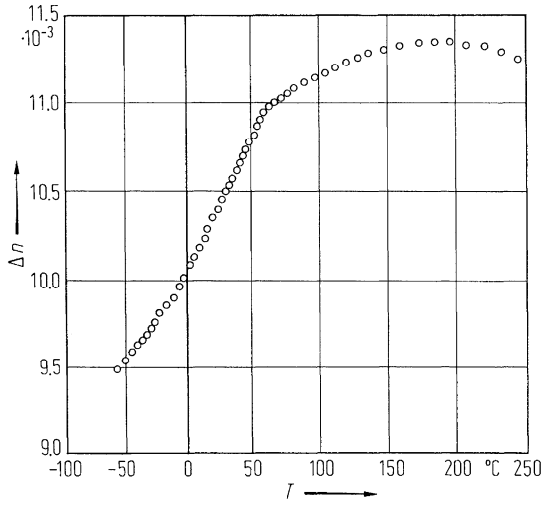

Fig. 58A-3-024. $Ca_2Pb(CH_3CH_2COO)_6$ (DLP). Δn vs. T [76Tak]. $\Delta n = n_c - n_a$.

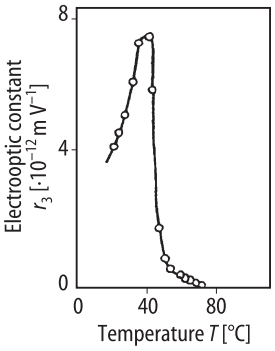

Fig. 58A-3-025. $Ca_2Pb(CH_3CH_2COO)_6$ (DLP). r_3 vs. T [89Vlo]. r_3: electrooptic constant defined as $r_3 = n_3^3 r_{33} - n_1^3 r_{13}$. $\lambda = 632.8$ nm.

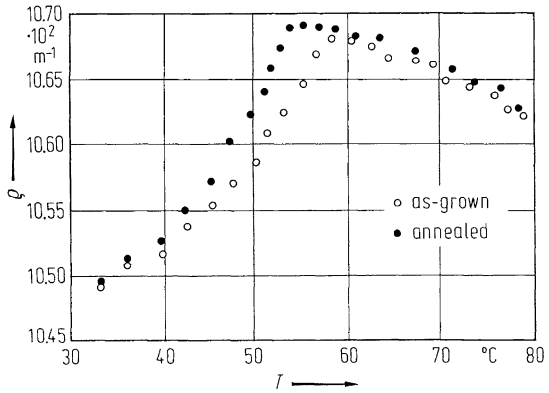

Fig. 58A-3-026. $Ca_2Pb(CH_3CH_2COO)_6$ (DLP). ρ vs. T [76Tak]. ρ: optical rotatory power.

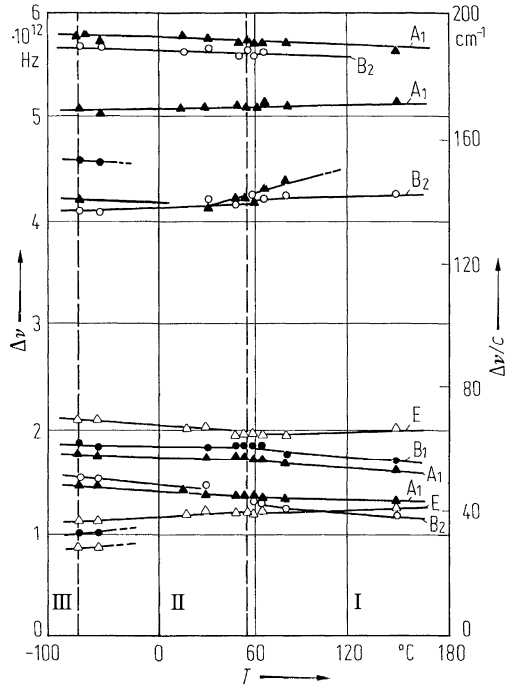

Fig. 58A-3-027. $Ca_2Pb(CH_3CH_2COO)_6$ (DLP). $\Delta\nu$ vs. T [76Nag2]. $\Delta\nu$: Raman frequency shift.

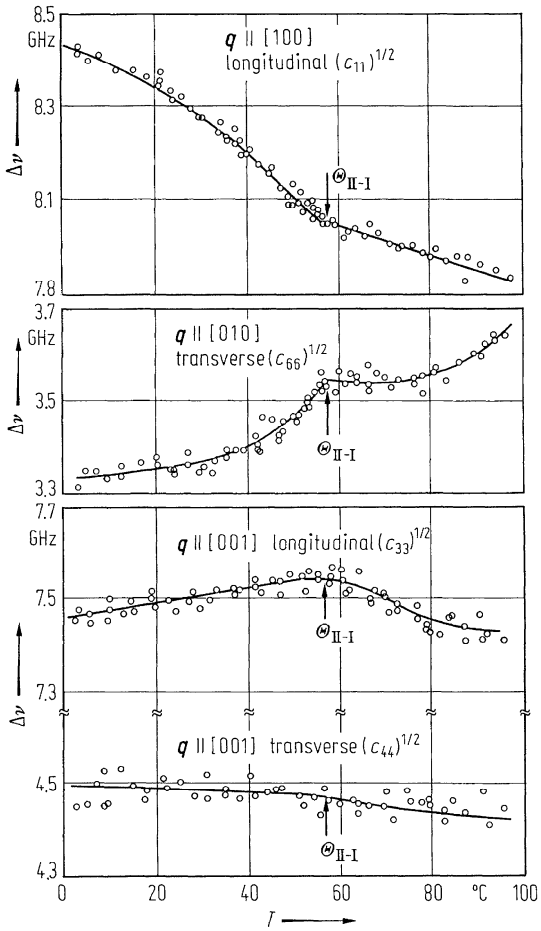

Fig. 58A-3-028. $Ca_2Pb(CH_3CH_2COO)_6$ (DLP). $\Delta\nu$ vs. T [74Yag]. $\Delta\nu$: frequency shift of Brillouin scattering. Scattering angle: 90°. $\lambda = 632.8$ nm.

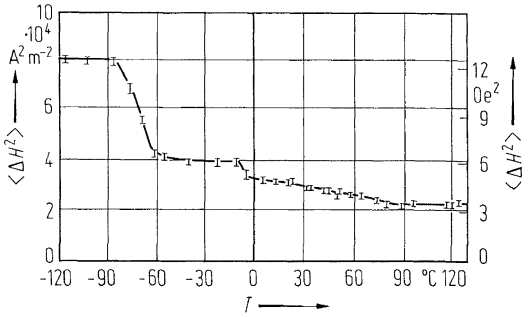

Fig. 58A-3-029. $Ca_2Pb(CH_3CH_2COO)_6$ (DLP). $\langle\Delta H^2\rangle$ vs. T [67Ale]. $\langle\Delta H^2\rangle$: second moment for proton NMR line.

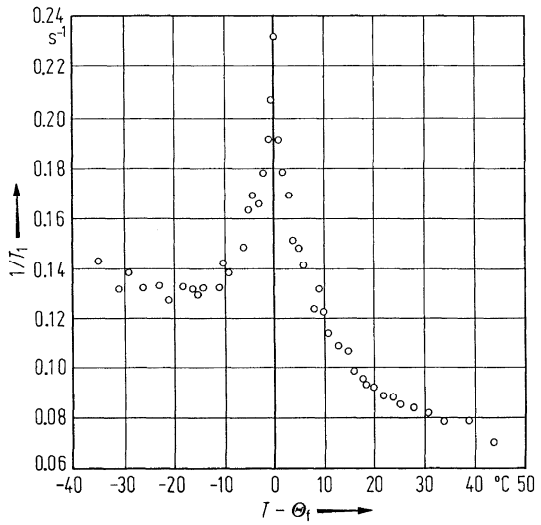

Fig. 58A-3-030. $Ca_2Pb(CH_3CH_2COO)_6$ (DLP). $1/T_1$ vs. $T - \Theta_f$ [72Tat]. T_1: spin-lattice relaxation time for proton. $\boldsymbol{H} \parallel \boldsymbol{c}$ axis.

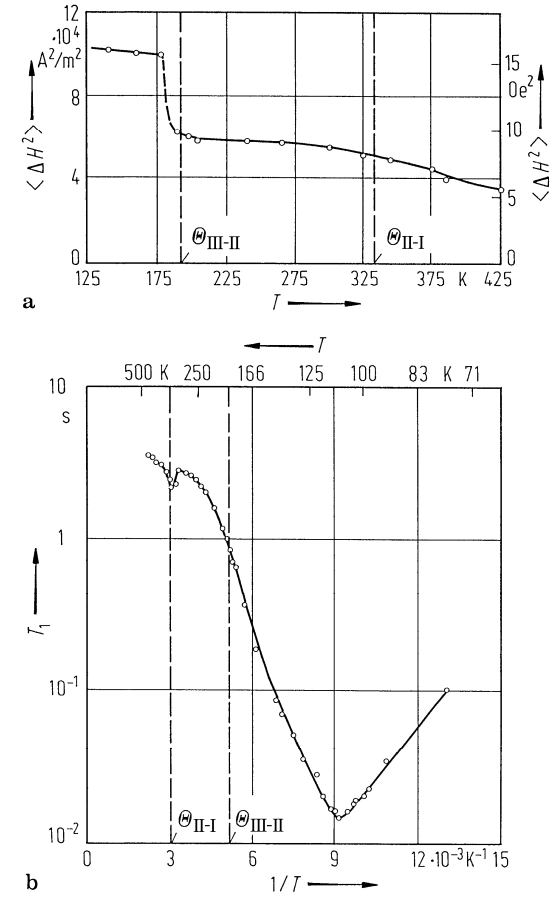

Fig. 58A-3-031. $Ca_2Pb(CH_3CH_2COO)_6$ (DLP). Proton NMR [85Sun]. (**a**) $\langle \Delta H^2 \rangle$ vs. T. $\langle \Delta H^2 \rangle$: second moment of NMR line for powdered sample. (**b**) T_1 vs. T^{-1}. T_1: spin-lattice relaxation time.

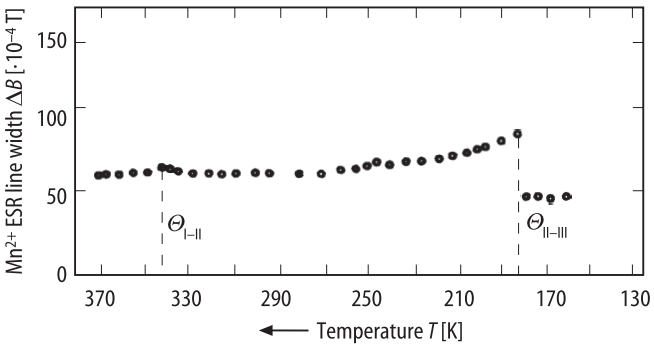

Fig. 58A-3-032. $Ca_2Pb(CH_3CH_2COO)_6$ (DLP). ΔB vs. T [89Mis2]. ΔB: Mn^{2+} ESR line width of the highest-field line.

References

59Fer Ferroni, E., Orioli, P.: Z. Kristallogr. **111** (1959) 362.
65Nak Nakamura, N., Suga, H., Chihara, H., Seki, S.: Bull. Chem. Soc. Jpn. **38** (1965) 1779.
67Ale Aleksandrova, I.P., Zherebtsova, L.I., Aleksandrov, K.S.: Kristallografiya **12** (1967) 894; Sov. Phys. Crystallogr. (English Transl.) **12** (1968) 780.
72Tat Tatsuzaki, I., Sakata, K., Todo, I., Tokunaga, M.: J. Phys. Soc. Jpn. **33** (1972) 438.
72Tod Todo, I., Tatsuzaki, I.: Phys. Lett. A **38** (1972) 41.
74Tod Todo, I., Tatsuzaki, I.: Phys. Status Solidi (a) **23** (1974) 591.
74Yag Yagi, T., Tatsuzaki, I.: J. Phys. Soc. Jpn. **37** (1974) 1038.
75Dim Dimir, V., Osredkar, M.: Phys. Status Solidi (a) **30** (1975) K63.
75Ges Gesi, K., Ozawa, K.: J. Phys. Soc. Jpn. **39** (1975) 1026.
75Osa Osaka, T., Makita, Y., Gesi, K.: J. Phys. Soc. Jpn. **38** (1975) 292.
75Tak Takashige, M., Iwamura, K., Hirotsu, S., Sawada, S.: J. Phys. Soc. Jpn. **38** (1975) 1217.
76Nag1 Nagae, Y., Ishibashi, Y., Takagi, Y., Kameyama, H.: J. Phys. Soc. Jpn. **41** (1976) 1300.
76Nag2 Nagae, Y., Wada, M., Ishibashi, Y., Takagi, Y.: J. Phys. Soc. Jpn. **41** (1976) 1659.
76Tak Takashige, M., Iwamura, H., Hirotsu, S., Sawada, S.: Ferroelcctrics **11** (1976) 431.
78Tak Takashige, M., Hirotsu, S., Sawada, S., Hamano, K.: J. Phys. Soc. Jpn. **45** (1978) 558.
84Bad Badarinath, K.V.S., Radhakrishna, S.: J. Mater. Sci. Lett. **3** (1984) 575.
84Sin Singh, S.: J. Phys. C **17** (1984) 5421.
85Sun Sundaram, C.S., Ganesan, K., Ramakrishna, J., Chandrasekhar, K., Sastry, V.S.S.: Phase Transitions **5** (1985) 169.
88Ues Uesu, Y., Inoue, M., Okada, N.: J. Phys. C **21** (1988) L391.
89Mis1 Misra, S.K., Jerzak, S.: Phys. Rev. B **39** (1989) 2041.
89Mis2 Misra, S.K., Jerzak, S.: Acta Phys. Pol. A **76** (1989) 943.
89Ues Uesu, Y., Inoue, M., Okada, N.: Ferroelectrics **96** (1989) 319.
89Vlo Vlokh, R.O., Biletsky, I.N., Franko, I.V.: Ferroelectrics **90** (1989) 183.
90Kas Kasatani, H.: J. Phys. Soc. Jpn. **59** (1990) 1647.
90Ues Uesu, Y., Okada, N., Inoue, M., Hara, S.: Ferroelectrics **107** (1990) 33.
91Ara Arahira, S., Uesu, Y.: J. Phys. Soc. Jpn. **60** (1991) 2461.
92Deg Deguchi, K., Takeuchi, M., Nakamura, E.: J. Phys. Soc. Jpn. **61** (1992) 1362.
92Ito Itoh, K., Niwata, A., Abe, W., Kasatani, H., Nakamura, E.: J. Phys. Soc. Jpn. **61** (1992) 3593.